AN ABSTRACT OF THE
DISSERTATION OF

Siriporn Sasimontonkul for the degree of Doctor of Philosophy in Exercise and Sport Science presented on August 25, 2004.
Title: Do Running and Fatigued Running Relate to Tibial Stress fractures?

Abstract approved: Redacted for Privacy

Brian R. Bay

Tibial stress fractures are common in runners. However, it is unclear what factors are associated with tibial stress fractures. This study aimed to investigate 1) magnitudes of bone contact forces occurring while running 2) whether or not repeated application of running loads is sufficient to explain tibial stress fractures and 3) whether or not muscle fatigue alters the potential of tibial stress fractures. Tibial stress fractures were predicted through an estimation of the minimum number of cycles to failure (Nfail) using an integrated experimental and mathematical modeling approach. Short running trials within a speed range of 3.5-4 m/s of ten male runners were evaluated with a coupled force plate and 3 dimensional motion analysis system. The collected data were used to estimate joint reaction forces (JRF) and joint moments. Using these JRF and muscle forces predicted from optimization, 2-D bone contact forces at the distal end of the tibia were determined. Next, tibial stresses were estimated by applying these bone contact forces to a tibial model, which were then used to predict the Nfail. All procedures were repeated after plantarflexors fatigued from prolonged running. This study found that peaks of compressive and posterior shear forces occurred during mid stance, and these peaks equaled 8.91 $\pm$ 1.14 BW and -0.53 $\pm$ 0.16 BW, respectively. These bone contact forces led to a backward bending of the tibia during most of the stance phase and resulted in the maximum stresses of -43.4 $\pm$ 10.3 MPa on the posterior face of the tibia. These maximum stresses predicted the group mean of Nfail as being $5.28*10^6$ cycles. However, 2.5% to 56% of population of runners have a chance of getting tibial stress fractures within 1 million

cycles of a repeated foot impact. Within the context of muscle force and stress estimation procedures used in this study, Nfail appeared to increase after fatigue, not decrease as we hypothesized.

Do Running and Fatigued Running Relate to Tibial Stress Fractures?

by
Siriporn Sasimontonkul

A DISSERTATION

Submitted to

Oregon State University

In partial fulfillment of
the requirements for the
degree of

Doctor of Philosophy

Presented August 25, 2004
Commencement June 2005

Doctor of Philosophy dissertation of Siriporn Sasimontonkul presented on August 25, 2004.

APPROVED:

Redacted for Privacy

Major Professor, representing Exercise and Sports Science

Redacted for Privacy

Chair of the Department of Exercise and Sports Science

Redacted for Privacy

Dean of the Graduate School

I understand that my dissertation will become part of the permanent collection of Oregon State University libraries. My signature below authorizes release of my dissertation to any reader upon request.

Redacted for privacy

Siriporn Sasimontonkul, Author

ACKNOWLEDGMENTS

I gained pleasure and inspiration through conducting this dissertation. As expected, I was confronted with many obstacles to overcome and often times felt like giving up, yet the hard work and love that my parents modeled and gave to me are what have helped me to successfully pass through all trials. I am most indebted to my parents who love me with unending love, Prasong and Normjit Sasimontonkul. Although my parents are no longer in this world, I hope that they know my success is because of them. A part of me completed this degree for them. I thank my sisters and brother, Kanitha, Suchada, Thamarat and Ampawan Sasimontonkul, for their thoughtfulness and encouragement.

I take pleasure in expressing my gratitude to those who have helped me with this dissertation. I am especially indebted to committee members, Dr. Brian Bay, Dr. Mike Pavol, Dr. Michael Schuyler, Dr. Rod Harter, Dr. Jeff Widrick and Dr. Marjorie Reed, for their guidance and valuable suggestions. I am delighted to thank Dr. Terry Wood and Dr. DeWayne Derryberry for their useful suggestions in statistic. Many thanks are due to Wayne Robertson and Cami Bradley for their contributions in editing this dissertation.

I acknowledge all of the volunteer runners. I was pleased to work with them and was impressed by their incredible dedication. Through assistance from friends, the data collection was completed. I would like to thank Yingrodge Suntiwuth, Weerasak Ussawawongaraya, Chairat Choosakul, Sarawuth Naramngam and Charirat Kusonwiriyawong. I am also thankful for the great support from friends, Prangtip Chayaput, Pasakorn Watanatada and Jeremy Bauer.

I am grateful to the department of exercise and sports science at Kasetsart University, Dr. Timothy White and Dr.Supitr Samahito for the wonderful opportunity to study Biomechanics at Oregon State University. I am also indebted to Vullee Bhatharobhas for nominating me to the Royal Thai Government Scholarship, through which I received partial financial support. I also greatly appreciate the partial financial

support from Kasetsart University, Thailand and for the GRA and GTA positions provided by Dr. Gerald Smith and Dr. Anthony Wilcox, chair of the department of exercise and sport science, Oregon State University.

TABLES OF CONTENTS

LIST OF FIGURES

LIST OF TABLES

LIST OF APPENDICES FIGURES

DO RUNNING AND FATIGUED RUNNING RELATE TO TIBIAL STRESS FRACTURES?

CHAPTER 1

INTRODUCTION

Stress fractures are localized, generally incomplete bone fractures caused by low-level repetitive loading, not a single traumatic event. They are common in athletes, particularly those involved in endurance sports accounting for between 0.7% and 15.6% of all injuries (Spitz and Newberg, 2002; Bennell and Brukner, 1997). The highest incidence rate of stress fractures has been reported in runners, with a wide range of 9.7% to 72% (Bennell et al., 1996; Bennell and Brukner, 1997; Brukner et al., 1996; Hulkko and Orava, 1987). Among different types of runners, long distance runners had the highest percentage of athletes (31%) who sustained the stress fractures (Bennell et al., 1996). The most common site and common region of stress fractures found in runners were the tibia, and the posterior-medial crest at its distal third, respectively (Hulkko and Orava, 1987; Fredericson et al., 1995; Brukner et al., 1998).

There is no conclusive evidence regarding the causation of the tibial stress fracture in runners. Beck (1998) reported that the incidence of tibial stress fractures was associated with the activity volume and alterations in tibial loading. Runners, who got stress fractures, had a mean weekly running mileage of 117 km, but the association between the weekly running mileage and the frequency of fractures was not found (Korpelainen et al., 2001). In contrast, Bennell and team (1996) reported for their own study that the incidence of stress fractures was 0.7 per 1000 hours of training. From these previous reports, the possible factors causing tibial stress fractures in runners may be either the large magnitude of loads applied to the tibia during running, the number of running cycles, the change in tibial loading after muscle fatigue, or some combination of these factors.

Micro-damage and fatigue failure of materials is a function of cyclic loading magnitude and duration. A number of *in vitro* studies have documented the response of cortical bone to the application of repetitive loads (Carter et al., 1981; Carter and Caler, 1983; Carter and Caler, 1985; Schaffler et al., 1990). These studies showed that loads deforming bone about 3000-10,000 με were able to fail bone within 10^3 to 10^5 cycles of the repetitive application (Table 1). If the stride length is about 2.68 m at the running speed of 3.83 m/s (Cavanagh and Kram, 1990), 10^3 and 10^5 cycles will be equivalent to running distances of 2.68 km (1.67 miles) and 268 km (167.5 miles), respectively. However, bone will not fail if the applied loads result in a smaller strain range of 1,200-1,500 με. This strain range is within the normal physiologic range, which has been estimated to be between 50 and 1500 με (Martin, 2000).

Table 1. Fatigue life of cortical bone at various strain levels.

Type of Loads	**Strain (με)**	**Cycles to failure* (cycles)**
Reversed uniaxial loading (Carter et al., 1981)	5,000-10,000	10^3 to 10^4
Uniaxial tensile loading (Carter and Caler, 1985)	3000	10^5
Uniaxial tensile loading (Schaffler et al., 1990)	1,200-1,500	Bone did not fail after $13*10^6$

*Cycles to failure is the number of loading cycles that results in the failure of cortical bone. Failure was defined as the complete fracture of the specimens.

At the stance phase of running, the foot applies compressive and shear forces to the leg with peak magnitudes in the range of 8-14 BW and 0.4-5 BW, respectively, for a running speed range of 3.5 – 5.3 m/s (Scott and Winter, 1990; Burdett, 1982). However, the simplicity of mathematical techniques used in these studies, such as the reduction in the number of active muscles, may lead to inaccuracy of the prediction. Moreover, whether or not these forces could lead to the micro-damage of the tibia is unknown.

To investigate the possibility of micro-damage of the tibia from running, strain gauge staples were mounted to the medial aspect of the mid tibial diaphysis of live humans (Milgrom et al., 2000a &b; Milgrom et al., 2002; Burr et al., 1996; Milgrom et al., 2003; Ekenman et al., 1998). The results showed that the strains occurring during running were not large enough to induce the micro-damage of bone. The maximum compressive axial strain was in the range of -350 με to -2500 με while the maximum tensile axial strain was in the range of 630 με to 1469 με. Factors that affect the difference in the magnitudes of the reported peak strains were the differences in running speed, running shoes, and the material of the running track used in those experiments. However, these peak strains were not the actual maximum strains found in the tibia because they were measured from only specific sites of the tibia. Maximum strain is the peak of the strain's distribution around the tibia, which can be recorded by bonding the rosette strain gauges around the tibia. However, the experimental technique requires an invasive surgery and has not been done in live humans (Milgrom et al., 2000a).

In contrast, the measurement of peak strains in the tibia can be taken during *in vitro* experiments. Petermann and colleagues (2001) mounted seven strain gauges around cadaveric tibiae, approximately 9 cm above the malleoli. Strains were recorded from simulated gait in micro-gravity. Authors reported that bending was a primary mode of loading on the tibia. The peak compressive and tensile strains were found in the posterior and anterior regions of the tibia, respectively. The medial aspect of the tibia was the location of the neutral axis of bending. It was the place that the previous *in vivo* studies used for mounting the strain gauge staples to the human tibia. Therefore, those reported strains from the *in vivo* studies were not the maximum and were far below maximum strains. It is then possible that running causes larger strains in the tibia than those reported. It may large enough to fail bone during long running events, but this has not been confirmed in human studies.

The finite element modeling method has also been used for the estimation of bone stresses. The proximal tibia (Little et al., 1986) and the whole tibia (Mehta et al.,

1999) were modeled in 3 dimensions. A compressive force of 2450 N was applied to their models. The magnitude of this applied force corresponded to the joint reaction force (JRF) measured experimentally. An increasing compressive stress from the anterior to the posterior aspect was found in the proximal tibial model. The maximal stress of 24.8 MPa occurred in the cortical bone of the posterior surface. In contrast, a maximum compressive stress of 43.35 MPa was found in the whole tibial model. It occurred at approximately 7 cm from the distal end and at the lateral side of the tibia. Sonada and colleagues (2003) applied a compressive force of 2790 N and bending forces of 240 N to a 3-dimensional (3-D) finite element model simultaneously. The approximate peak stress at the posteriomedial distal third of the tibia was in the range of 19-32 MPa, however the type of this stress was not reported. The reported peak stresses from these finite element models were not the actual peak stresses because forces corresponding to the JRF were applied to the models rather than bone contact force. Bone contact force is the actual force found across the articulating surfaces of the bone ends but JRF is not (Winter, 1990). Bone contact force includes the effect of muscle activities and its magnitude is larger than that of JRF. The application of bone contact force to the finite element model of the tibia should predict a larger peak stress than those reported. As a result, it is unclear whether or not peak tibial stress occurring during running is large enough to damage bone.

Muscle fatigue resulting from prolonged running may be associated with tibial stress fractures because there was a report about an increase in peak strain in the tibiae of foxhounds after their muscles fatigued (Yoshikawa et al., 1994). These foxhounds were instrumented with strain gauges in their tibiae and subjected to 20 minutes of running exercise on their hind limbs. After the quadriceps fatigued, peak principal strain increased about 26-35 % compared to before fatigue. Fyhrie and colleagues (1998) attempted to observe the effect of muscle fatigue on bone strains in live humans. They mounted two strain gage equipped K-wires in the anteromedial side of the tibia. Unfortunately, the impact shock from heel strike caused too much noise in the signals, leading to inconclusive results. Therefore, the further study is necessary to

investigate the effect of muscle fatigue on the change of peak strain in the human tibia and to observe the relationship between this change and the stress fracture of the tibia.

At this time, it is unclear if the initiation of micro damage of the tibia is the result of the repetitive application of large loads to the bone during running or the result of an increase in the magnitude of applied loads to the bone after muscle fatigue. Several investigations have been conducted as previously mentioned but the limitations prevent them from drawing definitive conclusions. Furthermore, stress fractures of the tibia do occur at a high incidence rate in runners, in contradiction of the small strains and stresses found in the tibia, as reported by those studies. It is then possible that the maximum stresses and strains found in the tibia are larger than those reported. Therefore, two research questions were posed in this study, which were 1) whether, in the absence of muscle fatigue, the tibial stresses occurring while running could result in stress fractures, and 2) whether muscle fatigue from prolonged running increases the probability that stress fractures will occur.

An integrated experimental and mathematical modeling approach was used in this study. Bone contact force components were predicted from running trials and applied to a tibial model for the estimation of the stresses acting in the tibia. These stresses were then used for the prediction of the number of cycles to failure (Nfail). It has been reported that Nfail of bone is more than 10^6 cycles under physiological loading (Schaffler et al., 1990). Physiological loading is generally thought to produce strains in the range of 50-1500 $\mu\varepsilon$ (Martin, 2000). However, forces occurring while running might produce strains greater than this range and result in a smaller Nfail. Two hypotheses were then proposed here. First, the minimum Nfail of the tibia is less than 10^6 cycles under the force acting during running. Second, muscle fatigue alters the potential for stress fractures; therefore the minimum Nfail of the tibia found after muscle fatigue will not equal that found before muscle fatigue.

1.1 The mathematical calculations

Experimental procedures have been conducted in this study to gather data for the estimation of minimum Nfail in the tibia. Kinetic and kinematic data have been collected from short running trials, conducted in a gait evaluation laboratory. Running speed range was set at 3.5 - 4 m/s. During running, six cameras captured the 3 dimensional (3-D) spatial orientations of reflective markers taped to the skin at the left leg and the hip of runners. Simultaneously, a force plate recorded the 3-D ground reaction force (GRF) signals. The 3-D spatial coordinates and GRF signals were synchronized and used for the estimation of the resultant joint moments and JRF using an inverse dynamic method as shown in the Figure 1.1. Thereafter, the sequential calculations were performed to estimate minimum Nfail of the tibia at each time instant of the stance phase of running at the frequency of 120 Hz.

The determination of bone and muscle's orientations and the muscle moment arm lengths. The left lower limb was modeled as four rigid body segments consisting of (1) pelvis, (2) femur, (3) tibia, and (4) foot, with 21 muscles attached to them. The origin and insertion coordinates of individual muscles in the segmental reference frames were derived from Delp (1990) and were transformed to the global reference frame (Amirouche, 1992; Kepple et al., 1994). The coordinates of muscle landmarks were fixed in segmental reference frames; however the spatial orientations of muscle landmarks relative to the global reference frame were changed according to the movement of the runners' leg. Moment arm length of individual muscles in the sagittal plane was estimated from the coordinates of the muscle's origin and insertion and joint center using method of Hawkins (1992). It was estimated at each time instant of the stance phase of running.

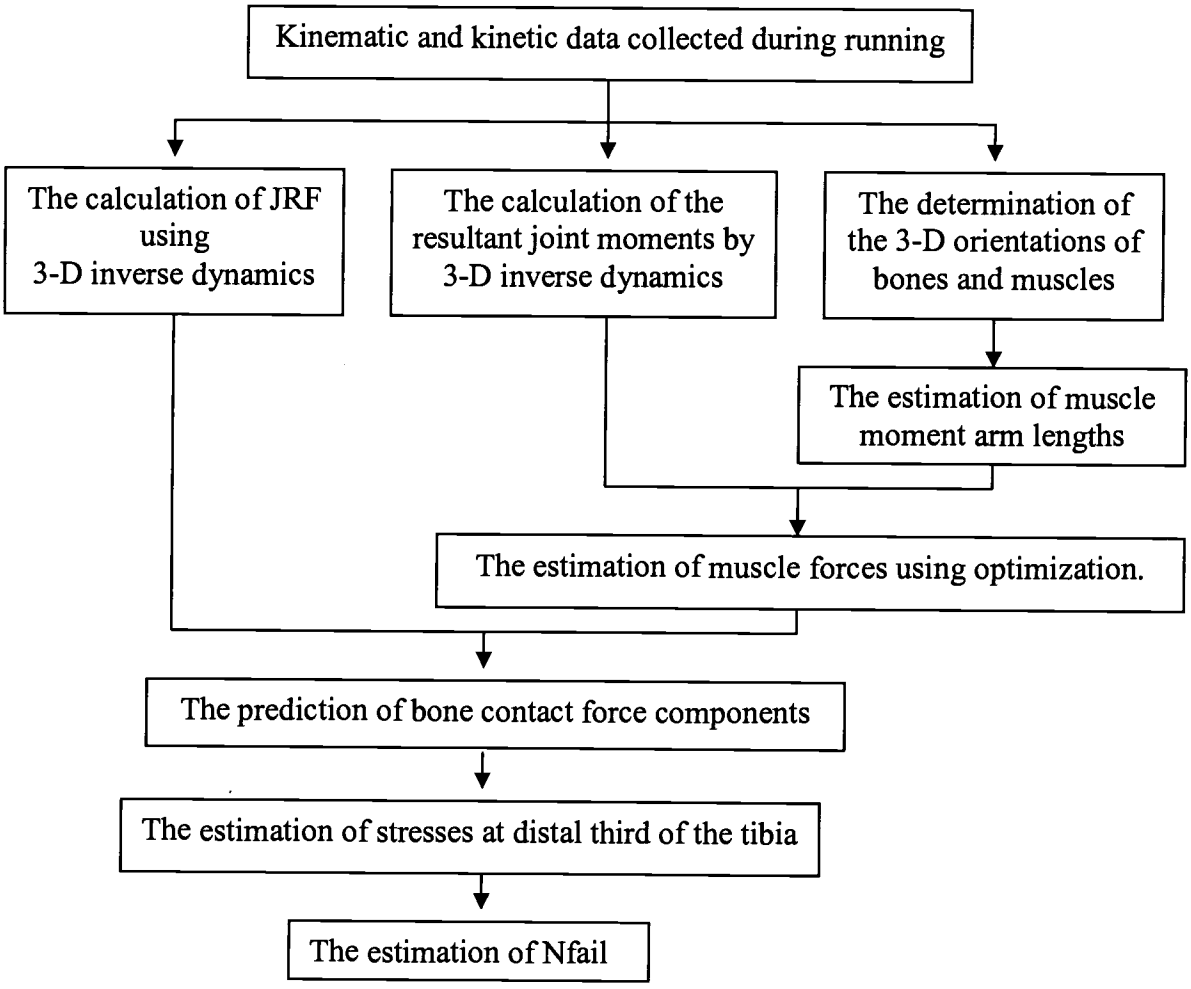

Figure 1. Schematic of the Nfail calculation method.

The muscle force calculation. 2-D muscle forces were estimated from the static optimization method. The minimized sum of cubed muscle stresses has been chosen to serve as the objective function instead of the minimized metabolic energy expenditure, even though there is evidence that more skilled runners used less metabolic energy cost (Williams, 1990). The later criterion requires more calculation time but results in similar predicted muscle forces (Anderson and Pandy, 2001), and is therefore not preferable. The criterion used in this study has been shown to predict muscle activation patterns similar to those recorded from electromyography (Prilutsky and Zatsiorsky, 2002). Moreover, it predicts the synergist and co-activation of the

muscles. To restrict predicted muscle forces to within physiologically realistic bounds, the objective function was subjected to equality and inequality constraints (Collin, 1995). The equality constraints were the muscle-moment equations, which were constructed from muscle moment arm lengths and the resultant joint moments calculated from the inverse dynamic method. In addition, the physiological upper and the lower bounds of muscle forces were applied as inequality constraints.

The estimation of bone contact force. Bone contact force components were composed of compressive and anterior-posterior shear forces. They were estimated from muscle forces and JRF.

The estimation of stresses and Nfail at the distal third of the tibia. Bending moment at the distal third of the tibia was calculated from a shear force-bending moment diagram. Axial compressive force and bending moment were then applied to a simple beam model of the tibia to estimate stresses in the anterior and posterior faces of the tibia. Finally, Nfail was predicted by fitting the estimated stresses at each time instant of the stance phase to published regression equations (Caler and Carter, 1989).

To observe the effect of muscle fatigue, the 3-D kinematic and kinetic data of running trials were re-collected after muscle fatigued from prolonged running. The same mathematical methods as previously described were used for estimating stresses and Nfail. By comparing stresses and Nfail before and after muscle fatigue, an association between muscle fatigue and the possibility of stress fractures could be investigated.

1.2 The dissertation overview.

The next two chapters are intended as stand-alone papers, thus some of the literature reviews from this chapter are repeated in them. Chapter 2 reports the magnitudes of bone contact force components found on the articulating surfaces of the tibia at each time instant the stance phase of running. Since they are calculated from muscle forces, the optimization method used for the prediction of muscle forces is

described in more detail. Chapter 3 describes the stress and Nfail found in the distal third of the tibia. Their changes after muscle fatigue are also reported in this chapter. The final chapter is the summary of the results. The review of the literature, that is not included in this chapter, is in the appendix A. Appendix B explains the calculation method in more detail while appendix C shows the orientations of muscles relative to the rigid segments of the leg. An informed consent form is in the appendix D.

REFERENCES

Amirouche, F.M.L. (1992). *Computational methods in multibody dynamics.* (pp.16-22). Prentice-Hall, Englewood Cliffs, New Jersey.

Anderson, F.C., & Pandy, M.G. (2001). Static and dynamic optimization solutions for gait are practically equivalent. *Journal of Biomechanics*, **34**, 153-161.

Beck, B.R. (1998). Tibial stress injuries: an aetiological review for the purposes of guiding management. *Injury Clinic*, **26**, 265-279.

Bennell, K.L., Malcolm, S.A., Thomas, S.A., Wark, J.D., & Brukner, P.D. (1996). The incidence and distribution of stress fractures in competitive track and field athletes: a twelve-month prospective study. *The American Journal of Sports Medicine*, **24**, 211-217.

Bennell, K.L., & Brukner, P.D. (1997). Epidemiology and site specificity of stress fractures. *Clinics in Sports Medicine*, **16**, 179-196.

Brukner, P., Bradshaw, C., Khan, K.M., White, S., & Crossley, K. (1996). Stress fractures: a review of 180 cases. *Clinical Journal of Sport Medicine*, **6**, 85-9.

Brukner, P., Bradshaw, C., & Bennell, K. (1998). Managing common stress fractures: let risk level guide treatment. *The Physician and Sport Medicine*, **26**, 39-47.

Burdett, R.G. (1982). Forces predicted at the ankle during running. *Medicine and Science in Sports and Exercise.* **14**, 308-316.

Burr, D.B., Milgrom, C., Fyhrie, D., Forwood, M.R., Nyska, M., Finestone, A., Hoshaw, S., Saiag, E., & Simkin, A. (1996). In-vivo Measurement of human tibia strains during vigorous activity. *Bone*, **18**, 405-410.

Caler, W.E., & Carter, D.R. (1989). Bone creep-fatigue damage accumulation. *Journal of Biomechanics*, **22**, 625-35.

Carter, D.R., & Caler, W.E. (1983). Cycle-dependent and time-dependent bone fracture with repeated loading. *Journal of Biomechanical Engineering*, **105**, 166-170.

Carter, D.R., & Caler, W.E. (1985). A cumulative damage model for bone fracture. *Journal of Orthopaedic Research*, **3**, 84-90.

Carter, D.R., Caler, W.E., Spengler, D.M., & Frankel, V.H. (1981). Fatigue behavior of adult cortical bone. The influences of mean strain and strain range. *Acta Orthopaedica Scandinavica*, **52**, 481-490.

Cavanagh, P.R., & Kram, R. (1990). Stride length in distance running: velocity, body dimensions, and added mass effects. In P.R. Cavanagh (Ed.), Biomechanics of distance running. Human Kinetics Books, Champaign, Illinois, pp.35-60.

Collins, J.J. (1995). The redundant nature of locomotor optimization laws. *Journal of Biomechanics*, **28**, 251-267.

Delp, S.L. (1990). Surgery simulation: a computer graphics system to analyze and design musculoskeletal reconstructions of the lower limb. Dissertation, Stanford University, California.

Ekenman, I., Halvorsen, K., Westblad, P., Fellander-Tsai, L., & Rolf, C. (1998). Local bone deformation at two predominant sites for stress fractures of the tibia: an in vivo study. *Foot and Ankle International*, **19**, 479-484.

Federicson, M., Bergman, G., Hoffman, K.L., & Dillingham, D.S. (1995). Tibial stress reaction in runners: correlation of clinical symptoms and scintigraphy with a new magnetic resonance imaging grading system. *American Journal of Sports Medicine*, **23**, 472-81.

Fyhrie, D.P., Milgrom, C., Hoshaw, S.J., Simkin, A., Dar, S., Drumb, D., & Burr, D.B. (1998). Effect of fatiguing exercise on longitudinal bone strain as related to stress fracture in humans. *Annals of Biomedical Engineering*, **26**, 660-5.

Hawkins, D. (1992). Software for determining lower extremity muscle-tendon kinematics and moment arm lengths during flexion/extension movements. *Computer Biological Medicine,* **22**, 59-71.

Hulkko, A., & Orava, S. (1987). Stress fractures in athletes. *International Journal of Sports Medicine*, **8**, 221-6.

Kepple, T.M., Arnold, A.S., Stanhope, S.J., & Siegel, K.L. (1994). Assessment of a method to estimate muscle attachments from surface landmarks: a 3D computer graphics approach. *Journal of Biomechanics*, **27**, 365-371.

Korpelainen, R., Orava, S., Karpakka, J., Siira, P., & Hulkko, A. (2001). Risk factors for recurrent stress fractures in athletes. *The American Journal of Sports Medicine*, **29**, 304-10.

Little, R.B., Wevers, H.W., Siu, D., & Cooke, T.D.V. (1986). A three-dimensional finite element analysis of the upper tibia. *Journal of Biomechanical Engineering*, **108**, 111-119.

Martin, R.B. (2000). Toward a unifying theory of bone remodeling. *Bone*, **26**, 1-6.

Mehta, B.V., Rajani, S., & Griffith, R. (1999). Finite element analysis of the tibia [On-line]. Available: http://www.ent.ohiou.edu/~mehta/BIOMED/tibia_fea.htm

Milgrom, C., Finestone, A., Levi, Y., Simkin, A., Ekenman, I., Mendeloson, S., Millgram, M., Nyska, M., BenJuya, N., & Burr, D. (2000a). Do high impact exercises produce higher tibial strains than running? *British Journal of Sports Medicine*, **34**, 195-199.

Milgrom, C., Finstone, A., Simkin, A., Ekenman, I., Mendelson, S., Millgram, M., Nyska, M., & Larsson, E.B. (2000b). In-vivo strain measurements to evaluate the strengthening potential of exercises on the tibial bone. *Journal of Bone and Joint Surgery*, **82**, 591-4.

Milgrom, C., Finstone, A., Sharkey, N., Hamel, A., Mandes, V., Burr, D., Arndt, A., & Ekenman, I. (2002). Metatarsal strains are sufficient to cause fatigue fracture during cyclic overloading. *Foot and Ankle International*, **23**, 230-235.

Milgrom, C., Finestone, A., Segev, S., Olin, C., Arndt, T., & Ekenman, I. (2003) Are overground or treadmill runners more likely to sustain tibial stress fracture? *British Journal of Sports Medicine*, **37**, 160-163.

Petermann, M.M., Hamel, A.J., Cavanagh, P.R., Piazza, S.J., & Sharkey, N.A. (2001). In vitro modeling of human tibial strains during exercise in micro-gravity. *Journal of Biomechanics*, **34**, 693-8.

Prilutsky, B.I., & Zatsiorsky, V.M. (2002). Optimization-based models of muscle coordination. *Exercise and Sport Science Reviews*, **30**, 32-38.

Schaffler, M.B., Radin, E.L., & Burr, D.B. (1990). Long-Term fatigue behavior of compact bone at low strain magnitude and rate. *Bone,* **11**, 321-6.

Scott, S.H., & Winter, D.A. (1990). Internal force of chronic running injury sites. *Medicine and Science in Sports and Exercise*, **22**, 357-69.

Sonada, N., Chosa, E., Totoribi, K., & Tajima, N. (2003). Biomechanical analysis for stress fractures of the anterior middle third of the tibia in athletes: nonlinear analysis using a three-dimensional finite element method. *Journal of Orthopaedic Science*, **8**, 505-513.

Spitz, D.J., & Newberg, A.H. (2002). Imaging of stress fractures in the athlete. *Radiologic Clinics of North America,* **40**, 313-331.

Williams, R.K. (1990). Relationships between distance running biomechanics and running economy. In P.R. Cavanagh (Ed.), Biomechanics of distance running. Human Kinetics Books, Champaign, Illinois, pp.271-305.

Winter, D.A. (1990). Biomechanics and motor control of human movement (2nd Ed.). A Wiley-Interscience Publication, New York, pp. 78-79.

Yoshikawa, T., Mori, S., Santiesteban, A.J., Sun, T.C., Hafstad, E., Chen, J., & Burr D.B. (1994). The effects of muscle fatigue on bone strain. *Journal of Experimental Biology*, **188**, 217-233.

Chapter 2

The Estimated Muscle and Bone Contact Forces from the Normal Running Trials

Siriporn Sasimontonkul and Brian K. Bay

Department of Exercise and Sports Science
Oregon State University, Corvallis, Oregon

Abstract

This study aimed to estimate bone contact forces applied directly to the distal end of the tibia during the stance phase of running. This estimation helps in the understanding of how tibial stress fractures occur in runners. An integrated experimental and mathematical modeling approach was used in this study. Ten volunteer recreational male runners were evaluated with a coupled force plate and 3 dimensional (3-D) motion analysis system while running in the speed range of 3.5-4 m/s. Using the collected data, 3-D joint reaction forces (JRF) and joint moments were calculated. Since both JRF and muscle forces contributed to bone contact forces, muscle forces were also estimated. Muscle forces were estimated by optimization using a 2-dimensional model of the lower limb composed of 4 link segments with 21 attached muscles. Sum of cubed muscle stresses was the objective function, with physiological constraints of experimental joint moments, muscle moment arm lengths, and lower and upper boundaries of muscle forces. This study found that the distal end of the tibia was compressed during the entire stance. A peak compressive force of 8.91 $\pm$ 1.14 BW was found during mid stance. Both vertical muscle force and tibial JRF contributed to the compressive force. The peak vertical muscle force and tibial JRF occurred during mid stance and were equal to -7.10 $\pm$ 0.96 BW and 1.95 $\pm$ 0.2 BW, respectively. The tibia was also sheared by a posterior shear force during most of stance. The peak posterior shear force of -0.53 $\pm$ 0.16 BW occurred at mid stance. The horizontal tibial JRF caused this peak posterior shear force while the horizontal muscle force reduced it. Since both compressive and shear forces peak at mid stance, superimposing these forces on the tibia may result in its injury.

Introduction

Tibial stress fractures are common among runners (Hulkko and Ovara, 1987; Johnson et al., 1994; Bennell et al., 1996; Bennell and Brukner, 1997; Spitz and Newberg, 2002). Experiments have also shown that cyclic loading can induce micro-damage in bone tissue (Mori and Burr, 1993; Burr et al., 1997; Schaffler and Jepsen, 2000). Therefore, several *in vivo* experiments were performed to record tibial deformations resulting from an application of running loads to the tibia in order to determine whether or not running loads occurring at the stance phase of running were large enough to damage bone (Milgrom et al., 2000 a & b; Milgrom et al., 2002; Burr et al., 1996; Milgrom et al., 2003; Ekenman et al., 1998). However, these previous experiments failed to record peak tibial deformations. As a result, the cause and effect relationship between running loads and tibial stress fractures are unknown.

Unlike direct measurement of tibial deformations in live humans, peak tibial deformations can be determined by applying estimated bone contact forces calculated from experimental running data to a tibial model. Additionally, maximum stress on the tibia can also be predicted by using the estimated bone contact forces. These bone contact forces are forces applied directly across the articulating surfaces of the tibia. An estimation of bone contact forces shows how the tibia is loaded in the stance phase of running. However, no study has estimated the bone contact forces on the distal end of the tibia although previous studies have estimated bone contact forces on the leg (Burdett, 1982; Scott and Winter, 1990). In one of these studies Scott and Winter (1990) reported that the foot pressed on the leg with a peak compressive force of 10.3 – 14.1 times body weight (BW) while in another study Burdett (1982) reported peak compressive forces of 8-13 BW. Both studies also reported that the foot sheared on the leg posteriorly but the magnitudes of the reported peak shear forces were substantially different. Scott and Winter (1990) reported a posterior shear force of 0.4 - 0.7 BW, in contrast to the range of 3.3 - 5.5 BW reported by Burdett and team (1982).

Besides a discrepancy in the magnitudes of reported bone contact forces, the accuracy of the reported values is questioned for several reasons. First, bone contact forces are the results of both ground reaction forces and muscle activities; however, these previous studies did not account for all active muscles when solving their equations. This may induce an error and ignore the mechanical actions of individual muscles (Dul et al., 1984). Moreover, bi-articular muscle action and co-activation of muscles are also ignored by the previous studies (Collins, 1995). In contrast to the previous studies, Nilsson and team (1985) showed that muscle co-contraction occurred during the stance phase of running, such as the co-contraction of the gastrocnemius and knee extensors. Second, muscle forces used for the estimation of bone contact forces were calculated from muscle moment arm lengths of grouped muscles instead of those of individual muscles. In addition, previous studies assumed a constant muscle moment arm length during the entire stance phase. In contrast, moment arm lengths of individual muscles actually vary according to the joint angle (Spoor et al., 1990; Rugg et al., 1990; Fukunaka et al., 1996; Maganaris, 2000). Consequently, the previously predicted muscle forces and bone contact forces were inaccurate. Finally, an inaccuracy in muscle paths leads to error in the estimated bone contact forces. Kepple and team (1994) found that the muscle path used in a study of Scott and Winter (1990) passed through bone, which was an unrealistic condition.

Using another technique, optimization, Glitsch and Baumann (1997) estimated the load sustained by the foot of forefoot runners. The optimization could predict synergistic and co-activation of muscles, which resulted in an approximation of bone contact forces at the ankle between 10 and 12.5 BW. However, the accuracy of their predicted muscle forces and bone contact forces, as in the previous studies (Burdett, 1982; Scott and Winter, 1990), was questioned. Delp and team (1990) found that muscle attachment points used in this previous study resulted in muscle paths that passed through bones or deeper muscles.

Unlike the previous studies, this study aimed to estimate the bone contact forces applied directly to the tibia at the ankle during the stance phase of running. This

study was performed because the tibia is a common site of stress fractures in runners. The estimated bone contact forces accounted for forces born by the fibula (Lambert, 1971; Calhoun et al., 1994; Funk et al., 2003). Muscle forces contributing to bone contact forces were estimated by optimization because it could predict individual muscle forces, synergist activation, and co-activation of muscles (Binding et al., 2000; Prilutsky and Zatsiorsky, 2002). Joint moments and muscle moment arm lengths at each time instant of the stance phase were used for predicting muscle forces. In addition, muscle paths were estimated from either muscle origins and insertions or wrapping points according to the segmental position (Delp, 1990; Delp et al., 1990).

Methods

Subject. Ten recreational male runners volunteered to participate in this study. They were 23 $\pm$ 2.7 years old. Their height and mass were 175.9 $\pm$ 8.4 cm and 71.5 $\pm$ 6.9 kg, respectively. They were heel strikers with average running mileages per week of 32.05 $\pm$ 9.9 miles. They were injury free and had no abnormal running patterns. Approval was obtained from the university institutional review board for the protection of human subjects and all volunteers signed an informed consent form (see appendix D) before participating in this study.

The determination of running kinetics and kinematics. Reflective markers were taped to the runners' skin at the left anterior superior iliac spine (ASIS), right ASIS, left posterior superior iliac spine (PSIS), right PSIS, left thigh, left femoral epicondyle, left shank, left lateral malleolus, left heel, and the base of the left second toe. They ran 6 successful trials, of approximately 10 meters each, across a force plate at a speed of 3.5 - 4 m/s. This distance was long enough to reach steady-state running. In addition, this speed was chosen because it was a running pace that many recreational runners use (Cavanagh and Kram, 1990). A pair of timing lights (model 63501-IR, Lafayette Instrument Company, Indiana, USA) measured running speed. If the target running speed range was met and the entire left foot hit on the force plate, it was considered a

successful trial. The force plate (Bertec, model 4060-08, Bertec Corporation, Columbus Ohio, USA) collected ground reaction force (GRF) signals at a frequency of 1080 Hz; simultaneously, six cameras captured spatial orientations of the reflective markers at a frequency of 120 Hz. Using the Vicon Motion System (Lake Forest California, USA), signals from six cameras and the force plate were synchronized. The spatial coordinates of the markers were filtered using Woltring's general cross-validatory quintic spline algorithm with a mean square error (MSE) of 7 mm. Plug-In Gait of Vicon Motion Systems then calculated 3-D joint reaction forces (JRF) and joint moments at 120 Hz using Euler's equations (Hibbeler, 1997) and the inverse dynamics method.

Mathematical calculations. Data from experimental running trials were used for estimating bone contact forces using mathematical calculations as presented in Figure 2.1.

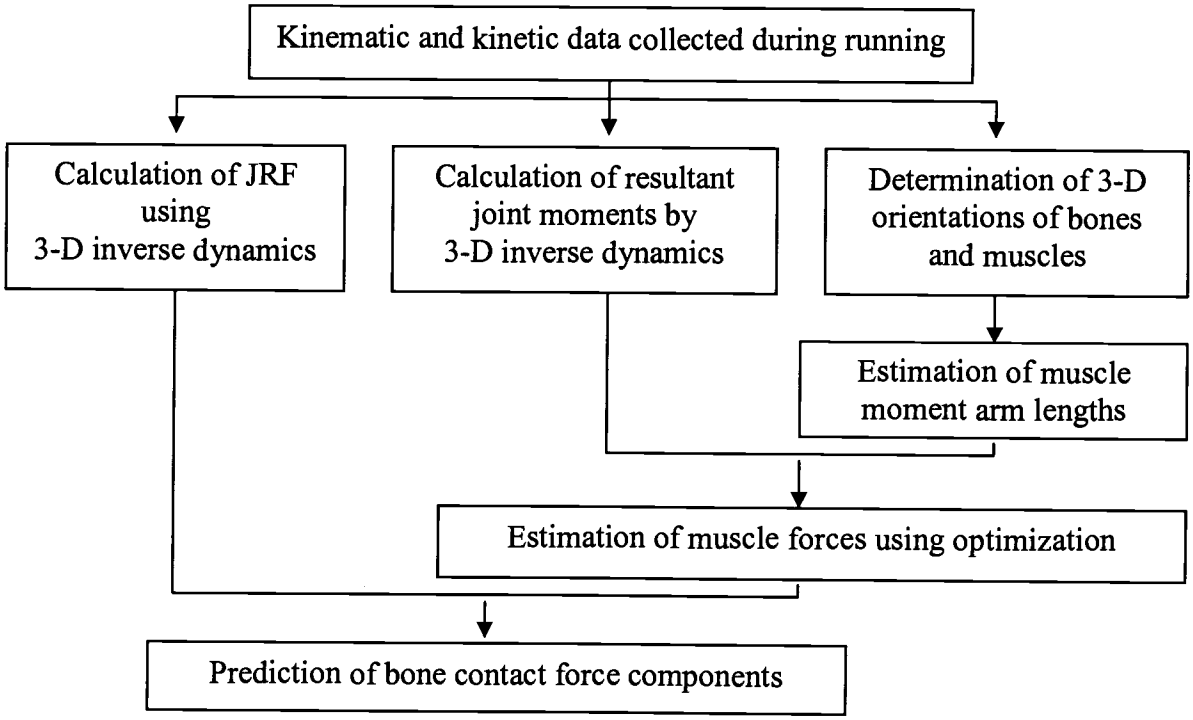

Figure 2.1 Procedures for estimating bone contact forces.

Determination of muscle origin and insertion and muscle moment arm lengths. Using the spatial positions of the reflective markers collected from the running trials, the left lower limb was modeled as a 3-dimensional, four rigid-body, segmented model composed of (1) pelvis, (2) femur, (3) tibia, and (4) foot (Figure 2.2). In total, 21 muscles were attached to the model. Origin and insertion coordinates of individual muscles in segmental reference frames were derived from Delp (1990) and scaled to suite individual volunteer runners (Brand et al., 1982; Kepple et al., 1994). To estimate muscle moment arm lengths at each time instant of the stance phase using the method of Hawkins (1992), origin and insertion coordinates in the segmental reference frames were transformed to the global reference frame (Amirouche, 1992; Kepple et al., 1994).

Prediction of muscle forces. Muscle forces were predicted using an optimization method. The optimization criterion used was the minimized sum of the cubed muscle stresses. A mathematical equation for this criterion, or objective function, is shown in equation (1).

$$\text{Minimize} \qquad \sum_{i=1}^{j} (f_i(t)/PCSA_i)^3 \qquad (1)$$

i is the number of muscle force. j is the 21 muscles. f_i is unknown tensile force developed in the i^{th} muscle at each time instant of the stance phase. $PCSA_i$ is the physiological cross-sectional area of the i^{th} muscle and is averaged across a reported PCSA of a male cadaver and a reported PCSA from Pierrynowski's study, as reported by Brand and team (1986).

Two further assumptions were made: 1) joint reaction force (JRF) and bone contact forces are applied at the center of contact point between each segment, and 2) no action of ligaments occurs around joints. Thus, resultant moments at each joint, calculated from the inverse dynamics, were the result of active muscles crossing an involved joint and could be written in mathematical equations as the following:

$$M_a(t) = \sum_{i=1}^{j} d_{ai}(t) * f_{ai}(t) \qquad (2)$$

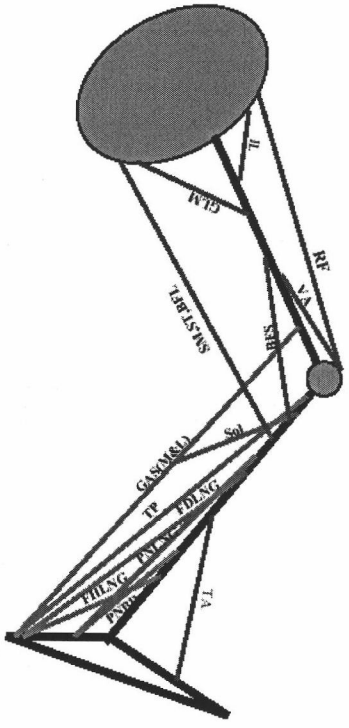

Abbreviations	Muscle	Abbreviations	Muscle
GASM	medial gastrocnemius	BFS	biceps femoris short head
GASL	lateral gastrocnemius	BFL	biceps femoris long head
FDLNG	flexor digitorum longus	ST	semitendinosus
PNBR	peroneus brevis	SM	semimembranosus
Sol	soleus	RF	rectus femoris
TP	tibialis posterior.	VA	Vastii is composed of vastus mediallis (VAM), vastus intermedius (VAI), and vastus laterallis (VAL).
FHLNG	flexor hallucis longus	GLM	Gluteus maximus is composed of superior, middle and inferior components.
PNLNG	peroneus longus	IL	iliacus
TA	tibialis anterior		

Figure 2.2 A 2-dimensional optimization model of the lower limb with 21 attached muscles.

$$M_k(t) = \sum_{i=1}^{j} d_{ki}(t) * f_{ki}(t) \quad (3)$$

$$M_h(t) = \sum_{i=1}^{j} d_{hi}(t) * f_{hi}(t) \quad (4)$$

M_a, M_k, and M_h are resultant moments at the ankle, knee and hip joints, respectively. The resultant moments came from experimental data at each time instant of the stance phase and are positive when acting counterclockwise. $d_i(t)$ is the moment arm length of the i^{th} muscle at each time instant of the stance phase and is positive when it results in counterclockwise moments. f_i is the force of the i^{th} muscle at each time instant of the stance phase that produces the resultant moment at a certain joint.

Equation (2), (3), and (4) were equality constraints that the objective function was subjected to. In addition, the objective function was also subjected to an inequality physiological constraint (Equation 5).

$$0 \leq f_1, f_2, f_3, f_4, \ldots, f_j \leq \text{maximum muscle force} \quad (5)$$

The maximum muscle force of the i^{th} muscle was estimated from $\sigma * PCSA_i$. σ was maximum muscle stress and assumed to be equal for all muscles. The reported value of σ was in a range of 30-150 N/cm^2 (Dul et al., 1984). $PCSA_i$ is the physiological cross-sectional area of the i^{th} muscle. The routine *fmincon* from the optimization toolbox of MATLAB (The Math Works Inc, version 6.1, Natick MA, USA) solved this optimization problem at each time instant of the stance phase. Solutions were 2-D muscle forces.

Calculation of bone contact force components relative to the tibia. Bone contact force components are composed of compressive and shear forces and were calculated from equation (6). The sums of muscle forces are separate summations of the vertical and horizontal components of the plantarflexor and dorsiflexor forces. Lines of action of individual plantarflexors and dorsiflexors were determined as vectors according to the position of the body. They were drawn either from muscle

insertion to muscle origin or from wrapping points at the most proximal end of the foot to the most distal end of the tibia.

Bone contact forces = AJRF – sum of muscle forces (6)

AJRF are the vertical and horizontal ankle JRF on the foot segment and were determined experimentally from running trials. These bone contact forces were the vertical and horizontal forces applied to the foot segment. The bone contact forces applied to the tibia had the same magnitudes but opposite directions. Approximately ten percent of bone contact forces are borne by the fibula (Lambert, 1971; Calhoun et al., 1994; Funk et al., 2003). Therefore, 90 % of bone contact forces were reported in this study and represented the forces being applied to the tibia. Next, these bone contact forces, JRF, and sum of muscle forces were transformed from the global reference frame to the tibial reference frame.

Statistical analysis: Stance times were normalized to be a percentage of the total stance time for each subject. All forces were normalized by subject body weight (BW). Kinetics, kinematics, and bone contact forces were interpolated every 0.2% stance across the stance phase using a piecewise cubic hermite interpolating polynomial. The kinetics, kinematics, and bone contact forces were then averaged across 6 trials within individual runners to represent their data. Next, group means and standard deviations of kinetics, kinematics, and bone contact forces were calculated across runners using MATLAB (Matlab® 6.1). The association between means of the kinetics, and bone contact forces was investigated using Pearson product moment correlation (SPSS 10.0 for Windows).

Results

Ankle angle. The ankle was in dorsiflexion during the first 85 % of the stance phase while plantarflexion occurred thereafter (Figure 2.3).

Ground reaction forces (GRF). GRF were reported in the global reference frame. The vertical GRF includes an impact peak and an active peak. The impact peak of the GRF is the first vertical force peak that occurs after the first ground contact. The

active peak of the GRF is the second vertical force peak of the vertical GRF. The impact and active peaks of the GRF were equal to 1.52 $\pm$ 0.24 and 2.56 $\pm$ 0.26 times body weight (BW), respectively (Figure 2.4 a). The braking peak, the peak of the backward GRF occurring at the heel impact, and the propulsive peak, the peak of the forward GRF occurring during push-off, were equal to -0.33 $\pm$ 0.06 BW and 0.35 $\pm$ 0.05 BW, respectively (Figure 2.4 b).

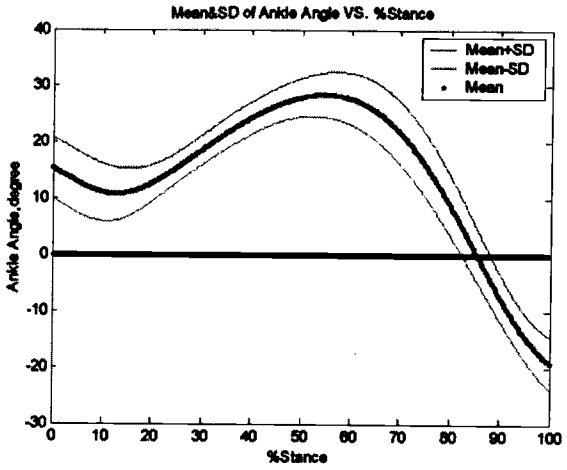

Figure 2.3 The group mean and SD of ankle angle. Positive and negative angles represent dorsiflexion and plantarflexion, respectively.

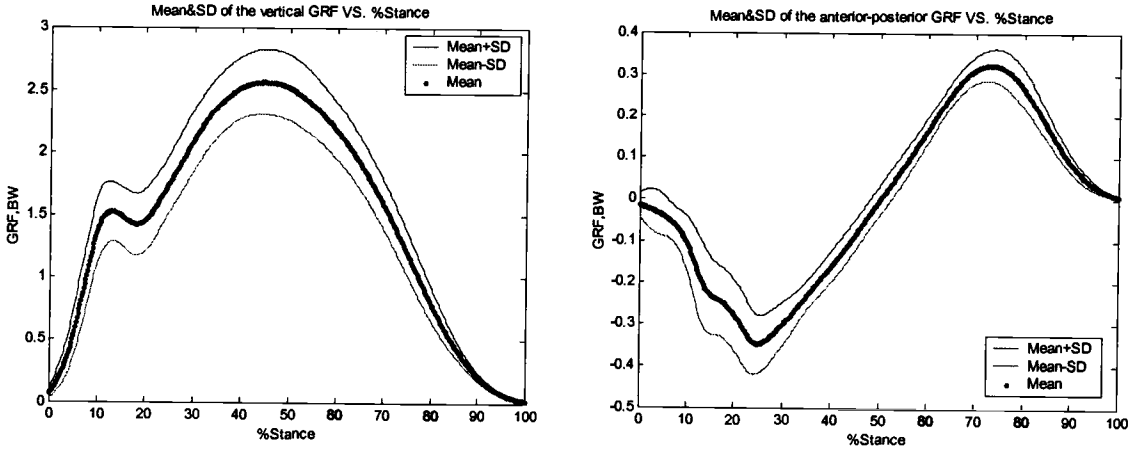

a) vertical GRF

b) horizontal GRF

Figure 2.4 The group mean and SD of GRF across stance phase. Positive forces represent the force being applied either in an upward direction or forward direction.

Tibial joint reaction forces (JRF). The vertical and horizontal tibial JRF were reported relative to the orientation of the tibial shaft in the sagittal plane. Two peaks of vertical tibial JRF were found at impact and at mid stance, and they were equal to 1.30 $\pm$ 0.2 and 1.95 $\pm$ 0.2 BW, respectively (Figure 2.5 a). The horizontal tibial JRF was applied anteriorly to the distal tibia during the first 10 % of the stance phase before being applied posteriorly (Figure 2.5 b). The peak posteriorly-directed tibial JRF occurred at mid stance and was equal to -1.22 $\pm$ 0.14 BW. The large horizontal tibial JRF in the tibial reference frame resulted from a transformation of JRF components found in the global coordinate system to the tibial coordinate system.

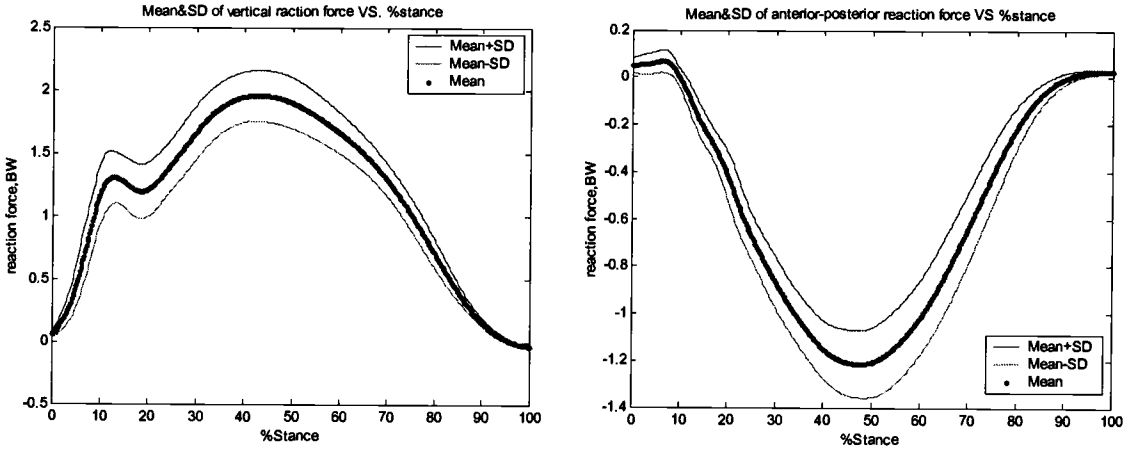

a) vertical tibial JRF

b) horizontal tibial JRF

Figure 2.5 The group mean and SD of the tibial JRF at the distal end of the tibia across the stance phase. Positive forces represent the force being applied either in an upward direction or forward direction.

Joint moments about the mediolateral axis. Patterns and magnitudes of moments about the mediolateral axis of all joints are presented in Figure 2.6. At the ankle joint, a dorsiflexion moment occurred from initial impact through 15 % of the stance phase followed by a plantarflexion moment occurring throughout the remainder of the stance phase (Figure 2.6 a). Peaks of dorsiflexion and plantarflexion moments were equal to -0.21 $\pm$ 0.72 and 2.96 $\pm$ 0.26 Nm/kg, respectively.

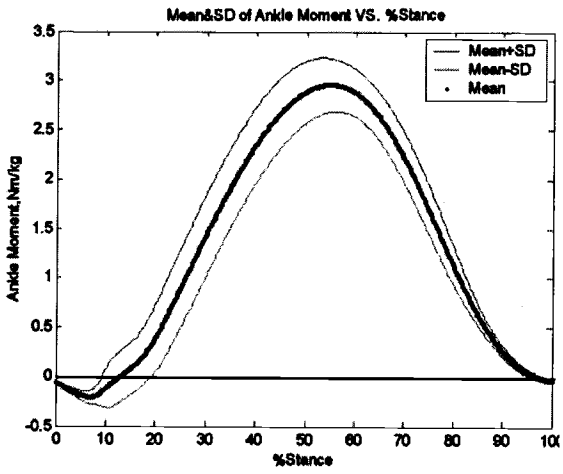

a) ankle joint moment

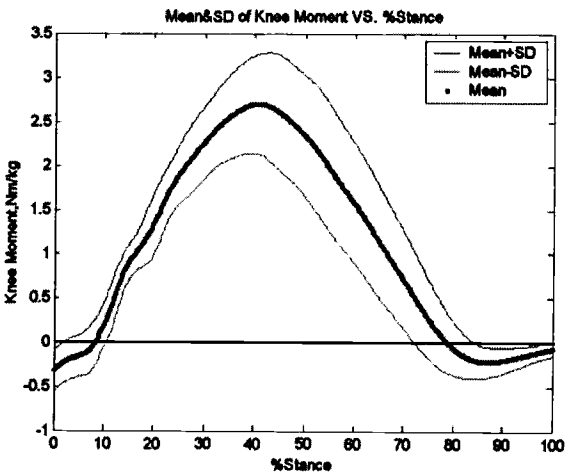

b) knee joint moment

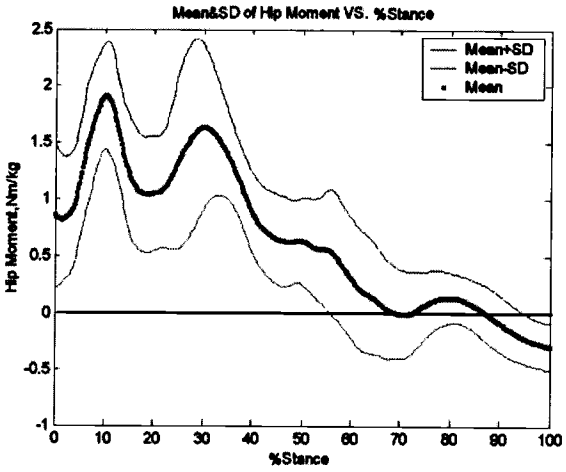

c) hip joint moment

Figure 2.6 The group mean and SD of resultant ankle, knee and hip moments about the mediolateral axis across the stance phase. Positive moments represent the extension moments.

At the knee joint, flexors caused a flexion moment through the first 10 % of the stance phase and then the extensors acted throughout the rest of the stance phase (Figure 2.6 b). Peaks of knee flexion and extension moments were equal to – 0.33 $\pm$ 0.24 and 2.70 $\pm$ 0.55 Nm/kg, respectively.

At the hip joint, a hip extension moment occurred during the first 85 % of the stance phase and then the flexors acted on the hip (Figure 2.6 c). Peaks of hip extension and flexion moments were equal to 1.91 $\pm$ 0.47 and –0.3 $\pm$ 0.21 Nm/kg, respectively.

Muscle Forces. Optimization was successfully able to solve for the muscle forces of all trials when the maximum muscle force was calculated using a maximum muscle stress of 80 N/cm^2. Though the effects of higher muscle stresses were studied, the optimizations resulted in the same magnitude of muscle forces. A muscle stress of 80 N/cm^2 was the minimal muscle stress that resulted in the successful optimization of all trials and was used in this study. The group means of predicted muscle forces across the stance phase are shown in Figure 2.7.

At the ankle joint. During the impact phase (0 % to 20 % of stance), tibialis anterior contracted, while soleus co-contracted with the tibialis anterior during the latter portion of the impact phase (Figure 2.7 a). From 20% to 90% of the stance phase, soleus, gastrocnemius medialis, and gastrocnemius lateralis were active. Other plantarflexors also contracted during this period (Figure 2.7 b), but their forces were smaller than those of soleus and gastrocnemius. During late stance (90 % to 100 %), soleus diminished its activity while gastrocnemius medialis, an agonist, co-contracted with tibialis anterior, an antagonist.

At the knee joint. A co-activation of the knee flexors semimembranosus and biceps femoris long head, and the knee extensors vastii was found during the period of knee flexion moment (Figure 2.7 c & d). In contrast, primarily the knee extensors were active during the period of knee extension moment and the largest forces were produced by, in descending order, vastus laterallis (VAL), vastus intermedius (VAI) and vastus mediallis (VAM), respectively.

At the hip joint. The hip extension moment resulted from an activity of semimembranosus and gluteus maximus (Figure 2.7 f). Semimembranosus produced a larger force during the first 40 % of the stance phase while gluteus maximus (GLMS, GLMI & GLMM) peaked between 30% and 40 % of the stance phase. Rectus femoris worked as an antagonist of the hip extensors during mid stance (Figure 2.7 e). During late stance, iliacus flexed the hip.

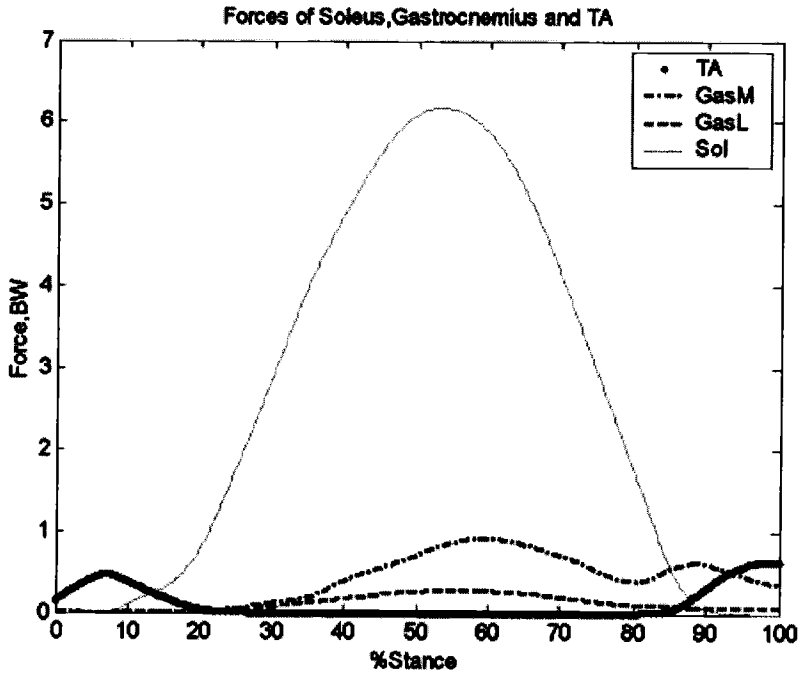

a) large plantarflexors & dorsiflexor

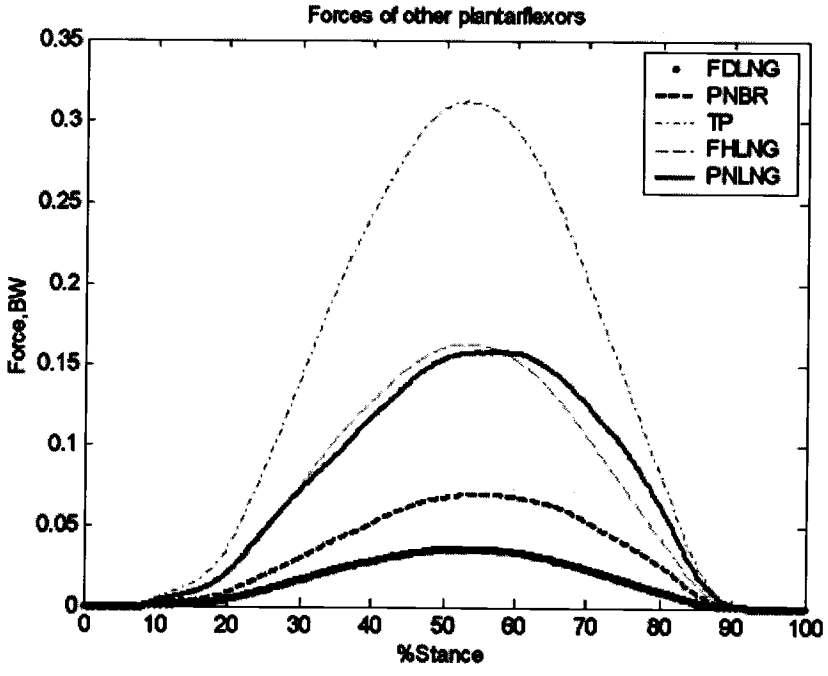

b) small plantarflexors

Figure 2.7 The group means of muscle forces from optimization.

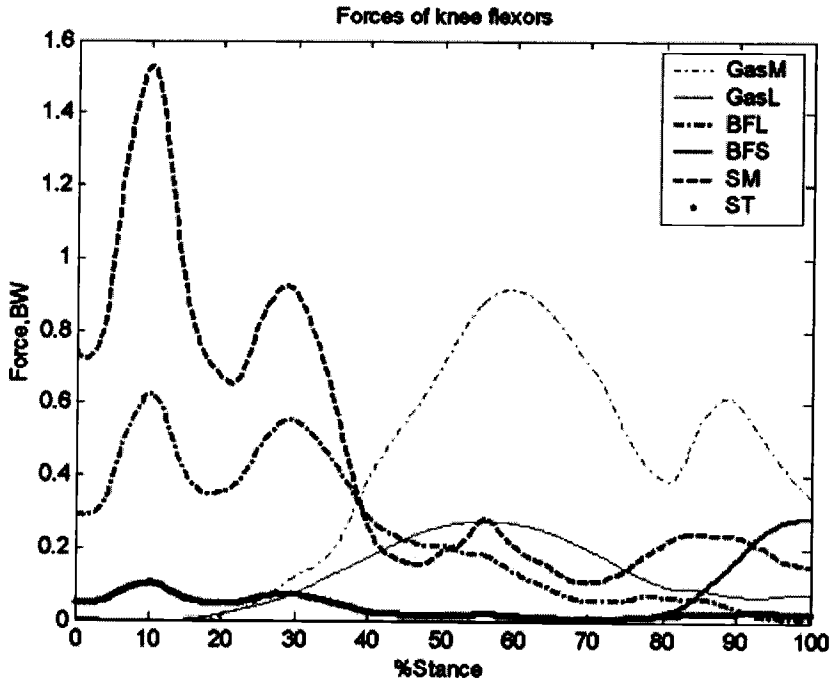

c) knee flexors

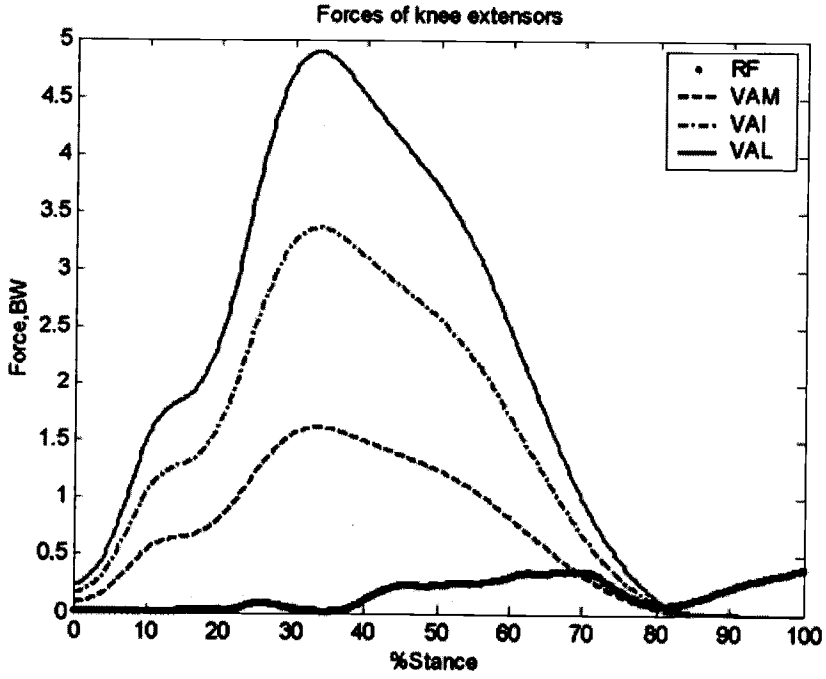

d) knee extensors

Figure 2.7. (Continued).

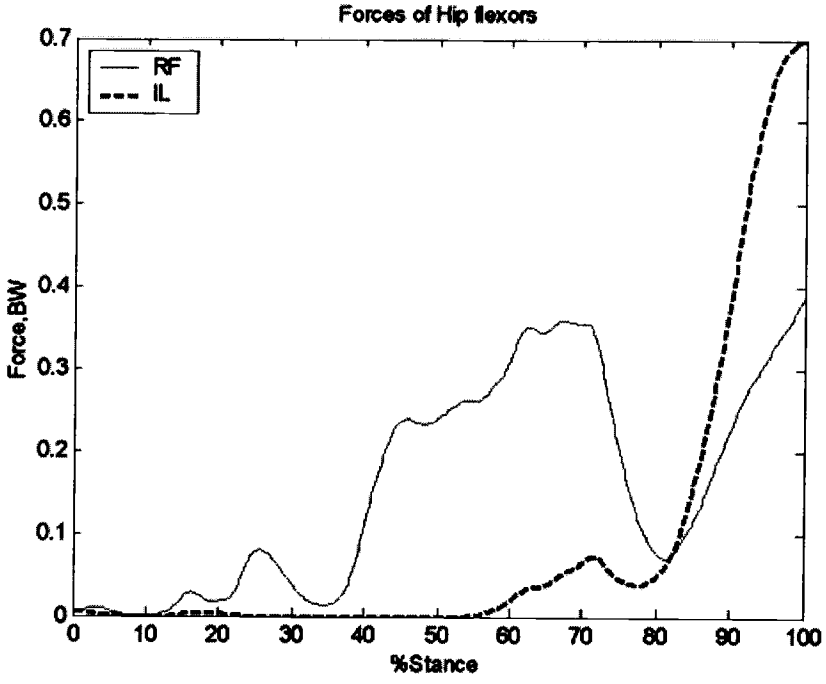

e) hip flexors

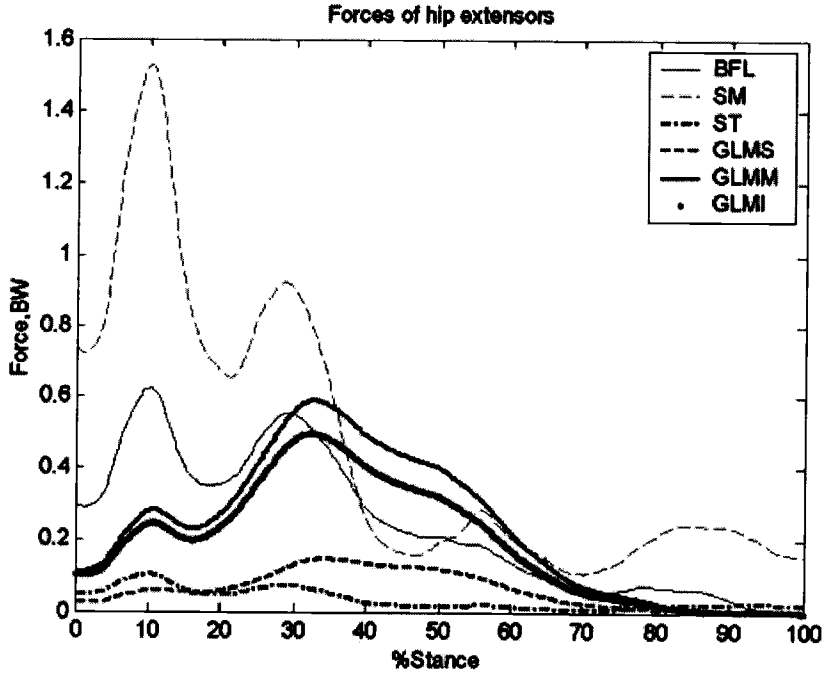

f) hip extensors

Figure 2.7. (Continued).

The vertical component of bone contact force. The distal end of the tibia was compressed during the entire stance. A peak compressive force of 8.91 $\pm$ 1.14 BW was found during mid stance. Figure 2.8(a) illustrates that the peak vertical muscle force caused a larger peak compressive force than the tibial JRF did. This peak vertical muscle force, equal to -7.10 $\pm$ 0.96 BW, contributed to a peak compressive force that was approximately 4.5 times the tibial JRF.

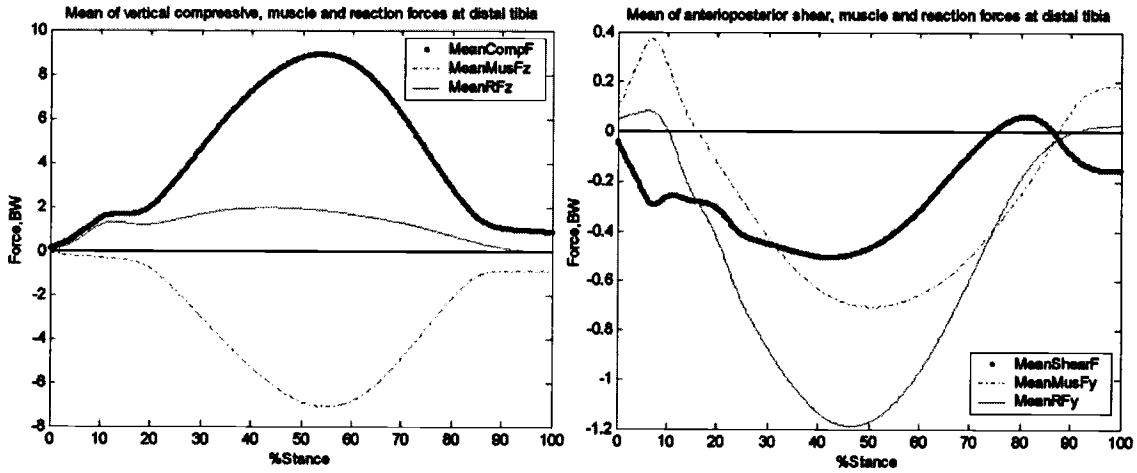

a) vertical forces

b) horizontal forces

Figure 2.8 The group means of bone contact, muscle, and the tibial joint reaction forces at the distal end of the tibia across the stance phase. Positive forces represent the force being applied either in an upward direction or forward direction.

z = vertical component
CompF= compressive force
MusF = muscle force

y = horizontal component.
ShearF = shear force
RF = the tibial joint reaction force.

The horizontal component of bone contact force. During the first 75 % of the stance phase, the distal end of the tibia was sheared posteriorly (Figure2.8 b). From 75 % to 90 % and from 90 % to the end of the stance phase, the tibia was sheared anteriorly and posteriorly, respectively. The muscle forces caused a larger shear than the tibial JRF did at the impact (between 0 % and 15 % of the stance) and during late stance (between 75 % and 90 % of stance), but the overall magnitude was small. In

contrast, between 15 % and 75 % of stance, the tibial JRF caused a large shear force while muscle force counteracted the tibial JRF to reduce shear force. The peak posterior shear force occurred a little bit before mid-stance and was equal to -0.53 $\pm$ 0.16 BW.

Association among forces. Associations among peaks of kinetics and bone contact forces are shown in Table 2.1. A large correlation coefficient was found between the active peak of the vertical GRF and the vertical muscle forces. The active peak of the vertical GRF also had a strong relationship with both the vertical and horizontal tibial JRF.

Table 2.1 Correlation coefficients among the maximum values of kinetics and bone contact forces (n=10).

	GRFz	GRFy	JRFz	JRFy	CompF	ShearF	MusFz	MusFy
GRFz	1.00							
GRFy	0.39	1.00						
JRFz	0.97**	0.30	1.00					
JRFy	0.83**	0.53	0.67*	1.00				
ComF	0.90**	0.62	0.89**	0.70*	1.00			
ShearF	0.62	0.31	0.59	0.58	0.45	1.00		
MusFz	0.84**	0.68*	0.85**	0.67*	0.99**	0.46	1.00	
MusFy	0.04	-0.14	-0.09	0.26	0.00	-0.56	-0.06	1.00

z = vertical component y = horizontal component
ComF =compressive force ShearF = shear force
MusF = muscle force
* = significant different from zero at p-value < 0.05 (2-tailed)
* * = significant different from zero at p-value < 0.01 (2-tailed)

Discussion

Ground reaction forces, moments, and muscle forces. The active peak of the GRF found in this study was in the range of those reported by Burdett (1982) and

Scott and his team (1990). Patterns and magnitudes of resultant moments about the mediolateral axis of all joints were also similar to those previously reported (Harrison et al., 1986; Buczek and Cavanagh, 1990; Scott and Winter, 1990; McCaw and De Vita, 1995; Farley and Ferris, 1998). Using the resultant moments as optimization constraints resulted in patterns of muscular activity similar to those provided by electromyography (Nilsson et al., 1985; Reber et al., 1993). Moreover, the model used in this study could predict co-activation and synergy of muscular activities as previously reported (Binding et al., 2000; Prilutsky and Zatsiorsky, 2002).

Bone contact forces. In this study, bone contact forces on the distal end of the tibia were not substantially different from those on the distal end of the leg as reported by previous studies (Burdett, 1982; Scott and Winter, 1990; Glitsch and Baumann, 1997). We found that the tibia sustained a large compressive force and a small posterior shear force during the stance phase of running. The peak compressive force sustained by the tibia in this study was similar to that sustained by the leg in Burdett's study (Burdett, 1982). In contrast, the peak posterior shear force on the tibia of this study was much smaller than that reported by Burdett yet still supported the same force found on the leg by Scott and Winter (1990). The peak compressive and shear forces on the tibia in this study resulted in the resultant bone contact force of 8.93 BW, which was smaller than that found by Glitsch and Baumann (1997).

We refined the results of the previous studies by calculating bone contact forces from muscle forces 1) that accounted for synergies and co-activation of muscles rather than assuming no co-contraction or ignoring some of the active muscles, as in previous studies (Burdett, 1982; Scott and Winter, 1990), 2) whose muscle paths wrapped over bone according to the segmental positions. In contrast, the muscle paths used in Scott and Winter (1990) and Glitsch and Baumann (1997) passed through bone in selected body positions (Kepple et al., 1994; Delp et al., 1990), 3) that were calculated from moment arm lengths that varied with joint angle at each time instant of the stance phase, and 4) that were calculated from joint moments about the mediolateral axis resulting from real 3-D analysis rather than 2-D analysis or unreal 3-

D analysis as in previous studies (Burdett, 1982; Scott and Winter, 1990). Moreover, the bone contact forces reported in this study were averaged both across trials of individual runners and across the group of these same runners rather than drawing results from either individual running trials or individual runners in previous studies (Burdett, 1982; Scott and Winter, 1990; Glitsch and Baumann, 1997).

A compressive force applied to the tibia at the centroid of tibia plafond should result in backward bending of the tibia. This is because the centroid at 15%-85% of the tibial length is located anteriorly to the line connecting the centroids of tibia plateau and tibia plafond, due to curvature of the tibia (Funk et al., 2003). Besides the compressive forces, a posterior shear force found at the distal end of the tibia also bends the tibia backward. As a result, compression should occur in the posterior face of the tibia. However, either tension or compression also occurs in the anterior face of the tibia depending on the magnitudes of the compressive and shear forces. Previous studies showed that both compressive and tensile strains were found in the anterior face (Ekenman et al., 1998; Peterman et al., 2001), whereas compressive strain developed in the posterior crest of the tibia (Peterman et al., 2001).

This study found that peak bone contact forces occurred at mid stance during dorxiflexion of the foot. Leardini and his team (1999) reported that the articular contact point is located in the anterior part of the tibial mortise during dorxiflexion. This may either reduce or increase the amount of backward bending of the tibia, depending on the location of this contact point relative to a centroid of the tibial midshaft. However, currently no study has reported the location of a contact point relative to the centroid of the tibia.

The vertical muscle force and horizontal tibial JRF are major factors that cause peak compressive and posterior shear forces at mid stance during running, respectively. Both vertical muscle force and horizontal tibial JRF had a strong relationship with the active peak of the vertical GRF (Table 2.1). Thus, the large active peak of vertical GRF found at mid stance may be a major source of tibia stress fractures. A reduction of this peak vertical GRF would be necessary to prevent tibial

injury. Moreover, a forward leaning of the shank at mid stance resulted in a large posterior tibial JRF relative to the tibial axis, which led to a more backward bending of the tibia. Hence, changes in running styles may also be necessary for some runners.

Limitation. More skilled runners have a lower metabolic energy cost than unskilled runners (Williams, 1990). However, a fatigue criterion, the minimized sum of cubed muscle stresses, was chosen as an objective function of the optimization for two reasons: 1) it maximizes endurance time, which is similar to minimizing metabolic energy expenditure, and 2) static optimization was used to solve the minimized sum of cubed muscle stresses and required a much shorter amount of time for calculation than dynamic optimization that solves for the minimized metabolic energy expenditure. The static and dynamic optimization methods have been found to result in similar muscle forces and bone contact forces (Anderson and Pandy, 2001). The greatest similarities in the results of these two criteria were found when the minimizing muscle stress was raised to the power of 2 as opposed to any other exponents. However, the minimizing muscle stress in this study was raised to the power of 3 because this exponent was the average exponent of the muscle endurance-force relationship (Crowninshield, 1983). In addition, the minimized sum of cubed muscle stresses provided patterns of muscular activities that were similar to those provided by electromyography (Prilutsky and Zatsiorsky, 2002). Nonetheless, a pilot calculation was performed in this study to compare the predicted muscle forces resulting from the minimized sum of squared muscle stresses and the minimized sum of cubed muscle stress. The predicted muscle forces resulting from both criteria were almost equal. This supported previous reports that patterns and predicted values of muscle forces were not sensitive to small changes in exponents of objective functions (Crowninshield, 1983; Glitsch and Baumann, 1997). Currently, it is unclear which criterion the body uses for controlling muscle activities. Thus, any conclusions drawn from comparing the results of mathematical models to those of the real world should be inferred with caution.

The accuracy of muscle force prediction is dependent on the accuracy of the physiological data used, such as PCSA, muscle stresses and moment arm lengths. Currently, those complete data reports from live humans are unavailable. This study used PCSA reported from cadavers, and a single data set was used for PCSA and origin and insertion locations, not individualized to each subject except by generalized scaling. Errors in muscle force prediction may occur if the PCSA reported from cadavers is different from that in live humans.

Conclusion. During the stance phase of running, the distal end of the tibia was compressed. It was also sheared both posteriorly or anteriorly. However, the amount of posterior shear force was larger than that of anterior shear force. Peak compressive and posterior shear forces occurred during mid stance. Both compressive and posterior shear forces may lead to tibial stress fractures. Vertical muscle force (i.e. along the tibia's longitudinal axis) is a major factor causing a large compressive force while horizontal tibial JRF is a major factor causing posterior shear force. The active peak of the GRF during mid stance is related to both vertical muscle force and horizontal tibial JRF. Thus, a reduction of this GRF's peak may help prevent tibial stress fractures.

REFERENCES

Amirouche, F.M.L. (1992). *Computational methods in multibody dynamics.* (pp.16-22). Prentice-Hall, Englewood Cliffs, New Jersey.

Anderson, F.C., & Pandy, M.G. (2001). Static and dynamic optimization solutions for gait are practically equivalent. *Journal of Biomechanics*, **34**, 153-161.

Bennell, K.L., Malcolm, S.A., Thomas, S.A., Wark, J.D., & Brukner, P.D. (1996). The incidence and distribution of stress fractures in competitive track and field athletes: a twelve-month prospective study. *The American Journal of Sports Medicine*, **24**, 211-217.

Bennell, K.L., & Brukner, P.D. (1997). Epidemiology and site specificity of stress fractures. *Clinics in Sports Medicine*, **16**, 179-196.

Binding, P., Jinha, A., & Herzog, W. (2000). Analytic analysis of the force sharing among synergistic muscles in one-and two-degree of freedom models. *Journal of Biomechanics*, **33**, 1423-1432.

Brand, R.A., Crowninshield, R.D., Wittstock, C.E., Pedersen, D.R., Clark, C.R., & Krieken, F.M.V. (1982). A model of lower extremity muscular anatomy. *Journal of Biomechanical Engineering*, **104**, 304-310.

Brand, R.A., Pederson, D.R., & Friederich, J.A. (1986). The sensitivity of muscle force predictions to changes in physiologic cross-sectional area. *The Journal of Biomechanics*, **19**, 589-596.

Buczek, F.L., & Cavanagh, P.R. (1990). Stance phase knee and ankle kinematics and kinetics during level and downhill running. *Medicine and Science in Sports and Exercise,* **22**, 669-667.

Burdett, R.G. (1982). Forces predicted at the ankle during running. *Medicine and Science in Sports and Exercise*, **14**, 308-316.

Burr, D.B., Forwood, M.R., Fyhrie, D.P., Martin, R.B., Schaffler, M.B., & Turner, C.H. (1997). Perspective: bone microdamage and skeletal fragility in osteoporotic and stress fractures. *Journal of Bone and Mineral Research*, **12**, 6-15.

Burr, D.B., Milgrom, C., Fyhrie, D., Forwood, M.R., Nyska, M., Finestone, A., Hoshaw, S., Saiag, E., & Simkin, A. (1996). In-vivo Measurement of human tibia strains during vigorous activity. *Bone*, **18**, 405-410.

Calhoun, J.H., Li, F., Ledbetter, B.R., & Viegas, S.F. (1994). A comprehensive study of pressure distribution in the ankle joint with inversion and eversion. *Foot & Ankle*, **15**, 125-133.

Cavanagh, P.R., & Kram, R. (1990). Stride length in distance running: velocity, body dimensions, and added mass effects. In P.R. Cavanagh (Ed.), Biomechanics of distance running. Human Kinetics Books, Champaign, Illinois, pp.35-60.

Collins, J.J. (1995). The redundant nature of locomotor optimization laws. *Journal of Biomechanics*, **28**, 251-267.

Crowninshield, R.D. (1983). A physiologically based criterion for muscle force predictions on locomotion. *Bulletin of the Hospital for Joint Diseases Orthopaedic Institute*, **XLIII**, 164-170.

Delp, S.L. (1990). Surgery simulation: a computer graphics system to analyze and design musculoskeletal reconstructions of the lower limb. Dissertation, Stanford University, California.

Delp, S.L., Loan, J.P., Hou, M.G., Zajac, F.E., Topp, E.L., & Rosen, J.M. (1990). An interactive graphics-based model of the lower extremity to study orthopaedic surgical procedures. *IEEE Transaction on Biomedical Engineering*, **37**, 757-767.

Dul, J., Johnson, G.E., Shiavi, R., & Townsend, M.A. (1984). Muscular synergism II: A minimum-fatigue criterion for load sharing between synergistic muscles. *Journal of Biomechanics*, **17**, 675-684.

Ekenman, I., Halvorsen, K., Westblad, P., Fellander-Tsai, L., & Rolf, C. (1998). Local bone deformation at two predominant sites for stress fractures of the tibia: an in vivo study. *Foot and Ankle International*, **19**, 479-484.

Farley, C.T., & Ferris, D.P. (1998). Biomechanics of walking and running: center of mass movements to muscle action. *Exercise and Sports Science Reviews*, **26**, 253-285.

Fukunaka, T., Roy, R.R., Shellock, F.G., Hodgson, J.A., & Edgerton, V.R. (1996). Specific tension of human plantar flexors and dorsiflexors. *The Journal of Applied Physiology*, **80**, 158-165.

Funk, J.R., Rudd, R.W., Kerrigan, J.R., & Candrall, J.R. (2003). Analysis of tibial curvature, fibular loading, and the tibia index [On-line]. Available: www.people.virginia.edu/~rwr4a/papers/ircobi2003.pdf

Glitsch, U., & Baumann, W. (1997). The three-dimensional determination of internal loads in the lower extremity. *Journal of Biomechanics*, **30**, 1123-1131.

Harrison, R.N., Lees, A., McCullagh, P.J.J., & Rowe, W.B. (1986). A bioengineering analysis of human muscle and joint forces in the lower limbs during running. *Journal of Sports Sciences*, **4**, 201-218.

Hawkins, D. (1992). Software for determining lower extremity muscle-tendon kinematics and moment arm lengths during flexion/extension movements. *Computer Biological Medicine,* **22**, 59-71.

Hibbeler, R.C. (1997). Engineering mechanics statics and dynamics (8^{th} Ed.). Prentice- Hall, Upper Saddle River, New Jersey.

Hulkko, A., & Orava, S. (1987). Stress fractures in athletes. *International Journal of Sports Medicine*, **8**, 221-6.

Johnson, A.W., Weiss, C.B., & Wheeler, D.L. (1994). Stress fractures of the femoral shaft in athletes more common than expected: A new clinical test. *The American Journal of Sports Medicine*, **22**, 248-256.

Kepple, T.M., Arnold, A.S., Stanhope, S.J., & Siegel, K.L. (1994). Assessment of a method to estimate muscle attachments from surface landmarks: a 3-D computer graphics approach. *Journal of Biomechanics*, **27**, 365-371.

Lambert, K.L. (1971). The weight bearing function of the fibula: a strain gauge study. *The Journal of Bone and Joint Surgery*, **53A**, 507-513.

Leardini, A., O'Connor, J.J., Catani, F., & Giannini, S. (1999). A geometric model of the human ankle joint. *Journal of Biomechanics*, **32**, 585-591.

Maganaris, C.N. (2000). In vivo measurement-based estimation of the moment arm in the human tibialis muscle-tendon unit. *Journal of Biomechanics*, **33**, 375-379

McCaw, S.T., & DeVita, P. (1995). Errors in alignment of center of pressure and foot coordinates affect predicted lower extremity torques. *Journal of Biomechanics*, **28**, 985-988.

Milgrom, C., Finestone, A., Levi, Y., Simkin, A., Ekenman, I., Mendelson, S., Millgram, M., Nyska, M., BenJuya, N., & Burr, D. (2000a). Do high impact exercises produce higher tibial strains than running? *British Journal of Sports Medicine*, **34**, 195-199.

Milgrom, C., Finstone, A., Simkin, A., Ekenman, I., Mendelson, S., Millgram, M., Nyska, M., & Larsson, E.B. (2000b). In-vivo strain measurements to evaluate the strengthening potential of exercises on the tibial bone. *Journal of Bone and Joint Surgery*, **82**, 591-4.

Milgrom, C., Finstone, A., Sharkey, N., Hamel, A., Mandes, V., Burr, D., Arndt, A., & Ekenman, I. (2002). Metatarsal strains are sufficient to cause fatigue fracture during cyclic overloading. *Foot and Ankle International*, **23**, 230-235.

Milgrom, C., Finestone, A., Segev, S., Olin, C., Arndt, T., & Ekenman, I. (2003) Are overground or treadmill runners more likely to sustain tibial stress fracture? *British Journal of Sports Medicine*, **37**, 160-163.

Mori, S., & Burr, D.B. (1993). Increased intracortical remodeling following fatigue damage. *Bone*, **14**, 103-109.

Nilsson, J., Thorstensson, A., & Halbertsma, J. (1985). Changes in leg movements and muscle activity with speed of locomotion and mode of progression in humans. *Acta Physiologica Scandinavica*, **123**, 457-475.

Petermann, M.M., Hamel, A.J., Cavanagh, P.R., Piazza, S.J., & Sharkey, N.A. (2001). In vitro modeling of human tibial strains during exercise in micro-gravity. *Journal of Biomechanics*, **34**, 693-8.

Prilutsky, B.I., & Zatsiorsky, V.M. (2002). Optimization-based models of muscle coordination. *Exercise and Sport Science Reviews*, **30**, 32-38.

Reber, L., Perry, J., & Pink, M. (1993). Muscular control of the ankle in running. *The American Journal of Sports Medicine,* **21**, 805-810.

Rugg, S.G., Gregor, R.J., Mandelbaum, B.R., & Chiu, L. (1990). In vivo moment arm calculations at the ankle using magnetic resonance imaging (MRI). *Journal of Biomechanics*, **23**, 495-501.

Schaffler, M.B., & Jepsen, K.J. (2000). Fatigue and repair in bone. *International Journal of Fatigue*, **22**, 839-846.

Scott, S.H., & Winter, D.A. (1990). Internal force of chronic running injury sites. *Medicine and Science in Sports and Exercise*, **22**, 357-69.

Spitz, D.J., & Newberg, A.H. (2002). Imaging of stress fractures in the athlete. *Radiologic Clinics of North America*, **40**, 313-331.

Spoor, C.W., Van Leeuwen, J.L., Meskers, C.G.M., Titulaer, A.F., & Huson A. (1990). Estimation of instantaneous moment arms of lower-leg muscles. *Journal of Biomechanics*, **23**, 1247-1259.

Williams, R.K. (1990). Relationships between distance running biomechanics and running economy. In P.R. Cavanagh (Ed.), Biomechanics of distance running. Human Kinetics Books, Champaign, Illinois, pp.271-305.

Chapter 3

Estimation of Stresses and Cycles to Failure of the Tibia during Rested and Fatigued Running.

Siriporn Sasimontonkul and Brian K. Bay

Department of Exercise and Sports Science
Oregon State University, Corvallis, Oregon

Abstract

Tibial stress fractures are common in runners. However, it is unclear which factors cause the occurrence of tibial stress fractures in runners. This study aimed to determine, through an estimation of the cycles to failure (Nfail) of the distal third of the tibia, whether or not repeated application of running loads over typical distances adequately explains tibial stress fractures. Moreover, this study observed whether or not muscle fatigue altered the potential of tibial stress fractures. An integrated experimental and mathematical modeling approach was used to estimate tibial stresses and the Nfail. To gather the experimental data, ten runners labeled with reflective markers on their left lower limb ran across a force plate within the speed range of 3.5-4 m/s. Six cameras and a force plate recorded the spatial orientations of these markers and the ground reaction force signals, respectively. Inverse dynamics analysis was applied to the collected data to estimate joint reaction forces (JRF) and joint moments. Muscle forces were estimated by an optimization procedure. Using these JRF and muscle forces, the 2-D bone contact forces at the distal end of the tibia were determined. Next, tibial stresses were estimated by applying the bone contact forces to a tibial model and were then used to predict the Nfail. All experimental procedures and calculations were repeated after the onset of muscle fatigue from prolonged running. This study found a backward bending of the tibia during most of the stance phase of running. This led to occurrences of compressive stresses on the posterior face and of compressive and tensile stresses on the anterior face of the tibia. However, the maximum stresses occurring during mid stance were the compressive stresses found on the posterior face and equaled - 43.4 $\pm$ 10.3 MPa. These maximum stresses predicted the group mean of Nfail as being $5.28*10^6$ cycles. However, 2.5% to 56% of the population of runners have a chance of getting tibial stress fractures within 1 million cycles of a repeated foot impact. There was no evidence that muscle fatigue accelerated tibial stress fractures. This was because the Nfail significantly increased after plantarflexors fatigued.

Introduction

Stress fractures are micro-damage of bone tissue (Spitz and Newberg, 2002), which are caused by low-level repetitive loading, not a single traumatic event. The highest incidence rate of stress fractures was found in runners with a wide range of 9.7% to 72% (Hulkko and Orava, 1987; Johnson et al., 1994; Bennell et al., 1996; Bennell and Brukner, 1997). A posterior-medial crest at the distal third of the tibia is the most common site of stress fractures found in runners (Brukner et al., 1998). Although tibial stress fractures are common in runners, especially long distance runners (Brukner et al., 1996), its mechanisms are not well understood.

Causations of tibial stress fractures found in runners are unclear. However, a repeated application of certain loads to bone leads to degradations of bone stiffness and microdamage accumulations (Burr et al., 1997). The previous studies found that loads resulting in the strain range of 3000-10,000 με could fail bone within 10^3 to 10^5 cycles of the repetitive application (Carter et al., 1981; Carter and Caler, 1983; Carter and Caler, 1985). However, bone won't fail if the applied loads result in a smaller strain range of 1,200-1,500 με (Schaffler et al., 1990). Loads occurring at the stance phase of running may result in large strains, which lead to tibial stress fractures after a certain number of running steps. In contrast, *in vivo* experiments found small tibial strains, not large, occurring while running (Milgrom et al., 2000a & b; Milgrom et al., 2002; Burr et al., 1996; Milgrom et al., 2003; Ekenman et al., 1998). However, Petermann and colleagues (2001) found that those reported peak strains from the *in vivo* studies were far below maximum strains because strains were recorded near the location of neutral axis or zero strain. Consequently, it is unknown if loads occurring while running are large enough to damage bone. Since the tibial stress fracture occurs in many runners, running may result in larger peak tibial strains, which could initiate a microdamage of bone, than those previously reported.

In contrast to a direct measurement of strains in the human tibia, the mathematical method, which is a finite element model of the tibia, provides a stress

distribution and a peak stress in the tibia. Unfortunately, the previous finite element models of the tibia were loaded by forces corresponding to experimental joint reaction forces (JRF) rather than bone contact forces (Little et al., 1986; Mehta et al., 1999; Sonada et al., 2003). Bone contact forces are forces found across articulating surfaces of bone ends (Winter, 1990), which include the effects of muscle activities. Magnitudes of bone contact forces are larger than those of JRF; therefore, an application of bone contact forces to a finite element model of the whole tibia should result in a larger peak stress than those previously reported (Mehta et al., 1999; Sonada et al., 2003). Hence, it is unclear whether or not a peak tibial stress occurring during running is large enough to injure the tibia.

It is also possible that either the number of running steps or muscle fatigue from a long distance run is associated with stress fractures. It was more likely for stress fractures to occur if the runners ran longer distances or had longer training hours (Bennell et al., 1996; Korpelainen et al., 2001). In addition, Yoshikawa and colleague (1994) reported that the fatigue of quadriceps resulting from a 20 minute running exercise increased peak principal and shear strains in the tibiae of foxhounds by an average of 26-35%. The effect of muscle fatigue was also observed in human tibia but noisy signals led to inconclusive results (Fyhrie et al., 1998). As a result, it is not understood whether it is the number of running steps, muscle fatigue, or both that lead to tibial stress fractures.

Since the relationship between running and tibial stress fractures is unclear, this study evaluated the potential for stress fractures in human subjects running immediately after a rested state, and compared this with running after the onset of muscle fatigue. Unlike the previous study, an integrated experimental and mathematical modeling approach was used to estimate stresses at the distal third of the tibia during each time instant of the stance phase. Thereafter, the probability of tibial stress fractures was determined from an estimation of the minimum cycle to failure (Nfail). Schaffler and colleague (1990) reported that the Nfail of bone specimens was more than 10^6 cycles if physiological loads were applied to bone. The physiological

loads are loads resulting in a strain range of 50-1500 με (Martin, 2000). Since running is a vigorous activity, running loads may result in larger strains and stresses than the physiological loads applied to bone. Thus, the running loads may result in a smaller Nfail than those reported by Schaffler (1990). Two hypotheses were posed here. First, the minimum Nfail was less than 10^6 cycles under running loads. Second, muscle fatigue altered the potentials of stress fractures; therefore, Nfail found after muscle fatigue was not equal to that found before fatigue.

Methods

Subject. Ten recreational male-runners volunteered to participate in this study. They were 23 ± 2.7 years old. Their height and mass were 175.9 ± 8.4 cm and 71.5 ± 6.9 kg, respectively. They were heel strikers with average running mileages per week of 32.05 ± 9.9 miles. They were injury free, especially from stress fractures, and had no abnormal running patterns. An approval was obtained from the university institutional review board for the protection of human subjects and all participants signed an informed consent (see appendix D) before participating in this study.

The measurement of peak torque of plantarflexors. A baseline peak torque of plantarflexors was determined before running using an isokinetic dynamometer (Biodex system 3 pro, Biodex Medical System, Inc., New York, USA). After warm-up and adjusting a proper position for ankle plantar flexion and dorsiflexion, the plantarflexors were tested using a concentric/concentric mode of isokinetic contraction at a speed of 30 degrees/s. Runners performed a concentric plantarflexion followed by a concentric dorsiflexion totaling 5 repetitions each without rest in between. During test, a full range of motion of both plantarflexion and dorsiflexion were required.

The determination of kinetics and kinematics. Reflective markers were taped to the runners' skin at the left anterior superior iliac spine (ASIS), right ASIS, left posterior superior iliac spine (PSIS), right PSIS, left thigh, left femoral epicondyle, left shank, left lateral malleolus, left heel and the base of the left second toe. The

participants ran 6 successful trials, less than 10 meters each, across a force plate at a speed range of 3.5 - 4 m/s because it was a common running pace for many recreational runners (Cavanagh and Kram, 1990). A pair of timing lights (model 63501-IR, Lafayette Instrument Company, Indiana, USA) controlled the running speed. If the running speed was met and the entire left foot hit on a force plate, it was consider a successful trial. This force plate (Bertec, model 4060-08, Bertec Corporation, Columbus Ohio, USA) collected ground reaction force (GRF) signals at a frequency of 1080 Hz; simultaneously, six cameras captured spatial orientations of the reflective markers at a frequency of 120 Hz. Using the Vicon Motion System (Lake Forest California, USA), signals from the six cameras and the force plate were synchronized. The procedures were repeated immediately after plantarflexors became fatigued following a running exercise. To reduce noise, Woltring's general cross-validatory quintic spline algorithm with a mean square error (MSE) of 7 mm was used to filter the spatial coordinates of the reflective markers. Next, Plug-In Gait of Vicon Motion System (Plug in Gait, Vicon Motion System, Inc., California, USA) calculated 3-D joint reaction forces (JRF) and joint moments at 120 Hz using Euler's equations (Hibbeler, 1997) and inverse dynamic method.

Running exercise. Before running, the reflective markers were taken off of the runners. Their locations on the runners' skin were marked so that after fatigue the same individual reflective markers were placed in the same spots as before fatigue. A running exercise was performed on a treadmill located near the testing area. The rating of perceived exertion (RPE) was used for periodically rating the perception of exertion in participants' leg muscles while running (Borg, 1998). A speed corresponding to lightly heavy exertion (scale of 11) was used in this study. The scale of 11 is associated with the lactate threshold of an individual runner (Weltman, 1995). Runners maintained this running speed and rated their perception of muscle exertion every 15 minutes of running. They stopped running when a scale of 17 was met. The strength of the plantarflexors was then re-evaluated immediately using the Biodex dynamometer. If the peak torque of the plantarflexors was about 25-30% less than its baseline value,

it was considered a complete running exercise. If this condition was not met, without taking a rest, runners were required to continue their running on the treadmill using either the previous pace or their preferred speed. The strength of the plantarflexors was evaluated every 15 minutes. The running was completed either when the peak torque of plantarflexors was about 25-30% less than its initial value or when runners became exhausted, whichever occurred first.

The estimation of muscle and bone contact forces. A left lower limb was constructed as a 3 dimensional four rigid-body segmented model composed of (1) pelvis, (2) femur, (3) tibia, and (4) foot. In total, 21 muscles were attached to the model. A 3-D origin and insertion of muscles relative to segmental reference frames was derived from Delp (1990) and scaled to suit individual runners (Brand et al., 1982; Kepple et al., 1994). Thereafter, the 3-D origin and insertion of muscles was transformed from the segmental reference frames to the global reference frame for estimating muscle moment arm lengths at each time instant of the stance phase (Amirouche, 1992; Hawkins, 1992; Kepple et al., 1994).

2-D muscle forces in a sagittal plane were estimated from an optimization procedure using a 2-D model of the leg attached with 21 muscles (Figure 2.2 of chapter 2). The minimized sum of cubed muscle stresses was used as an objective function of the optimization (Equation 1). Both joint moments about the mediolateral axis and muscle moment arm lengths in the sagittal plane resulting from the experimental running trials served as equality constraints (Equation 2-4) that the optimizations were subjected to. The lower and upper boundaries of muscle forces also served as inequality constraints of the optimizations (Equation 5). The objective function and constraints of the optimizations are shown in the following:

$$\text{Objective function:} \quad \text{Minimize} \quad \sum_{i=1}^{j} (f_i(t)/PCSA_i)^3 \tag{1}$$

$$\text{Equality Constraints:} \quad M_a(t) = \sum_{i=1}^{j} d_{ai}(t) * f_{ai}(t) \tag{2}$$

$$M_k(t) = \sum_{i=1}^{j} d_{ki}(t) * f_{ki}(t) \quad (3)$$

$$M_h(t) = \sum_{i=1}^{j} d_{hi}(t) * f_{hi}(t) \quad (4)$$

Inequality constraint: $0 \leq f_1, f_2, f_3, f_4, \ldots, f_j \leq$ maximum muscle force (5)

i is the number of muscle forces. j is the 21 muscles. M_a, M_k, and M_h are resultant moments at ankle, knee and hip joints, respectively. The resultant moments came from experimental data at each time instant of the stance phase and are positive when rotating counterclockwise. $d_i(t)$ is a moment arm length of the i^{th} muscle at each time instant of the stance phase and is positive when it results in counterclockwise moments. f_i is a force of the i^{th} muscle at each time instant of the stance phase that results in the resultant moment at a certain joint. The maximum muscle force of the i^{th} muscle was estimated from $\sigma * PCSA_i$ while σ represents muscle stress. The muscle stress of 80 N/cm^2 was used for all muscles (Refer to Chapter 2). $PCSA_i$ is the physiological cross-sectional area of the i^{th} muscle and is averaged across a reported PCSA of a male cadaver and a reported PCSA of Pierrynowski's study (Brand et al., 1986).

The routine *fmincon* of the optimization toolbox of MATLAB (The math Works Inc, version 6.1, Natick MA, USA) solved this optimization problem at each time instant of the stance phase and predicted muscle forces. Bone contact forces were then estimated from equation (6).

Bone contact forces = AJRF – summation of muscle forces (6)

AJRF are the vertical and horizontal ankle JRF on the foot segment and determined experimentally from running trials. The sums of muscle forces are separate summations of the vertical and horizontal components of plantarflexor and dorsiflexor forces. Muscle paths of individual plantarflexors and dorsiflexors, used for calculating muscle forces, were position vectors. According to the position of the body, they were drawn either from muscle insertion to muscle origin or from the wrapping points at the most proximal end of the foot to the most distal end of the tibia. These bone contact

forces were compressive and shear forces applied to the foot segment. The bone contact forces applied to the tibia in this study had the same magnitudes but opposite directions.

The calculation of stresses at the distal end of the tibia. To exclude loads transmitting through the fibula, only 90 % of bone contact forces were used for estimating normal stresses on the tibia (Lambert, 1971; Calhoun et al., 1994; Funk et al., 2003). These bone contact forces were forces transformed from the global reference frame to the tibial reference frame and were applied to the tibial model.

The tibia was modeled as a simple beam, and its cross-section was an elliptical ring with an eccentric hole as used in the study of Milgrom (1989). A complex finite element model of the tibia was not used because it was beyond the scope of this study. Stresses at 13.7 cm from the distal end of the tibia were calculated at each time instant of the stance phase using equations (7) and (8). The tibial geometry used in these equations, such as A, I and Y, comes from the previous reports (Giladi et al., 1987; Milgrom et al., 1989).

$$\sigma_{N \text{ at posterior face}} = \frac{\text{compressive force}}{A_{tibia}} - \frac{MY}{I_{tibia}} \quad (7)$$

$$\sigma_{N \text{ at anterior face}} = \frac{\text{compressive force}}{A_{tibia}} + \frac{MY}{I_{tibia}} \quad (8)$$

A_{tibia} (m^2) is the cross-sectional area of the tibia and equal to $397.31*10^{-6}$ m^2. I_{tibia} (m^4) is the area moment of inertia about the mediolateral axis of the tibia. It was averaged across the groups of recruits including both all stress fractures and non stress fractures (Milgrom et al., 1989). I_{tibia} is equal to $25{,}355*10^{-12}$ m^4. Y (m) is either the distance of the posterior or anterior outer surfaces of the tibia beginning from the centroid and is only positive. Y of the posterior and anterior faces are equal to 14.658 and $13.54*10^{-3}$ m, respectively. M (N·m) is the calculated bending moment at 13.7 cm above the distal end of the tibia using a shear-force and bending-moment diagram (Figure 3.1).

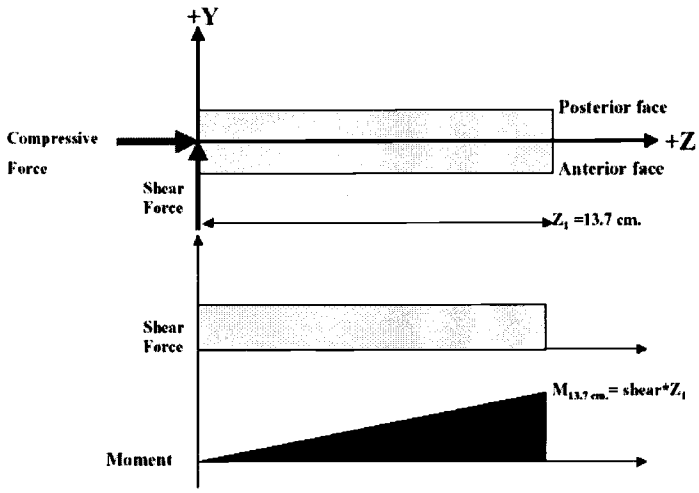

Figure 3.1 A diagram of shear force and the bending moment at the tibia. +Y is positive Y-axis. +Z is positive Z-axis. $M_{13.7\,cm}$ is moment at 13.7 cm from the distal end of the tibia.

The prediction of Nfail. The estimated stresses were fitted to a regression equation of Caler & Carter (1989) to predict Nfail as shown in equation (9).

$$T = F\,(\Delta\sigma/E)^{-G} \qquad (9)$$

$\Delta\sigma$ is the estimated stress at each time instant of the stance phase. E is Young's modulus and is equal to 17.0 GPa (Hayes and Bouxsein, 1997). F is creep coefficient and G is creep exponent. For tensile cyclic loading, F_t= 1.91*10 $^{-33}$ s and G_t= 14.74. For compressive cyclic loading, F_c= 4.79*10 $^{-25}$ s and G_c= 11.88. Time to failure (T) has a unit of seconds. Since Caler & Carter (1989) loaded bone specimens at a frequency of 2 cycles per second, T was multiplied by 2 to estimate the cycle to failure (Nfail).

The statistical analysis. The stance time was normalized to be a percentage of the total stance time. Kinetics, bone contact forces and stresses of individual running trials were interpolated every 0.2% stance across the stance phase using a piecewise cubic hermite interpolating polynomial. The kinetics, bone contact forces and stresses were then averaged across 6 trials within individual runners to represent their data. Next, group means and standard deviations of kinetics, bone contact forces and

stresses were calculated across runners using MATLAB (Matlab® 6.1). The reported Nfail was the minimum Nfail found during the period representing the active phase of the vertical GRF. This active phase covers a period from the relative minimum through the end of the vertical GRF. Since the distribution of Nfails was not normal, Nfails were transformed using the natural log, Ln(Nfail). Variations in Nfail between the 6 trials of individual runners were analyzed using a repeated measures ANOVA in a reliability analysis of SPSS (SPSS 10.0 for Windows). This analysis showed a consistency of Ln(Nfail) across the 6 trials (p-value > 0.05). Therefore, Ln(Nfail) of 6 trials were averaged to represent the Ln(Nfail) of individual runners.

Two statistical methods were used for testing the hypotheses. First, a t-test was used to analyze if a mean of Ln(Nfail) across runners was significantly different from $Ln(10^6)$ cycles. Since two t-tests were performed on the Ln(Nfail) of the posterior and anterior faces of the tibia, a Bonferroni adjustment was used to prevent an inflation of type I error. Therefore, the level of significance was set at 0.025. Second, the repeated measures multivariate analysis (SPSS 10.0 for Windows), a doubly multivariate, was performed twice to test the second hypothesis. A first doubly multivariate was used to test if Ln(Nfail) of all runners found prior to fatigue was different from that found after fatigue both at the anterior and posterior faces of the tibia. A second doubly multivariate was used to test if Ln(Nfail) of the anterior face was different from that of the posterior face of the tibia both before and after fatigue states. These two analyses showed statistically significant difference within subjects at the p-value of 0.015 and 0.000, respectively. To further investigate, the univariate F-test (SPSS 10.0 for Windows) was used to test within subject contrast. The level of significance of the univariate F-test was set at 0.025 using a Bonferroni adjustment.

Results:

The group mean and SD of the running speeds before and after fatigue were equal to 3.84 ± 1.2 and 3.76 ± 0.1 m/s, respectively. Using a paired t-test, they were

insignificantly different at a p-value of 0.074. The group mean and SD of the treadmill speed and total running time of the running exercise equaled 7.52 $\pm$ 0.8 m/s and 86 $\pm$ 21.3 min, respectively. Immediately after completing the running exercise, the peak torque of plantarflexors decreased 30.06 $\pm$ 11 % compared to before the running exercise.

Mean joint moments, muscle forces, JRF and bone contact forces across runners are shown in Figure 3.2-3.3. After fatigue, the peak plantarflexion moment tended to decrease (figure 3.2 a). The peak vertical muscle force (Figure 3.3 a) and tibial JRF (Figure 3.3 c, d) appeared to decrease during mid stance. Consequently, peak compressive and shear forces (Figure 3.3 e & f) tended to decrease during mid stance as well.

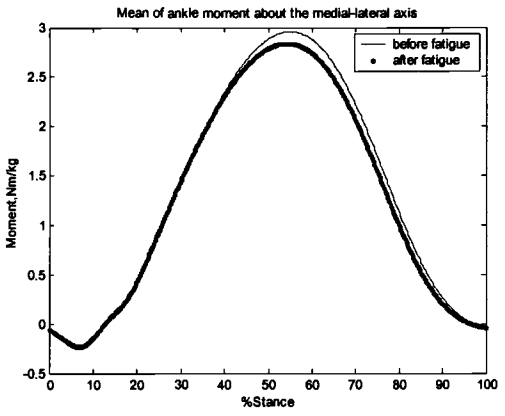

a) ankle moment

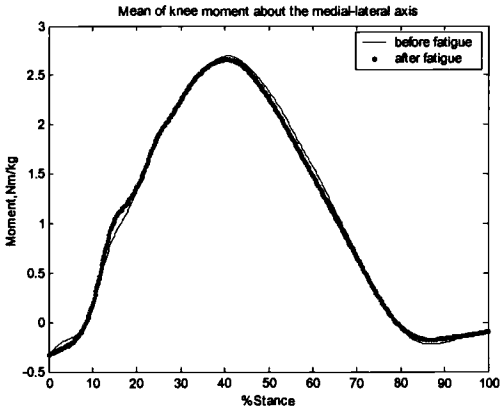

b) knee moment

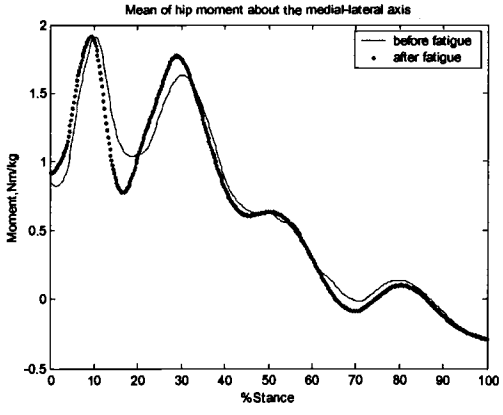

c) hip moment

Figure 3.2 Ankle, knee and hip moments before and after muscle fatigue. Positive moments represent extension moments.

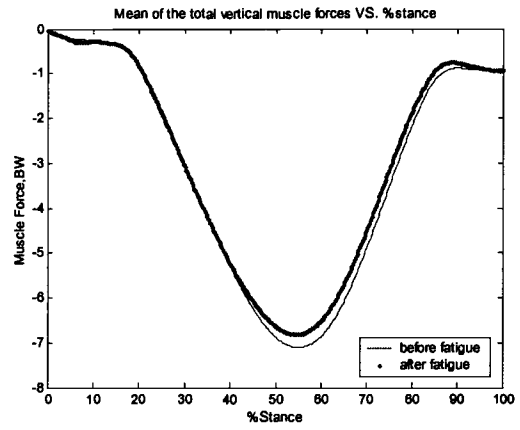

a) vertical muscle force

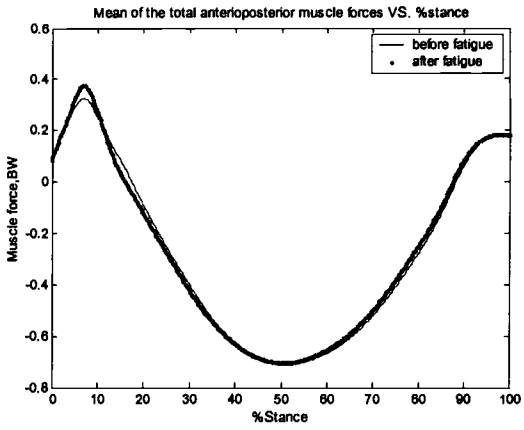

b) horizontal muscle force

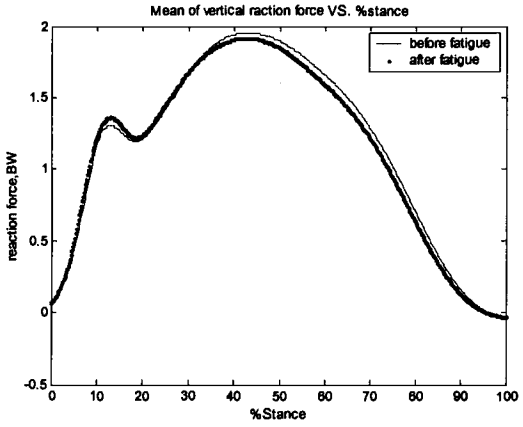

c) vertical tibial JRF

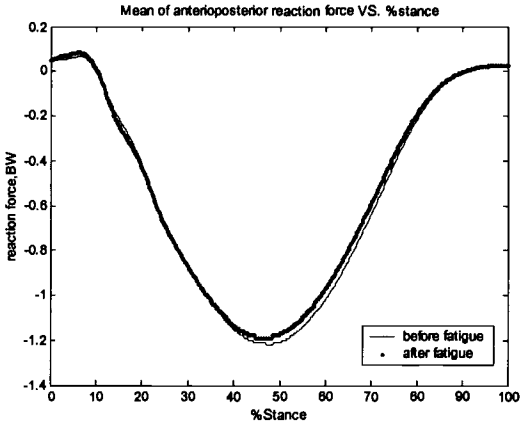

d) horizontal tibial JRF

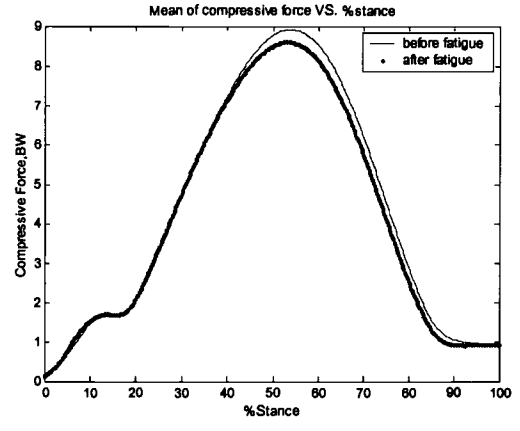

e) compressive force

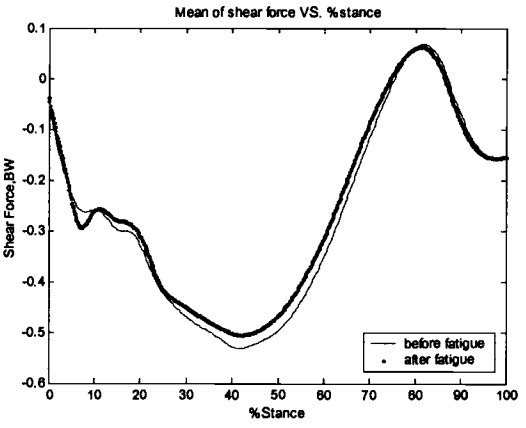

f) shear force

Figure 3.3 Muscle forces, tibial JRF and bone contact forces before and after muscle fatigue reported relative to the tibia's orientations. Positive forces represent the force being applied either in an upward direction or forward direction.

Tibial Stresses. Superimposing compressive and shear forces on the distal end of the tibia resulted in a backward bending of the tibia. This resulted in compressive stresses on the posterior face and both compressive and tensile stresses on the anterior face of the tibia. These mean stresses of all the runners are shown in Figure 3.4. Before fatigue, the maximum compressive stress found on the posterior face of the tibia was equal to - 43.4 $\pm$ 10.3 MPa and occurred during mid stance (Figure 3.4 a). Unlike the posterior face, small stresses were found on the anterior face of the tibia. The maximum tensile and compressive stresses found on the anterior face of the tibia were equal to 16.70 $\pm$ 5.95 MPa and -8.32 $\pm$ 3.13 MPa, respectively (Figure 3.4 b).

After muscle fatigue, the maximum stresses tended to decrease. The maximum compressive stress on the posterior face was equal to - 41.7 $\pm$ 9.64 MPa, and the maximum tensile and compressive stresses on the anterior face of the tibia were equal to 15.3 $\pm$ 4.56 and –7.94 $\pm$ 3.36 MPa, respectively.

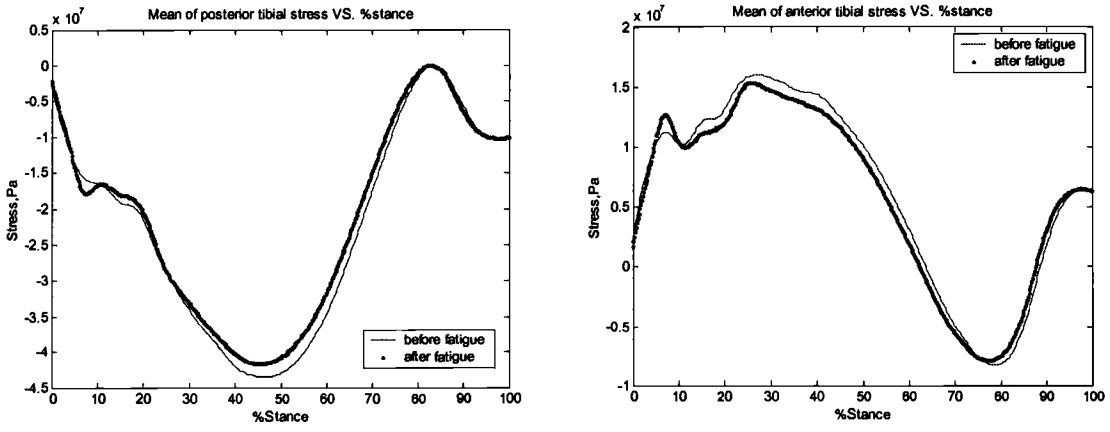

a) The posterior face of the tibia

b) The anterior face of the tibia

Figure 3.4. Tibial stresses found before and after muscle fatigue. Positive stress is tensile stress while negative stress is compressive stress.

Minimum cycle to failure, Ln(Nfail). The group mean and SD of Ln(Nfail) and the group mean of untransformed Nfail are shown in Table 3.1. Before fatigue, the group mean of Ln(Nfail) on the posterior face of the tibia was not significantly different from the hypothesized value of Ln(10^6), which equals 13.8. In contrast, the

group mean of Ln(Nfail) of the anterior face was significantly larger than its hypothesized value. Comparing the Ln(Nfail) of the two faces of the tibia, the group mean of Ln(Nfail) of the posterior face was significantly smaller than that of the anterior face both before and after fatigue states. As a result, Ln(Nfail) of the posterior face was the minimum Ln(Nfail).

Muscle fatigue resulted in the significant increase of the group mean of Ln(Nfail) of the posterior face. In contrast, the group mean of Ln(Nfail) of the anterior face was unchanged after muscle fatigue.

Table 3.1 The group mean and SD of Ln(Nfail) and the mean of untransformed Nfail of the posterior and anterior faces of the tibia.

Ln(Nfail)	**Before fatigue**	**After fatigue**	**P-value[a]**
a) Posterior face	15.48 ± 2.56	16.07 ± 2.44^{b}	0.004
b) Anterior face	$27.00 \pm 4.95^{b,c}$	$27.94 \pm 4.01^{b,c}$	0.095
Nfail (cycles)			
a) Posterior face	$5.28*10^{6}$	$9.53*10^{6}$	
b) Anterior face	$5.32*10^{11}$	$1.36*10^{12}$	

a = p-value of a comparison between before and after fatigue states.

b = Ln(Nfail) was significantly different from the hypothesized value of $Ln(10^{6})$, 13.8, at p-value < 0.025.

c = Ln(Nfail) of the anterior and posterior faces were significantly different with a p-value of 0.000.

A large variance in Ln(Nfail) was found between runners; therefore, the mean Ln(Nfail) of 6 trials of individual runners and its 95% confidence interval (CI) are shown in Figure 3.5. This figure presents only the Ln(Nfail) of the posterior face because it was the minimum Ln(Nfail) of the tibia. Before fatigue, 2 of the 10 runners had a predicted Ln(Nfail) of less than the hypothesized value of $Ln(10^{6})$, (Figure 3.5 a). A 95% CI of the previous proportion of runners, when inferred upon some larger population, equaled 2.5% to 56%. Thus, 2.5 to 56% of the population of runners

would have predicted Nfail as less than 10^6 cycles. Because of the small sample size, this range is large and does not precisely define stress fracture risk. After muscle fatigue, the Ln(Nfail) of individual runners increased (Figure 3.5 b). However, those two runners, who were more likely to get tibial stress fractures before fatigue, still had a chance to get tibial stress fractures after fatigue.

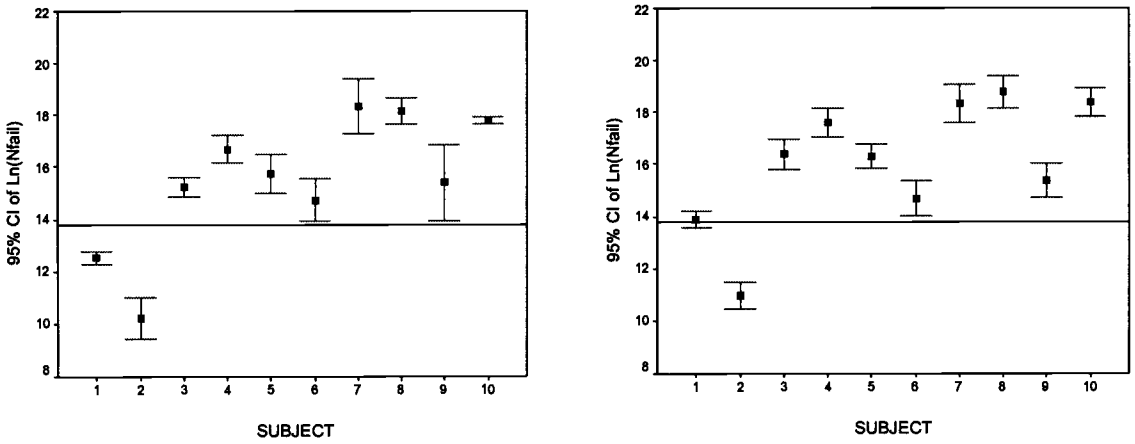

a) before fatigue b) after fatigue

Figure 3.5. The Ln(Nfail) of the posterior face of the tibia of individual runners and its 95% CI. A horizontal line is the hypothesized value of Ln(10^6), 13.8.

Discussion

Stresses and Nfail found in normal running. In contrast to the forward bending of the tibia reported by Scott and Winter (1990), the tibial model of this study showed a backward bending of the tibia during most of the entire stance. As a result, this study found compressive stresses on the posterior face and both tensile and compressive stresses on the anterior face of the tibia. The previous *in vivo* and *in vitro* studies (Ekenman et al., 1998; Peterman et al., 2001) supported that both tensile strains and compressive strains occurred in the anterior face while only compressive strains occurred in the posterior face of the tibia due to the backward bending of the tibia. A simulation of walking by Peterman and team (2001) showed that the peak compressive

strain was found on the posterior face; similarly, this study found the maximum compressive stress on the posterior face of the tibia.

Strains found from running trials at a speed range of 3 - 4.7 m/s have been reported from *in vivo* experiments (Burr et al., 1996; Milgrom et al., 2000a & b; Milgrom et al., 2001; Milgrom et al., 2002). The ranges of compressive and tensile strains were equal to -359 to -2,104 με and 646 to 1,415με, respectively. However, these reported strains were far below maximum strains (Peterman et al., 2001). In contrast to the previous *in vivo* studies, the integrated experimental and mathematical modeling approach of this study could estimate the maximum compressive and tensile stresses on the tibia. Thus, the maximal compressive and tensile stresses of –43.4 and 16.7 MPa were found to be on the posterior and anterior faces of the tibia, respectively. Assuming the linearly elastic material of bone and a Young's modulus of 17 GPa, these compressive and tensile stresses were equal to the compressive and tensile strains of -2553 and 982 με, respectively. This maximum compressive strain was larger than those reported by the previous *in vivo* studies (Burr et al., 1996; Milgrom et al., 2000a & b; Milgrom et al., 2001; Milgrom et al., 2002).

The maximum compressive stress found on the posterior face of the tibia resulted in the minimum Nfail of the tibia. Hence, the posterior face of the tibia was more prone to stress fractures, which supported the result of a previous epidemiological study (Brukner et al., 1998). However, the group mean of the minimum Nfail of the posterior face was not less than 1 million cycles, but, due to the previously unaccounted tibial curvature, it was possible that the minimum Nfail could have been less than 1 million cycles. This is because the centroid at 15%-85% of the tibial length is located anterior to the line connecting the centroids of tibia plateau and tibia plafond as reported by Funk and his team (2003). An application of compressive force at the centroid of tibia plafond results in an eccentric force applied to the tibia. Thus, the tibia would be bent more backward resulting in larger stresses than those reported in this study. However, the exact locations of contact points on tibia plafond found at various time instants of the stance phase are unknown.

The effect of muscle fatigue on the stresses and Nfail of the distal tibia. After muscle fatigue, peaks of JRF, muscle forces and bone contact forces appeared to decrease compared to the forces before fatigue. As a result, the maximum stress tended to decrease after muscle fatigue, which was different from the results of an animal experiment performed by Yoshikawa and team (1994). This animal experiment found that the fatigue of quadriceps resulting from a 20 minute running exercise increased peak principal and shear strains in the tibiae of foxhounds by an average of 26-35%. The difference in the results found by an animal model and this study may be due to the differences in running mechanics of the lower limbs of dogs and humans and in the alignment of dog and human tibiae. This difference may also be due to our method of predicting muscle force distributions. Thus, further studies are needed to confirm the effects of muscle fatigue on changes in either tibial strain or stress.

The maximum compressive stress on the posterior face of the tibia tended to decrease after muscle fatigue, which resulted in a significant increase in Nfail. This was because the stress and Nfail relationship was an exponential function. This increase in Nfail inferred that the fatigue of plantarflexors from prolonged running did not accelerate tibial stress fractures. Hence, tibial stress fractures should instead result from a repeated application of running loads. Based on the calculated Nfail before fatigue, two of the ten runners should have a micro-damage of the tibia after $2.7*10^4$ to $2.7*10^5$ cycles of foot impact. If a stride length is equal to 2.68 m at a running speed of 3.83 m/s (Cavanagh and Kram, 1990), the numbers of foot impact are equal to the running distance of 73 km (45.9 miles) and 733 km (458.5 miles), respectively. However, a rapid loss of bone stiffness resulting from a microdamage of bone-matrix could occur initially within the first 25% of Nfail (Turner and Burr, 1993) or within 11.5-114.6 miles of running .

Limitations of the study. A large variability of minimum Nfail was found across runners, and tibial stress fractures were likely to occur only in some of the runners. Although proportions of runners from some larger population, who would

have predicted Nfail as less than 10^6 cycles, were in the range of 2.5% to 56%; further studies should be performed with a larger sample size to confirm this result.

This study estimated stresses from a 2-D model of the tibia using geometry of the tibia reported by previous studies (Giladi et al., 1987; Milgrom et al., 1989). To get a more precise result, stress should be estimated from a 3-D tibial model of the tibial geometry of individual runners. In addition, 3-D bone contact forces should be applied to the tibial model to account for compressive, shear and torsional forces.

Conclusion. An integrated experimental and mathematical modeling approach used in this study showed the backward bending of the tibia. Only compressive stress was found on the posterior face of the tibia. In contrast, both compressive and tensile stresses were found on the anterior face. The maximum stress was the compressive stress that was found on the posterior face of the tibia. This maximum stress resulted in a minimum Nfail. Thus, the posterior face of the tibia was more prone to failure than the anterior face. The group mean of Nfail was larger than 1 million cycles with a large variance among runners. Tibial stress fractures could occur in some runners if they run past a specific distance. Hence, a repeated application of running loads on the tibia through long distance running could result in a tibial stress fracture in some runners. However, there was no evidence that muscle fatigue accelerated tibial stress fractures.

REFERENCES

Amirouche, F.M.L. (1992). *Computational methods in multibody dynamics.* (pp.16-22). Prentice-Hall, Englewood Cliffs, New Jersey.

Bennell, K.L., Malcolm, S.A., Thomas, S.A., Wark, J.D., & Brukner, P.D. (1996). The incidence and distribution of stress fractures in competitive track and field athletes: a twelve-month prospective study. *The American Journal of Sports Medicine*, **24**, 211-217.

Bennell, K.L., & Brukner, P.D. (1997). Epidemiology and site specificity of stress fractures. *Clinics in Sports Medicine*, **16**, 179-196.

Borg, G. (1998). Borg's perceive exertion and pain scales. Human Kinetics, Champaign, Illinois.

Brand, R.A., Crowninshield, R.D., Wittstock, C.E., Pedersen, D.R., Clark, C.R., & Krieken, F.M.V. (1982). A model of lower extremity muscular anatomy. *Journal of Biomechanical Engineering*, **104**, 304-310.

Brand, R.A., Pederson, D.R., & Friederich, J.A. (1986). The sensitivity of muscle force predictions to changes in physiologic cross-sectional area. *The Journal of Biomechanics*, **19**, 589-596.

Brukner, P., Bradshaw, C., Khan, K.M., White, S., & Crossley, K. (1996). Stress fractures: a review of 180 cases. *Clinical Journal of Sport Medicine*, **6**, 85-9.

Brukner, P., Bradshaw, C., & Bennell, K. (1998). Managing common stress fractures: let risk level guide treatment. *The Physician and Sport Medicine*, **26**, 39-47.

Burr, D.B., Forwood, M.R., Fyhrie, D.P., Martin, R.B., Schaffler, M.B., & Turner, C.H. (1997). Perspective: bone microdamage and skeletal fragility in osteoporotic and stress fractures. *Journal of Bone and Mineral Research*, **12**, 6-15.

Burr, D.B., Milgrom, C., Fyhrie, D., Forwood, M.R., Nyska, M., Finestone, A., Hoshaw, S., Saiag, E., & Simkin, A. (1996). In-vivo Measurement of human tibia strains during vigorous activity. *Bone*, **18**, 405-410.

Caler, W.E., & Carter, D.R. (1989). Bone creep-fatigue damage accumulation. *Journal of Biomechanics*, **22**, 625-35.

Calhoun, J.H., Li, F., Ledbetter, B.R., & Viegas, S.F. (1994). A comprehensive study of pressure distribution in the ankle joint with inversion and eversion. *Foot & Ankle*, **15**, 125-133.

Carter, D.R., & Caler, W.E. (1983). Cycle-dependent and time-dependent bone fracture with repeated loading. *Journal of Biomechanical Engineering*, **105**, 166-170.

Carter, D.R., & Caler, W.E. (1985). A cumulative damage model for bone fracture. *Journal of Orthopaedic Research*, **3**, 84-90.

Carter, D.R., Caler, W.E., Spengler, D.M., & Frankel, V.H. (1981) Fatigue behavior of adult cortical bone. The influences of mean strain and strain range. *Acta Orthopaedica Scandinavica*, **52**, 481-490.

Cavanagh, P.R., & Kram, R. (1990). Stride length in distance running: velocity, body dimensions, and added mass effects. In P.R. Cavanagh (Ed.), Biomechanics of distance running. Human Kinetics Books, Champaign, Illinois, pp.35-60.

Delp, S.L. (1990). Surgery simulation: a computer graphics system to analyze and design musculoskeletal reconstructions of the lower limb. Dissertation, Stanford University, California.

Ekenman, I., Halvorsen, K., Westblad, P., Fellander-Tsai, L., & Rolf, C. (1998). Local bone deformation at two predominant sites for stress fractures of the tibia: an in vivo study. *Foot and Ankle International*, **19**, 479-484.

Funk, J.R., Rudd, R.W., Kerrigan, J.R., & Candrall, J.R. (2003). Analysis of tibial curvature, fibular loading, and the tibia index [On-line]. Available: www.people.virginia.edu/~rwr4a/papers/ircobi2003.pdf

Fyhrie, D.P., Milgrom, C., Hoshaw, S.J., Simkin, A., Dar, S., Drumb, D., & Burr, D.B. (1998). Effect of fatiguing exercise on longitudinal bone strain as related to stress fracture in humans. *Annals of Biomedical Engineering*, **26**, 660-5.

Giladi, M., Milgrom, C., Simkin, A., Stein, M., Kashtan, H., Margulies, J., Rand, N., Chisin, R., Steinberg, R., Aharonson, Z., Kedem, R., & Frankel, V.H. (1987). Stress fractures and tibial bone width: a risk factor. *The Journal of Bone and Joint Surgery*, **69B**, 326-329.

Hawkins, D. (1992). Software for determining lower extremity muscle-tendon kinematics and moment arm lengths during flexion/extension movements. *Computer Biological Medicine,* **22**, 59-71.

Hayes, W.C., & Bouxsein, M.L. (1997). Biomechanics of cortical and trabecular bone: implications for assessment of fracture risk. In V.C. Mow & W.C. Hayes (Eds.), Basic orthopaedic biomechanics. Lippincott-Raven Publishers, Philadelphia, Pennsylvania, pp.85.

Hibbeler, R.C. (1997). Engineering mechanics statics and dynamics (8th Ed.). Prentice-Hall, Upper Saddle River, New Jersey.

Hulkko, A., & Orava, S. (1987). Stress fractures in athletes. *International Journal of Sports Medicine*, **8**, 221-6.

Johnson, A.W., Weiss, C.B., & Wheeler, D.L. (1994). Stress fractures of the femoral shaft in athletes more common than expected: A new clinical test. *The American Journal of Sports Medicine*, **22**, 248-256.

Kepple, T.M., Arnold, A.S., Stanhope, S.J., & Siegel, K.L. (1994). Assessment of a method to estimate muscle attachments from surface landmarks: a 3-D computer graphics approach. *Journal of Biomechanics*, **27**, 365-371.

Korpelainen, R., Orava, S., Karpakka, J., Siira, P., & Hulkko, A. (2001). Risk factors for recurrent stress fractures in athletes. *The American Journal of Sports Medicine*, **29**, 304-10.

Lambert, K.L. (1971). The weight bearing function of the fibula; a strain gauge study. *The Journal of Bone and Joint Surgery*, **53A**, 507-513.

Little, R.B., Wevers, H.W., Siu, D., & Cooke, T.D.V. (1986). A three-dimensional finite element analysis of the upper tibia. *Journal of Biomechanical Engineering*, **108**, 111-119.

Martin, R.B. (2000). Toward a unifying theory of bone remodeling. *Bone*, **26**, 1-6.

Mehta, B.V., Rajani, S., & Griffith, R. (1999). Finite element analysis of the tibia [On-line]. Available: http://www.ent.ohiou.edu/~mehta/BIOMED/tibia_fea.htm

Milgrom, C., Ekenman, I., & Finstone, A. (2001). Metatarsal strains are sufficiently high to cause fatigue fracture on the basis of cyclic overloading. *47th Annual meeting, Orthopaedic Research Society*, February 25-28, 2001.

Milgrom, C., Finstone, A., Levi, Y., Simkin, A., Ekenman, I., Mendelson, S., Millgram, M., Nyska, M., Benjuya, N., & Burr, D. (2000a). Do high impact exercises produce higher tibial strains than running? *British Journal of Sports Medicine*, **34**, 195-9.

Milgrom, C., Finstone, A., Simkin, A., Ekenman, I., Mendelson, S., Millgram, M., Nyska, M., & Larsson, E.B. (2000b). In-vivo strain measurements to evaluate the strengthening potential of exercises on the tibial bone. *Journal of Bone and Joint Surgery*, **82**, 591-4.

Milgrom, C., Finstone, A., Sharkey, N., Hamel, A., Mandes, V., Burr, D., Arndt, A., & Ekenman, I. (2002). Metatarsal strains are sufficient to cause fatigue fracture during cyclic overloading. *Foot and Ankle International*, **23**, 230-235.

Milgrom, C., Finestone, A., Segev, S., Olin, C., Arndt, T., & Ekenman, I. (2003) Are overground or treadmill runners more likely to sustain tibial stress fracture? *British Journal of Sports Medicine*, **37**, 160-163.

Milgrom, C., Giladi, M., Simkin, A., Rand, N., Kedem, R., Kashtan, H., Stein, M., & Gomori, M. (1989). The area moment of inertia of the tibia: a risk factor for stress fractures. *The Journal of Biomechanics*, **22**, 1243-1248.

Mori, S., & Burr, D.B. (1993). Increased intracortical remodeling following fatigue damage. *Bone*, **14**, 103-109.

Nilsson, J., Thorstensson, A., & Halbertsma, J. (1985). Changes in leg movements and muscle activity with speed of locomotion and mode of progression in humans. *Acta Physiologica Scandinavica*, **123**, 457-475.

Petermann, M.M., Hamel, A.J., Cavanagh, P.R., Piazza, S.J., & Sharkey, N.A. (2001). In vitro modeling of human tibial strains during exercise in micro-gravity. *Journal of Biomechanics*, **34**, 693-8.

Schaffler, M.B., Radin, E.L., & Burr, D.B. (1990). Long-Term fatigue behavior of compact bone at low strain magnitude and rate. *Bone,* **11**, 321-6.

Scott, S.H., & Winter, D.A. (1990). Internal force of chronic running injury sites. *Medicine and Science in Sports and Exercise*, **22**, 357-69.

Sonada, N., Chosa, E., Totoribi, K., & Tajima, N. (2003). Biomechanical analysis for stress fractures of the anterior middle third of the tibia in athletes: nonlinear analysis using a three-dimensional finite element method. *Journal of Orthopaedic Science*, **8**, 505-513.

Spitz, D.J., & Newberg, A.H. (2002). Imaging of stress fractures in the athlete. *Radiologic Clinics of North America*, **40**, 313-331.

Turner, C.H., & Burr, D.B. (1993). Basic biomechanical measurements of bone: A tutorial. *Bone*, **14**, 595-608.

Weltman, A. (1995). The blood lactate response to exercise. Human Kinetics, Champaign, Illinois.

Winter, D.A. (1990). Biomechanics and motor control of human movement (2nd Ed.). A Wiley-Interscience Publication, New York, pp. 78-79.

Yoshikawa, T., Mori, S., Santiesteban, A.J., Sun, T.C., Hafstad, E., Chen, J., & Burr D.B. (1994). The effects of muscle fatigue on bone strain. *Journal of Experimental Biology*, **188**, 217-233.

DO RUNNING AND FATIGUED RUNNING RELATE TO TIBIAL STRESS FRACTURES?

CHAPTER 4

THE SUMMARY OF THE OVERALL RESULTS

Stress fractures are micro-damage of bone tissue (Spitz and Newberg, 2002), which are caused by low-level repetitive loading, not a single traumatic event. They are common in runners (Hulkko and Orava, 1987; Johnson et al., 1994; Bennell et al., 1996; Bennell and Brukner, 1997). The most common site for stress fractures found in runners is at the posterior-medial crest in the distal third of the tibia (Brukner et al., 1998). A repeated application of a specific amount of loads to bone results in its micro-damage (Carter et al., 1981; Carter and Caler, 1983; Carter and Caler, 1985; Schaffler et al., 1990). A number of *in vivo* experiments were performed to investigate whether running loads led to stress fractures of the tibia (Milgrom et al., 2000a & b; Milgrom et al., 2002; Burr et al., 1996; Milgrom et al., 2003; Ekenman et al., 1998). However, their results could not explore this relationship due to the limitations of those previous experiments. The mathematical method, a finite element model, has been used for estimating bone stresses in the tibial models (Mehta et al., 1999; Sonada et al., 2003). Unfortunately, their studies did not result in an actual maximum stress because they applied forces to the models corresponding to experimental joint reaction forces (JRF) instead of bone contact forces. Bone contact forces are forces found across articulating surfaces of bone ends (Winter, 1990), and their magnitudes are larger than those of JRF. An application of bone contact forces would result in a larger maximum stress than those stresses previously reported.

The main goal of this dissertation was to explore a relationship between running and tibial stress fractures using an integrated experimental and mathematical modeling approach. This relationship could be observed through an estimation of bone

contact forces, tibial stresses and the minimum cycle to failure of the tibia (Nfail), sequentially. Bone contact forces were predicted during the stance phase of running and used to estimate tibial stresses at 13.7 cm from the distal end of the tibia. Thereafter, the Nfail was predicted from these tibial stresses to determine whether or not a repeated application of these bone contact forces to the tibia led to tibial stress fractures. Moreover, the effects of muscle fatigue from prolonged running on tibial stresses and Nfail were also investigated in this study. This was investigated because a previous study reported that muscle fatigue from prolonged running increased tibial strains (Yoshikawa et al., 1994). Yoshikawa and team (1994) reported that strains in the foxhounds' tibiae increased after their quadriceps fatigued from a 20 minute run. Fyhrie and team (1998) performed a similar study on humans (Fyhrie et al., 1998); however, no conclusive result could be drawn from this study.

To gather experimental data for estimating bone contact forces, both the spatial orientations of the reflective markers taped onto the left lower limb of runners and the ground reaction forces (GRF) were recorded from running trials within a speed range of 3.5-4.0 m/s. Next, the 3 dimensional (3-D) resultant joint moments and joint reaction forces (JRF) were calculated using a 3-D inverse dynamics method. These resultant joint moments and muscle moment arm lengths about the sagittal plane were used as constraints of optimization for estimating muscle forces. The objective function of the optimization was the minimized sum of cubed muscle stresses and was subjected to the previous constraints. Next, bone contact forces at the distal end of the tibia were calculated from muscle forces crossing the ankle joint and JRF. These bone contact forces were applied to a tibial model for estimating stresses at 13.7 cm from the distal end of the tibia. These stresses were estimated at each time instant of the stance phase and were fitted to regression equations for predicting the Nfail. All of these procedures were repeated after plantarflexors became fatigued from a running exercise on a treadmill.

Bone contact forces

The tibia was compressed by the foot during the entire stance. This resulted in an application of compressive forces on the distal end of the tibial. These compressive forces peaked during mid stance, and their peaks were equal to 8.91 $\pm$ 1.14 times body weight (BW). The distal end of the tibia was also sheared posteriorly by the foot during most of the stance phase. Peak posterior shear forces occurred during mid stance and were equal to -0.53 $\pm$ 0.16 BW.

Stress and Nfail occurring from normal running

Superimposing the estimated bone contact forces onto a tibial model resulted in a backward bending of the tibia during most of the entire stance. As a result, compressive stresses were found on the posterior face of the tibia while both compressive and tensile stresses were found on the anterior face. However, the maximum tibial stress was the compressive stress found on the posterior face of the tibia and was equal to - 43.4 $\pm$ 10.3 MPa. This maximum compressive stress resulted in a minimum Nfail. Therefore, tibial stress fractures are most likely to occur on the posterior face of the tibia, which supports a previous epidemiological report (Brukner et al., 1998). Assuming the linearly elastic material of bone and a Young's modulus of 17 GPa, a maximum stress of -43.4 MPa was equal to -2553 $\mu\epsilon$. This strain was larger than the compressive strains reported in the previous *in vivo* experiments (Burr et al., 1996; Milgrom et al., 2000a & b; Milgrom et al., 2001; Milgrom et al., 2002).

The group mean of Nfail predicted from the maximum stresses found on the posterior face of the tibia was equal to $5.28*10^6$ cycles, which was not less than 1 million cycles. However, a large variance in Nfails was found between runners. This study found that the mean Nfails of 2 out of 10 runners were less than 1 million cycles; these mean Nfails were $2.7*10^4$ and $2.7*10^5$ cycles. With the stride length equal to 2.68 m at a running speed of 3.83 m/s (Cavanagh and Kram, 1990), these Nfails corresponded to running distances of 73 km (45.9 miles) and 733 km (458.5

miles), respectively. Thus, tibial stress fractures were most likely to occur in these two runners if they ran past these distances in just a single trial. However, a microdamage of bone-matrix could be initiated within 11.5-114.6 miles of running (Turner and Burr, 1993) .

Stress and Nfail occurring after muscle fatigue

After prolonged running, peak torque of plantarflexors decreased about 30.06 $\pm$ 11 % compared to the peak torque before running. As a result, peak bone contact forces and tibial stresses tended to decrease, which led to an increase in the minimum Nfail. Thus, there was no evidence that muscle fatigue accelerated tibial stress fractures. In contrast, the increase in the minimum Nfail after muscle fatigue inferred that muscle fatigue reduced the likelihood of getting tibial stress fractures. However, the increase of the minimum Nfail after muscle fatigue was small. Thus, tibial stress fractures were likely to occur in 2 out of 10 runners; their Nfails were less than 1 million cycles before fatigue.

The limitations and suggestions for the future study

The limitation in the sample size. A large variance of the predicted Nfail was found between runners. This might be a result of differences in running styles and running kinetics of the individual runners. This study found that the proportion of runners from a large population, who would have predicted Nfail below 10^6 cycles, was in the range of 2.5% to 56%. However, further studies should be performed with a randomized design and a larger sample size to confirm and refine this result.

The limitation in the physiological and anatomical data. Maximum muscle forces of individual muscles were calculated from a product of the physiological cross-sectional area (PCSA) and the stress of that muscle. These maximum muscle forces were used as constraints for the optimization. Currently, there is no completed

data of PCSA and maximum muscle stress that has been studied in live humans. Thus, PCSA reported from cadaveric studies were used in this study. Since the optimization attributed more force to a larger muscle, an error in PCSA studied from cadavers could lead to an error in a muscle force prediction.

The limitation in the estimation of muscle forces. A lack of availability of precise muscle force measurements in live humans led to the use of a mathematical method for estimating these muscle forces. Currently, an optimization method has been widely used to predict muscle forces, but the optimization needs a physiological criterion to serve as its objective function. However, how the body controls muscular activities for certain movements is unclear. Although a fatigue criterion was used in this study to predict muscle forces both prior to and after muscle fatigue, regulation of muscular activities during both states may differ. Therefore, further studies should be performed to determine which strategies the body uses for activating muscles.

The limitation in the tibial geometry. Stresses were estimated from previously reported tibial geometry. However, they should be estimated from the tibial geometry of individual runners to increase the accuracy of the estimated stress and Nfail.

The limitation in the dimension of the approach. This study was a preliminary step to estimate stresses and Nfails using an integrated experimental and mathematical modeling approach. The results of this study successfully showed that tibial stress fractures are directly related to a long distance run. However, the tibial model used for estimating stress and the muscle model used for predicting muscle forces were constructed in 2 dimensions (2-D) instead of 3-D. Hence, the effects of a torsional force on tibial stresses were not observed by this study. To predict stresses more precisely, a 3-D approach should be applied in the future.

REFERENCES

Bennell, K.L., Malcolm, S.A., Thomas, S.A., Wark, J.D., & Brukner, P.D. (1996) The incidence and distribution of stress fractures in competitive track and field athletes: a twelve-month prospective study. *The American Journal of Sports Medicine*, **24**, 211-217.

Bennell, K.L., & Brukner, P.D. (1997) Epidemiology and site specificity of stress fractures. *Clinics in Sports Medicine*, **16**, 179-196.

Brukner, P., Bradshaw, C., & Bennell, K. (1998). Managing common stress fractures: let risk level guide treatment. *The Physician and Sport Medicine*, **26**, 39-47.

Burr, D.B., Milgrom, C., Fyhrie, D., Forwood, M.R., Nyska, M., Finestone, A., Hoshaw, S., Saiag, E., & Simkin, A. (1996). In-vivo Measurement of human tibia strains during vigorous activity. *Bone*, **18**, 405-410.

Carter, D.R., & Caler, W.E. (1983). Cycle-dependent and time-dependent bone fracture with repeated loading. *Journal of Biomechanical Engineering*, **105**, 166-170.

Carter, D.R., & Caler, W.E. (1985). A cumulative damage model for bone fracture. *Journal of Orthopaedic Research*, **3**, 84-90.

Carter, D.R., Caler, W.E., Spengler, D.M., & Frankel, V.H. (1981) Fatigue behavior of adult cortical bone. The influences of mean strain and strain range. *Acta Orthopaedica Scandinavica*, **52**, 481-490.

Cavanagh, P.R., & Kram, R. (1990). Stride length in distance running: velocity, body dimensions, and added mass effects. In P.R. Cavanagh (Ed.), Biomechanics of distance running. Human Kinetics Books, Champaign, Illinois, pp.35-60.

Ekenman, I., Halvorsen, K., Westblad, P., Fellander-Tsai, L., & Rolf, C. (1998). Local bone deformation at two predominant sites for stress fractures of the tibia: an in vivo study. *Foot and Ankle International*, **19**, 479-484.

Fyhrie, D.P., Milgrom, C., Hoshaw, S.J., Simkin, A., Dar, S., Drumb, D., & Burr, D.B. (1998). Effect of fatiguing exercise on longitudinal bone strain as related to stress fracture in humans. *Annals of Biomedical Engineering*, **26**, 660-5.

Hulkko, A., & Orava, S. (1987). Stress fractures in athletes. *International Journal of Sports Medicine*, **8**, 221-6.

Johnson, A.W., Weiss, C.B., & Wheeler, D.L. (1994). Stress fractures of the femoral shaft in athletes more common than expected: A new clinical test. *The American Journal of Sports Medicine*, **22**, 248-256.

Mehta, B.V., Rajani, S., & Griffith, R. (1999). Finite element analysis of the tibia [On-line]. Available: http://www.ent.ohiou.edu/~mehta/BIOMED/tibia_fea.htm

Milgrom, C., Finstone, A., Ekenman, I., Simkin, A., & Nyska, M. (2001). The effect of shoe sole composition on in vivo tibial strains. *Foot and Ankle International*, **22**, 598-602.

Milgrom, C., Finstone, A., Levi, Y., Simkin, A., Ekenman, I., Mendelson, S., Millgram, M., Nyska, M., Benjuya, N., & Burr, D. (2000a). Do high impact exercises produce higher tibial strains than running? *British Journal of Sports Medicine*, **34**, 195-9.

Milgrom, C., Finstone, A., Sharkey, N., Hamel, A., Mandes, V., Burr, D., Arndt, A., & Ekenman, I. (2002). Metatarsal strains are sufficient to cause fatigue fracture during cyclic overloading. *Foot and Ankle International*, **23**, 230-235.

Milgrom, C., Finestone, A., Segev, S., Olin, C., Arndt, T., & Ekenman, I. (2003) Are overground or treadmill runners more likely to sustain tibial stress fracture? *British Journal of Sports Medicine*, **37**, 160-163.

Milgrom, C., Finstone, A., Simkin, A., Ekenman, I., Mendelson, S., Millgram, M., Nyska, M., & Larsson, E.B. (2000b). In-vivo strain measurements to evaluate the strengthening potential of exercises on the tibial bone. *Journal of Bone and Joint Surgery*, **82**, 591-4.

Schaffler, M.B., Radin, E.L., & Burr, D.B. (1990). Long-Term fatigue behavior of compact bone at low strain magnitude and rate. *Bone,* **11**, 321-6.

Sonada, N., Chosa, E., Totoribi, K., & Tajima, N. (2003). Biomechanical analysis for stress fractures of the anterior middle third of the tibia in athletes: nonlinear analysis using a three-dimensional finite element method. *Journal of Orthopaedic Science*, **8**, 505-513.

Spitz, D.J., & Newberg, A.H. (2002). Imaging of stress fractures in the athlete. *Radiologic Clinics of North America*, **40**, 313-331.

Turner, C.H., & Burr, D.B. (1993). Basic biomechanical measurements of bone: A tutorial. *Bone*, **14**, 595-608.

Winter, D.A. (1990). Biomechanics and motor control of human movement (2nd Ed.). A Wiley-Interscience Publication, New York, pp. 78-79.

Yoshikawa, T., Mori, S., Santiesteban, A.J., Sun, T.C., Hafstad, E., Chen, J., & Burr D.B. (1994). The effects of muscle fatigue on bone strain. *Journal of Experimental Biology*, **188**, 217-233.

BIBLIOGRAPHY

Amirouche, F.M.L. (1992). *Computational methods in multibody dynamics*. (pp.16-22). Prentice-Hall, Englewood Cliffs, New Jersey.

Anderson, F.C., & Pandy, M.G. (2001). Static and dynamic optimization solutions for gait are practically equivalent. *Journal of Biomechanics*, **34**, 153-161.

Beck, B.R. (1998). Tibial stress injuries: an aetiological review for the purposes of guiding management. *Injury Clinic*, **26**, 265-279.

Bennell, K.L., Malcolm, S.A., Thomas, S.A., Wark, J.D., & Brukner, P.D. (1996). The incidence and distribution of stress fractures in competitive track and field athletes: a twelve-month prospective study. *The American Journal of Sports Medicine*, **24**, 211-217.

Bennell, K.L., & Brukner, P.D. (1997). Epidemiology and site specificity of stress fractures. *Clinics in Sports Medicine*, **16**, 179-196.

Binding, P., Jinha, A., & Herzog, W. (2000). Analytic analysis of the force sharing among synergistic muscles in one-and two-degree of freedom models. *Journal of Biomechanics*, **33**, 1423-1432.

Borg, G. (1998). Borg's perceive exertion and pain scales. Human Kinetics, Champaign, Illinois.

Brand, R.A., Crowninshield, R.D., Wittstock, C.E., Pedersen, D.R., Clark, C.R., & Krieken, F.M.V. (1982). A model of lower extremity muscular anatomy. *Journal of Biomechanical Engineering*, **104**, 304-310.

Brand, R.A., Pederson, D.R., & Friederich, J.A. (1986). The sensitivity of muscle force predictions to changes in physiologic cross-sectional area. *The Journal of Biomechanics*, **19**, 589-596.

Brukner, P., & Bennell, K. (1997). Stress fractures in female athletes: diagnosis, management and rehabilitation. *Sports Medicine*, **24**, 419-429.

Brukner, P., Bradshaw, C., Khan, K.M., White, S., & Crossley, K. (1996). Stress fractures: a review of 180 cases. *Clinical Journal of Sport Medicine*, **6**, 85-9.

Brukner, P., Bradshaw, C., & Bennell, K. (1998). Managing common stress fractures: let risk level guide treatment. *The Physician and Sport Medicine*, **26**, 39-47.

Buczek, F.L., & Cavanagh, P.R. (1990). Stance phase knee and ankle kinematics and kinetics during level and downhill running. *Medicine and Science in Sports and Exercise,* **22**, 669-667.

Burdett, R.G. (1982). Forces predicted at the ankle during running. *Medicine and Science in Sports and Exercise*, **14**, 308-316.

Burr, D.B., Forwood, M.R., Fyhrie, D.P., Martin, R.B., Schaffler, M.B., & Turner, C.H. (1997). Perspective: bone microdamage and skeletal fragility in osteoporotic and stress fractures. *Journal of Bone and Mineral Research*, **12**, 6-15.

Burr, D.B., Milgrom, C., Boyd, R.D., Higgins, W.L., Robin, G., & Radin, E.L. (1990). Experimental of the stress fractures of the tibia. *The Journal of Bone and Joint Surgery*, **72-B**, 370-375.

Burr, D.B., Milgrom, C., Fyhrie, D., Forwood, M.R., Nyska, M., Finestone, A., Hoshaw, S., Saiag, E., & Simkin, A. (1996). In-vivo Measurement of human tibia strains during vigorous activity. *Bone*, **18**, 405-410.

Caler, W.E., & Carter, D.R. (1989). Bone creep-fatigue damage accumulation. *Journal of Biomechanics*, **22**, 625-35.

Calhoun, J.H., Li, F., Ledbetter, B.R., & Viegas, S.F. (1994). A comprehensive study of pressure distribution in the ankle joint with inversion and eversion. *Foot & Ankle*, **15**, 125-133.

Carter, D.R., & Caler, W.E. (1983). Cycle-dependent and time-dependent bone fracture with repeated loading. *Journal of Biomechanical Engineering*, **105**, 166-170.

Carter, D.R., & Caler, W.E. (1985). A cumulative damage model for bone fracture. *Journal of Orthopaedic Research*, **3**, 84-90.

Carter, D.R., Caler, W.E., Spengler, D.M., & Frankel, V.H. (1981). Fatigue behavior of adult cortical bone. The influences of mean strain and strain range. *Acta Orthopaedica Scandinavica*, **52**, 481-490.

Cavanagh, P.R., & Kram, R. (1990). Stride length in distance running: velocity, body dimensions, and added mass effects. In P.R. Cavanagh (Ed.), Biomechanics of distance running. Human Kinetics Books, Champaign, Illinois, pp.35-60.

Challis, J.H. (1997). Producing physiologically realistic individual muscle force estimations by imposing constrains when using optimization techniques. *Medical Engineering and Physics*, **19**, 253-61.

Christina, K.A., White, S.C., & Gilchrist, L.A. (2001). Effect of localized muscle fatigue on vertical ground reaction forces and ankle joint motion during running. *Human Movement Science*, **20**, 257-276.

Collins, J.J. (1995). The redundant nature of locomotor optimization laws. *Journal of Biomechanics*, **28**, 251-267.

Crowninshield, R.D., & Brand, R.A. (1981). A physiologically based criterion of muscle force prediction in locomotion. *Journal of Biomechanics*, **14**, 793-801.

Crowninshield, R.D. (1983). A physiologically based criterion for muscle force predictions on locomotion. *BULLETIN of the Hospital for Joint Diseases Orthopaedic Institute*, **XLIII**, 164-170.

Delp, S.L. (1990). Surgery simulation: a computer graphics system to analyze and design musculoskeletal reconstructions of the lower limb. Dissertation, Stanford University, California.

Delp, S.L., Loan, J.P., Hou, M.G., Zajac, F.E., Topp, E.L., & Rosen, J.M. (1990). An interactive graphics-based model of the lower extremity to study orthopaedic surgical procedures. *IEEE Transaction on Biomedical Engineering*, **37**, 757-767.

Dul, J., Johnson, G.E., Shiavi, R., & Townsend, M.A. (1984). Muscular synergism II: A minimum-fatigue criterion for load sharing between synergistic muscles. *Journal of Biomechanics*, **17**, 675-684.

Ekenman, I., Halvorsen, K., Westblad, P., Fellander-Tsai, L., & Rolf, C. (1998). Local bone deformation at two predominant sites for stress fractures of the tibia: an in vivo study. *Foot and Ankle International*, **19**, 479-484.

Farley, C.T., & Ferris, D.P. (1998). Biomechanics of walking and running: center of mass movements to muscle action. *Exercise and Sports Science Reviews,* **26,** 253-285.

Federicson, M., Bergman, G., Hoffman, K.L., & Dillingham, D.S. (1995). Tibial stress reaction in runners: correlation of clinical symptoms and scintigraphy with a new magnetic resonance imaging grading system. *American Journal of Sports Medicine*, **23**, 472-81.

Forwood, M.R., & Parker, A.W. (1991). Repetitive loading, in vivo, of the tibiae and femora of rats: effects of repeated bouts of treadmill-running. *Bone and Mineral*, **13**, 35-46.

Fukunaka, T., Roy, R.R., Shellock, F.G., Hodgson, J.A., & Edgerton, V.R. (1996). Specific tension of human plantar flexors and dorsiflexors. *The Journal of Applied Physiology*, **80**, 158-165.

Fukushima, M., Mutoh, Y., Takasugi, S., Iwata, H., & Ishii, S. (2002). Characteristics of stress fractures in young athletes under 20 years. *The Journal of Sports Medicine and Physical Fitness*, **42**, 198-206.

Funk, J.R., Rudd, R.W., Kerrigan, J.R., & Candrall, J.R. (2003). Analysis of tibial curvature, fibular loading, and the tibia index [On-line]. Available: www.people.virginia.edu/~rwr4a/papers/ircobi2003.pdf

Fyhrie, D.P., Milgrom, C., Hoshaw, S.J., Simkin, A., Dar, S., Drumb, D., & Burr, D.B. (1998). Effect of fatiguing exercise on longitudinal bone strain as related to stress fracture in humans. *Annals of Biomedical Engineering*, **26**, 660-5.

Giladi, M., Milgrom, C., Simkin, A., Stein, M., Kashtan, H., Margulies, J., Rand, N., Chisin, R., Steinberg, R., Aharonson, Z., Kedem, R., & Frankel, V.H. (1987). Stress fractures and tibial bone width: a risk factor. *The Journal of Bone and Joint Surgery*, **69B**, 326-329.

Glitsch, U., & Baumann, W. (1997). The three-dimensional determination of internal loads in the lower extremity. *Journal of Biomechanics*, **30**, 1123-1131.

Harrison, R.N., Lees, A., McCullagh, P.J.J., & Rowe, W.B. (1986). A bioengineering analysis of human muscle and joint forces in the lower limbs during running. *Journal of Sports Sciences*, **4**, 201-218.

Hausswirth, C., Brisswalter, J., Vallier, J.M., Smith, D., & Lepers, R. (2000). Evolution of electromyographic signal, running economy, and perceived exertion during different prolonged exercises. *International Journal of Sports Medicine*, **21**, 429-36.

Hawkins, D. (1992). Software for determining lower extremity muscle-tendon kinematics and moment arm lengths during flexion/extension movements. *Computer Biological Medicine*, **22**, 59-71.

Hayes, W.C., & Bouxsein, M.L. (1997). Biomechanics of cortical and trabecular bone: implications for assessment of fracture risk. In V.C. Mow & W.C. Hayes (Eds.), Basic orthopaedic biomechanics. Lippincott-Raven Publishers, Philadelphia, Pennsylvania, pp.85.

Hibbeler, R.C. (1997). Engineering mechanics statics and dynamics (8th Ed.). Prentice-Hall, Upper Saddle River, New Jersey.

Hulkko, A., & Orava, S. (1987). Stress fractures in athletes. *International Journal of Sports Medicine*, **8**, 221-6.

Jensen, J. (1998). Stress fracture in the world class athlete: a case study. *Medicine and Science in Sports and Exercise*, **30**, 783-787.

Jeske, J.M., Lomasney, L.M., Demos, T.C., Vade, A., & Bielski, R.J. (1996). Longitudinal tibial stress fracture. *Orthopedics*, **19**, 225-230.

Johnson, A.W., Weiss, C.B., & Wheeler, D.L. (1994). Stress fractures of the femoral shaft in athletes more common than expected: A new clinical test. *The American Journal of Sports Medicine*, **22**, 248-256.

Kepple, T.M., Arnold, A.S., Stanhope, S.J., & Siegel, K.L. (1994). Assessment of a method to estimate muscle attachments from surface landmarks: a 3-D computer graphics approach. *Journal of Biomechanics*, **27**, 365-371.

Korpelainen, R., Orava, S., Karpakka, J., Siira, P., & Hulkko, A. (2001). Risk factors for recurrent stress fractures in athletes. *The American Journal of Sports Medicine*, **29**, 304-10.

Lambert, K.L. (1971). The weight bearing function of the fibula; a strain gauge study. *The Journal of Bone and Joint Surgery*, **53A**, 507-513.

Leardini, A., O'Connor, J.J., Catani, F., & Giannini, S. (1999). A geometric model of the human ankle joint. *Journal of Biomechanics*, **32**, 585-591.

Little, R.B., Wevers, H.W., Siu, D., & Cooke, T.D.V. (1986). A three-dimensional finite element analysis of the upper tibia. *Journal of Biomechanical Engineering*, **108**, 111-119.

Maganaris, C.N. (2000). In vivo measurement-based estimation of the moment arm in the human tibialis muscle-tendon unit. *Journal of Biomechanics*, **33**, 375-379

Martin, R.B. (2000). Toward a unifying theory of bone remodeling. *Bone*, **26**, 1-6.

McCaw, S.T., & DeVita, P. (1995). Errors in alignment of center of pressure and foot coordinates affect predicted lower extremity torques. *Journal of Biomechanics*, **28**, 985-988.

Mehta, B.V., Rajani, S., & Griffith, R. (1999). Finite element analysis of the tibia [On-line]. Available: http://www.ent.ohiou.edu/~mehta/BIOMED/tibia_fea.htm

Milgrom, C., Ekenman, I., & Finstone, A. (2001). Metatarsal strains are sufficiently high to cause fatigue fracture on the basis of cyclic overloading. *47th Annual meeting, Orthopaedic Research Society*, February 25-28, 2001.

Milgrom, C., Finstone, A., Ekenman, I., Simkin, A., & Nyska, M. (2001). The effect of shoe sole composition on in vivo tibial strains. *Foot and Ankle International*, **22**, 598-602.

Milgrom, C., Finestone, A., Levi, Y., Simkin, A., Ekenman, I., Mendeloson, S., Millgram, M., Nyska, M., BenJuya, N., & Burr, D. (2000a). Do high impact exercises produce higher tibial strains than running? *British Journal of Sports Medicine*, **34**, 195-199.

Milgrom, C., Finestone, A., Segev, S., Olin, C., Arndt, T., & Ekenman, I. (2003) Are overground or treadmill runners more likely to sustain tibial stress fracture? *British Journal of Sports Medicine*, **37**, 160-163.

Milgrom, C., Finstone, A., Sharkey, N., Hamel, A., Mandes, V., Burr, D., Arndt, A., & Ekenman, I. (2002). Metatarsal strains are sufficient to cause fatigue fracture during cyclic overloading. *Foot and Ankle International*, **23**, 230-235.

Milgrom, C., Finstone, A., Simkin, A., Ekenman, I., Mendelson, S., Millgram, M., Nyska, M., & Larsson, E.B. (2000b). In-vivo strain measurements to evaluate the strengthening potential of exercises on the tibial bone. *Journal of Bone and Joint Surgery*, **82**, 591-4.

Milgrom, C., Giladi, M., Simkin, A., Rand, N., Kedem, R., Kashtan, H., Stein, M., & Gomori, M. (1989). The area moment of inertia of the tibia: a risk factor for stress fractures. *The Journal of Biomechanics*, **22**, 1243-1248.

Millet, G.Y., Lepers, R., Maffiuletti, N.A., Babault, N., Martin, V., & Lattier, G. (2002). Alterations of neuromuscular function after an ultra marathon. *Journal of Applied Physiology*, **92**, 486-492.

Mizrahi, J., Verbitsky, O., & Isakov, E. (2000). Shock accelerations and attenuation in downhill and level running. *Clinical Biomechanics*, **15**, 15-20.

Mori, S., & Burr, D.B. (1993). Increased intracortical remodeling following fatigue damage. *Bone*, **14**, 103-109.

Nigg, B.M. (2001). The role of impact forces and foot pronation: a new paradigm. *Clinical Journal of Sport Medicine*, **11**, 2-9.

Nummel, A., Vuorimaa, T., & Rusko, H. (1992). Changes in force production, blood lactate and EMG activity in the 400-m sprint. *Journal of Sports Science*, **10**, 217-28.

Nummel, A., Rusko, H., & Mero, A. (1994). EMG activities and ground reaction forces during fatigued and nonfatigued sprinting. *Medicine and Science in Sports and Exercise*, **26**, 605-609.

Paavolainen, L., Nummela, A., Rusko, H., & Hakkinen, K. (1999). Neuromuscular characteristics and fatigue during 10 km running. *International Journal of Sports Medicine*, **20**, 516-21.

Peris, P. (2003). Stress fractures. *Best Practice and Research Clinical Rheumatology*, **17**, 1043-1061.

Petermann, M.M., Hamel, A.J., Cavanagh, P.R., Piazza, S.J., & Sharkey, N.A. (2001). In vitro modeling of human tibial strains during exercise in micro-gravity. *Journal of Biomechanics*, **34**, 693-8.

Petrofsky, J.C., & Lind, A.R. (1979). Isometric endurance in fast and slow muscles in cat. *American Journal of Physiology*, **236**, C185-C191.

Prilutsky, B.I., & Zatsiorsky, V.M. (2002). Optimization-based models of muscle coordination. *Exercise and Sport Science Reviews*, **30**, 32-38.

Reber, L., Perry, J., & Pink, M. (1993). Muscular control of the ankle in running. *The American Journal of Sports Medicine,* **21**, 805-810.

Ross, A., Leveritt, M., & Riek, S. (2001). Neural influences on sprint running: training adaptations and acute responses. *Sports Medicine*, **31**, 409-25.

Rugg, S.G., Gregor, R.J., Mandelbaum, B.R., & Chiu, L. (1990). In vivo moment arm calculations at the ankle using magnetic resonance imaging (MRI). *Journal of Biomechanics*, **23**, 495-501.

Schaffler, M.B., & Jepsen, K.J. (2000). Fatigue and repair in bone. *International Journal of Fatigue*, **22**, 839-846.

Schaffler, M.B., Radin, E.L., & Burr, D.B. (1990). Long-Term fatigue behavior of compact bone at low strain magnitude and rate. *Bone,* **11**, 321-6.

Scott, S.H., & Winter, D.A. (1990). Internal force of chronic running injury sites. *Medicine and Science in Sports and Exercise*, **22**, 357-69.

Siler, W.L., & Martin, P.E. (1991). Changes in running pattern during a treadmill run to volitional exhaustion: fast versus slower runners. *International Journal of Sport Biomechanics*, **7**, 12-28.

Sonada, N., Chosa, E., Totoribi, K., & Tajima, N. (2003). Biomechanical analysis for stress fractures of the anterior middle third of the tibia in athletes: nonlinear analysis using a three-dimensional finite element method. *Journal of Orthopaedic Science*, **8**, 505-513.

Spitz, D.J., & Newberg, A.H. (2002). Imaging of stress fractures in the athlete. *Radiologic Clinics of North America*, **40**, 313-331.

Spoor, C.W., Van Leeuwen, J.L., Meskers, C.G.M., Titulaer, A.F., & Huson A. (1990). Estimation of instantaneous moment arms of lower-leg muscles. *Journal of Biomechanics*, **23**, 1247-1259.

Turner, C.H., & Burr, D.B. (1993). Basic biomechanical measurements of bone: A tutorial. *Bone*, **14**, 595-608.

Van Der Velde, G.M., & Hsu, W.S. (1999). Posterior tibial stress fracture: a report of three cases. *Journal of Manipulative and Physiological Therapeutics*, **22**, 341-346.

Voloshin, A., Mizrahi, J., Verbitsky, O., & Isakove, E. (1998). Dynamic loading on the human musculoskeletal system: effect of fatigue. *Clinical Biomechanics*, **13**, 515-520.

Weltman, A. (1995). The blood lactate response to exercise. Human Kinetics, Champaign, Illinois.

Williams, R.K. (1990). Relationships between distance running biomechanics and running economy. In P.R. Cavanagh (Ed.), Biomechanics of distance running. Human Kinetics Books, Champaign, Illinois, pp.271-305.

Winter, D.A. (1990). Biomechanics and motor control of human movement (2nd Ed.). A Wiley-Interscience Publication, New York, pp. 78-79.

Yao, L., Johnson, C., Gentill, A., Lee, J., & Seeger, L.L. (1998). Stress injuries of bone: analysis of MR imaging staging criteria. *Academic Radiology*, **5**, 34-40.

Yoshikawa, T., Mori, S., Santiesteban, A.J., Sun, T.C., Hafstad, E., Chen, J., & Burr D.B. (1994). The effects of muscle fatigue on bone strain. *Journal of Experimental Biology*, **188**, 217-233.

APPENDICES

Appendix A

APPENDIX A
REVIEW OF THE LITERATURES

Stress fractures

Stress fractures are bone tissue micro-damage caused by repetitive loading. Its symptom is pain in the region of fracture, which increases with physical activity and decreases with rest (Brukner and Bennell, 1997; Peris, 2003). In severe cases, pain may persist after exercise. The signs that can be revealed by a physical examination are redness, swelling, and tenderness over the involved bone. Periosteal thickening may be palpable (Brukner and Bennell, 1997; Van Der Velde and Hsu, 1999).

Diagnostics. Plain radiographs are insensitive for detecting the early stages of stress fracture development (Spitz and Newberg, 2002; Yao et al., 1998). However, they can detect stress fractures at the late stage, specifically by showing the periosteal callus. Scintigraphy, computer tomography scans (CT scan) and magnetic resonance imaging (MRI) are able to detect stress fractures in the early stages. In scintigraphy, an injected radioisotope (^{99m}technetium-polyphosphate compounds) accumulates in areas of high blood flow and metabolic activity (Jensen, 1998). Therefore, it is highly sensitive to the stress fractures but not specific (Jeske et al., 1996). Any other focal bone abnormalities can result in a positive bone scan. Unlike scintigraphy, a CT scan is able to show the periosteal and endosteal new bone formations and the increasing of the medullary canal's density in stress fractures. To identify the progression of injury, MRI can be used. The progression starts with periosteal edema followed by a progressive marrow involvement and ultimately, the frank cortical stress fracture (Fredericson et al., 1995).

Epidemiological reports. An epidemiological report showed that the incidence rate of stress fractures did not differ among genders, but it differed among ages (Bennell and Brukner, 1997). The greatest percentage rate of the stress fractures was found in the younger group (mean age of 30 years old) compared to the older group

(mean age of 57 years old). Factors causing the difference in the percentage rate of stress fractures between the two age groups were unknown. Fukushima and team (2002) studied stress fractures in the young Japanese athletes whose ages were less than 20 years old. They reported that 16-year old athletes were the largest group who developed stress fractures. Comparing various types of sports, Johnson and colleagues (1994) found the highest incidence rate of stress fractures in track and field (9.7% in male and 31.1% in female). Hulkko and Orava (1987) also reported that the highest incidence rate of stress fractures was found in runners (72%). A twelve-month perspective study on track and field athletes performed by Bennell and colleagues (1996) showed that 31.6% of long-distance runners, 22.9% of middle-distance runners and 18.2% of hurdlers got stress fractures.

The distributed site of stress fractures was varied among different sports. However, it was reported that the most common sites were the tibia, metatarsal and fibula, respectively (Hulkko and Orava, 1987; Fredericson et al., 1995). In contrast, Bennell and team (1996) reported that 46 %, 15% and 12% of stress fractures were found in the tibia, navicular bone and fibula, respectively. Distance running and track were the most common sports that reported tibial stress fractures (Brukner et al., 1996). It was also reported that the distal third of the tibia and posteriomedial crest are the most common regions of the tibial stress fracture found in runners (Brukner et al., 1998).

The incidence of stress fractures was also associated with the activity volume. Korpelainen and colleagues (2001) reported that the highest percentage of stress fractures occurred in runners (61%) whose average weekly running mileage was 117 km. Bennell and colleagues (1996) reported the incidence rate of 0.7 per one stress fracture site per 1000 hours of training. The study of Fukushima and colleagues (2002) showed an increase of stress fractures in direct relation to how often the athletes train per week. Out of the athletes who trained 7, 6, and 5 day a week, 44.2%, 21.1%, and 13.8 % sustained stress fractures, respectively.

Strains in the tibia and hypothesized mechanisms of stress fractures

A repeated application of loads to materials could result in a microdamage of the materials that leads to a deterioration of their mechanical properties. The effects of the repeated bouts of exercise and loading on the stress fractures were observed in animals. Treadmill running at 20,000 cycles per day for 5 and 10 days resulted in the stiffness reduction of the tibia in exercising rats (Forwood and Parker, 1991). Nonetheless, rats used in this study were most likely skeletally immature. Rabbits were used in the similar study by Burr and colleagues (1990) who applied the repetitive impulsive loading of 1.5 BW 5 days a week, for a total of 9 weeks to the rabbits' hind limbs. The repetitive loading led to the development of stress fractures in the middle and the distal tibia between the third and sixth week. Microcracks were also observed in the damaged regions. Both previous studies showed that stress fractures in the animal tibia could be induced by repeated application of the small impulsive loads.

The behaviors of cortical bone in response to the application of repetitive loads have been investigated in the *in vitro* studies (Carter et al., 1981; Carter and Caler, 1983; Carter and Caler, 1985; Schaffler et al., 1990). They found that loads resulting in the strain range of 3000-10,000 με could fail bone within 10^3 to 10^5 cycles of the repetitive application. However, bone will not fail if the applied loads result in a smaller strain range of 1,200-1,500 με. Loads occurring at the stance phase of running may result in large strains, which lead to stress fractures at a certain number of running steps.

Tibial strains have been recorded in live humans during running by mounting strain gauge staples in the medial tibial cortex at the midshaft of bone. Strain magnitude and strain rate were recorded while running at 11 km/hr (Milgrom et al., 2001; Milgrom et al., 2002). The ranges of compressive and tensile strains were equal to 359-446 με, and 639-1225 με, respectively. Compressive and tensile strain rates were equal to 2028-3795 με/s, and 6895-10020 με/s, respectively. Compressive,

tensile and shear strains occurring when running at a higher speed (13.88 km/hr) were larger and reported as –968 ± 30 με, 646 ± 72 με, and 1583 ± 46 με, respectively (Burr et al., 1996). Compressive, tensile and shear strain rates were equal to –34, 457 ± 3,637 με/s, 20,237± 2,136 με/s, and 51,433± 5,244 με/s, respectively. Milgrom and colleagues (2000a & 2000b) also reported that larger strains were found in the mid-diaphysis of the tibia at the faster running speed of 17 km/hr. These ranges of compressive, tensile and shear strains were equal to –1,675 to –2,104 με, 1,378 to 1,415 με and 5,027 to 5,532 με, respectively. The recorded compressive, tensile and shear strain rates were equal to –9,766 to –14,543 με/s, 7,780 to 8,255 με/s, and 38,064 to 44,306 με/s, respectively. Therefore, it could be concluded that the faster the running speed, the larger the strains and strain rates were found in the tibia. Moreover, the hardness of shoe soles and the type of running track also affect them. The smallest peak tibial strain was found in those who wore the polyurethane embedded with air cell shoes compared to other types of shoes (Milgrom et al., 2001). Milgrom and colleagues (2003) also reported that strains and strain rates of over-ground running were 48-285 % larger than those of treadmill running.

The controversy about factors initiating tibial stress fractures in runners exists. Since the peak tibial strains found while running were smaller than 3000 με, Milgrom and colleagues (2002) reported that a repeated application of running loads to the tibia could not result in tibial stress fractures. In contrast, they hypothesized that the tibial stress fracture might be a result of the remodeling responses to the repetitive loading. As the cyclic loading continues before the laying down of new bone is finished, micro-damage accumulates and leads to stress fractures. However, Petermann and colleagues (2001) found that those reported peak strains from the *in vivo* studies were far below maximum strains because strains were recorded near the neutral axis of bending. Therefore, running may result in larger peak tibial strains than the previous *in vivo* studies showed, which could initiate a microdamage of bone.

An experiment has been performed to determine whether remodeling follows the accumulation of microcracks or vice versa (Mori and Burr, 1993). The repetitive

three-point bending loads of 2500 με were applied to the left forelimbs of foxhounds for 10,000 cycles. The same repetitive loads were also applied to the right forelimbs 8 days later. This study found that the remodeling occurred subsequent to microdamage initiation (Burr et al., 1997). Schaffler and Jepsen (2000) also reported that diffuse bone matrix microdamage processes are a major mode of early fatigue damage and associated with *in vivo* loading. The diffuse bone matrix microdamage may be a stimulus of matrix turnover and repair. Therefore, it can be summarized that stress fractures of bone are initiated by cyclic loading until microdamage of bone matrix occurs. However, no study has been proven that loads occurring while running can initiate microdamge of the tibia.

Muscle fatigue and its association with stress fractures

Muscle fatigue occurs both in sprinting and distance running and leads to various changes in kinetics and kinematics. However, the mechanism of fatigue varies depending on how fast and how long runners run. In the 100-meter sprint, muscle fatigue causes a decrease in stride rate. This was a result of neural fatigue because muscle activation decreased about 4.9-8.7% after the acceleration phase of the race (Ross et al., 2001).

The decreasing of running speed, stride length, stride rate, and ground reaction force (GRF) after a 400-m run was also reported (Nummel et al., 1992). Since the increasing of neural activation in rectus femoris, biceps femoris, vastus lateralis and gastrocnemius medialis was found, the fatigue that occurred in the 400-m sprint was the result of peripheral fatigue (Nummel et al., 1994).

Fatigue after a 10-km run led to the decreasing of running velocity and GRF (Paavolainen et al., 1999). Hausswirth and colleagues (2000) reported that the decreasing of neural activation was one factor leading to fatigue occurring in long distance running. One example of this factor was the decreasing of maximal voluntary

activation of knee extensors reported by Millet and team (2002). It decreased about $27.7 \pm 13.0\%$ after a 65-km ultra marathon race.

The previous studies showed that muscle fatigue from running resulted in the decreasing of running speed and stride length. In another study, the runner maintained a constant running speed even after muscle fatigue while running on a treadmill, this resulted in the runner having had to change their running patterns, such as an increase in stride length and range of motion of thighs (Siler and Martin, 1991). However, the range of motion of the knee was unaltered.

Christina and colleagues (2001) showed that a localized fatigue of the dorsiflexors resulted in the decreasing of dorsiflexion at heel contact and the increasing of loading rate of the impact peak of GRF. An increase in loading rate of GRF may relate to the increasing of shanks' acceleration at the impact phase. It has been reported that impact shock waves at the shank increased as a result of metabolic fatigue when running at a speed exceeding anaerobic threshold (Voloshin et al., 1998; Mizrahi et al., 2000). However, these previous studies did not prove that the increasing of shock waves related to muscle fatigue. Mizrahi and colleagues (2000) recorded accelerations of the runners' shank while running on a treadmill by attaching an accelerometer on their skin at the tibial tuberosity. They found an increase in peak accelerations propagating through the longitudinal direction of the shank after the development of metabolic fatigue. Using spectral analysis technique, median frequency of the entire power spectral density of the acceleration increased in the late stages of running. This shift in a higher impact shock wave propagating through the shank may lead to injuries of the tibia. However, wearing shoes with shock-absorbing insoles, which reduced the high impact shock waves, was still ineffective in reducing the incidence of stress fractures (Nigg, 2001). Therefore, the increasing of impact shock waves may not be a major contributing factor to stress fractures.

It has been reported that muscle fatigue led to the increasing of strains and changes in strain distribution. Yoshikawa and colleague (1994) reported that the fatigue of quadriceps resulting from a 20 minute running exercise increased peak

principal and shear strains in the tibiae of foxhounds by an average of 26-35%. The largest change of strains was found along the anterior and anterolateral surfaces of the tibia. A 25 ° clockwise rotation of neutral axis was also found when muscle became fatigued. Therefore, some regions of bone may experience abnormally high strains and are damaged. However, no evidence has proven this relationship. A similar experiment has been observed in humans but no conclusive result could be drawn due to noisy signals (Fyhrie et al., 1998). Thus, further studies are needed to confirm the results drawn from the animal model.

REFERENCES

Bennell, K.L., Malcolm, S.A., Thomas, S.A., Wark, J.D., & Brukner, P.D. (1996). The incidence and distribution of stress fractures in competitive track and field athletes: a twelve-month prospective study. *The American Journal of Sports Medicine*, **24**, 211-217.

Bennell, K.L., & Brukner, P.D. (1997) Epidemiology and site specificity of stress fractures. *Clinics in Sports Medicine*, **16**, 179-196.

Brukner, P., & Bennell, K. (1997). Stress fractures in female athletes: diagnosis, management and rehabilitation. *Sports Medicine*, **24**, 419-429.

Brukner, P., Bradshaw, C., Khan, K.M., White, S., & Crossley, K. (1996). Stress fractures: a review of 180 cases. *Clinical Journal of Sport Medicine*, **6**, 85-9.

Brukner, P., Bradshaw, C., & Bennell, K. (1998). Managing common stress fractures: let risk level guide treatment. *The Physician and Sport Medicine*, **26**, 39-47.

Burr, D.B., Forwood, M.R., Fyhrie, D.P., Martin, R.B., Schaffler, M.B., & Turner, C.H. (1997). Perspective: bone microdamage and skeletal fragility in osteoporotic and stress fractures. *Journal of Bone and Mineral Research*, **12**, 6-15.

Burr, D.B., Milgrom, C., Boyd, R.D., Higgins, W.L., Robin, G., & Radin, E.L. (1990). Experimental of the stress fractures of the tibia. *The Journal of Bone and Joint Surgery*, **72-B**, 370-375.

Burr, D.B., Milgrom, C., Fyhrie, D., Forwood, M., Nyska, N., Finestone, A., Hoshaw, S., Saiag, E., & Simkin, A. (1996). In vivo measurement of human tibial strains during vigorous activity. *Bone*, **18**, 405-410.

Carter, D.R., & Caler, W.E. (1983). Cycle-dependent and time-dependent bone fracture with repeated loading. *Journal of Biomechanical Engineering*, **105**, 166-170.

Carter, D.R., & Caler, W.E. (1985). A cumulative damage model for bone fracture. *Journal of Orthopaedic Research*, **3**, 84-90.

Carter, D.R., Caler, W.E., Spengler, D.M., & Frankel, V.H. (1981). Fatigue behavior of adult cortical bone. The influences of mean strain and strain range. *Acta Orthopaedica Scandinavica*, **52**, 481-490.

Christina, K.A., White, S.C., & Gilchrist, L.A. (2001). Effect of localized muscle fatigue on vertical ground reaction forces and ankle joint motion during running. *Human Movement Science*, **20**, 257-276.

Federicson, M., Bergman, G., Hoffman, K.L., & Dillingham, D.S. (1995). Tibial stress reaction in runners: correlation of clinical symptoms and scintigraphy with a new magnetic resonance imaging grading system. *American Journal of Sports Medicine*, **23**, 472-81.

Forwood, M.R., & Parker, A.W. (1991). Repetitive loading, in vivo, of the tibiae and femora of rats: effects of repeated bouts of treadmill-running. *Bone and Mineral*, **13**, 35-46.

Fukushima, M., Mutoh, Y., Takasugi, S., Iwata, H., & Ishii, S. (2002). Characteristics of stress fractures in young athletes under 20 years. *The Journal of Sports Medicine and Physical Fitness*, **42**, 198-206.

Fyhrie, D.P., Milgrom, C., Hoshaw, S.J., Simkin, A., Dar, S., Drumb, D., & Burr, D.B. (1998). Effect of fatiguing exercise on longitudinal bone strain as related to stress fracture in humans. *Annals of Biomedical Engineering*, **26**, 660-5.

Hausswirth, C., Brisswalter, J., Vallier, J.M., Smith, D., & Lepers, R. (2000). Evolution of electromyographic signal, running economy, and perceived exertion during different prolonged exercises. *International Journal of Sports Medicine*, **21**, 429-36.

Hulkko, A., & Orava, S. (1987). Stress fractures in athletes. *International Journal of Sports Medicine*, **8**, 221-6.

Jensen, J. (1998). Stress fracture in the world class athlete: a case study. *Medicine and Science in Sports and Exercise*, **30**, 783-787.

Jeske, J.M., Lomasney, L.M., Demos, T.C., Vade, A., & Bielski, R.J. (1996). Longitudinal tibial stress fracture. *Orthopedics*, **19**, 225-230.

Johnson, A.W., Weiss, C.B., & Wheeler, D.L. (1994). Stress fractures of the femoral shaft in athletes more common than expected: A new clinical test. *The American Journal of Sports Medicine*, **22**, 248-256.

Korpelainen, R., Orava, S., Karpakka, J., Siira, P., & Hulkko, A. (2001). Risk factors for recurrent stress fractures in athletes. *The American Journal of Sports Medicine*, **29**, 304-10.

Milgrom, C., Ekenman, I., & Finstone, A. (2001). Metatarsal strains are sufficiently high to cause fatigue fracture on the basis of cyclic overloading. *47th Annual meeting, Orthopaedic Research Society*, February 25-28, 2001.

Milgrom, C., Finstone, A., Levi, Y., Simkin, A., Ekenman, I., Mendelson, S., Millgram, M., Nyska, M., Benjuya, N., & Burr, D. (2000a). Do high impact exercises produce higher tibial strains than running? *British Journal of Sports Medicine*, **34**, 195-9.

Milgrom, C., Finestone, A., Segev, S., Olin, C., Arndt, T., & Ekenman, I. (2003) Are overground or treadmill runners more likely to sustain tibial stress fracture? *British Journal of Sports Medicine*, **37**, 160-163.

Milgrom, C., Finstone, A., Sharkey, N., Hamel, A., Mandes, V., Burr, D., Arndt, A., & Ekenman, I. (2002). Metatarsal strains are sufficient to cause fatigue fracture during cyclic overloading. *Foot and Ankle International*, **23**, 230-235.

Milgrom, C., Finstone, A., Simkin, A., Ekenman, I., Mendelson, S., Millgram, M., Nyska, M., & Larsson, E.B. (2000b). In-vivo strain measurements to evaluate the strengthening potential of exercises on the tibial bone. *Journal of Bone and Joint Surgery*, **82**, 591-4.

Milgrom, C., Finstone, A., Ekenman, I., Simkin, A., & Nyska, M. (2001). The effect of shoe sole composition on in vivo tibial strains. *Foot and Ankle International*, **22**, 598-602.

Millet, G.Y., Lepers, R., Maffiuletti, N.A., Babault, N., Martin, V., & Lattier, G. (2002). Alterations of neuromuscular function after an ultra marathon. *Journal of Applied Physiology*, **92**, 486-492.

Mizrahi, J., Verbitsky, O., & Isakov, E. (2000). Shock accelerations and attenuation in downhill and level running. *Clinical Biomechanics*, **15**, 15-20.

Mori, S., & Burr, D.B. (1993). Increased intracortical remodeling following fatigue damage. *Bone*, **14**, 103-109.

Nigg, B.M. (2001). The role of impact forces and foot pronation: a new paradigm. *Clinical Journal of Sport Medicine*, **11**, 2-9.

Nummel, A., Vuorimaa, T., & Rusko, H. (1992). Changes in force production, blood lactate and EMG activity in the 400-m sprint. *Journal of Sports Science*, **10**, 217-28.

Nummel, A., Rusko, H., & Mero, A. (1994). EMG activities and ground reaction forces during fatigued and nonfatigued sprinting. *Medicine and Science in Sports and Exercise*, **26**, 605-609.

Paavolainen, L., Nummela, A., Rusko, H., & Hakkinen, K. (1999). Neuromuscular characteristics and fatigue during 10 km running. *International Journal of Sports Medicine*, **20**, 516-21.

Peris, P. (2003). Stress fractures. *Best Practice and Research Clinical Rheumatology*, **17**, 1043-1061.

Petermann, M.M., Hamel, A.J., Cavanagh, P.R., Piazza, S.J., & Sharkey, N.A. (2001). In vitro modeling of human tibial strains during exercise in micro-gravity. *Journal of Biomechanics*, **34**, 693-8.

Ross, A., Leveritt, M., & Riek, S. (2001). Neural influences on sprint running: training adaptations and acute responses. *Sports Medicine*, **31**, 409-25.

Schaffler, M.B., & Jepsen, K.J. (2000). Fatigue and repair in bone. *International Journal of Fatigue*, **22**, 839-846.

Schaffler, M.B., Radin, E.L., & Burr, D.B. (1990). Long-Term fatigue behavior of compact bone at low strain magnitude and rate. *Bone,* **11**, 321-6.

Siler, W.L., & Martin, P.E. (1991). Changes in running pattern during a treadmill run to volitional exhaustion: fast versus slower runners. *International Journal of Sport Biomechanics*, **7**, 12-28.

Spitz, D.J., & Newberg, A.H. (2002). Imaging of stress fractures in the athlete. *Radiologic Clinics of North America,* **40**, 313-331.

Van Der Velde, G.M., & Hsu, W.S. (1999). Posterior tibial stress fracture: a report of three cases. *Journal of Manipulative and Physiological Therapeutics*, **22**, 341-346.

Voloshin, A., Mizrahi, J., Verbitsky, O., & Isakove, E. (1998). Dynamic loading on the human musculoskeletal system: effect of fatigue. *Clinical Biomechanics*, **13**, 515-520.

Yao, L., Johnson, C., Gentill, A., Lee, J., & Seeger, L.L. (1998). Stress injuries of bone: analysis of MR imaging staging criteria. *Academic Radiology*, **5**, 34-40.

Yoshikawa, T., Mori, S., Santiesteban, A.J., Sun, T.C., Hafstad, E., Chen, J., & Burr D.B. (1994). The effects of muscle fatigue on bone strain. *Journal of Experimental Biology*, **188**, 217-233.

Appendix B

APPENDIX B
THE CALCULATION METHODS

The estimation of joint reaction force (JRF) and the resultant joint moments

Three-dimensional JRF and moments were determined from Newton-Euler's equations (Hibbeler, 1997).

$$\sum F_x = ma_x \quad (1)$$

$$\sum F_y = ma_y \quad (2)$$

$$\sum F_z = ma_z \quad (3)$$

$$\sum M_x = I_x\alpha_x - (I_y - I_z)\,\omega_y\omega_z \quad (4)$$

$$\sum M_y = I_y\alpha_y - (I_z - I_x)\,\omega_z\omega_x \quad (5)$$

$$\sum M_z = I_z\alpha_z - (I_x - I_y)\,\omega_x\omega_y \quad (6)$$

F is force. m is segmental mass. a is linear acceleration of the center of mass. M is moment about the center of mass. I is principle moment of inertia. α is angular acceleration of the center of mass. ω is angular velocity of the center of mass. x is mediolateral axis. y is anterior-posterior axis. z is vertical axis.

The calculation of the origin, insertion and moment arm lengths of the muscles

The left lower limb was modeled as four rigid-body segments composed of (1) pelvis, (2) femur, (3) tibia, and (4) foot. In total, 21 muscles were attached to the model. The hip, knee and ankle joints were modeled as a ball and socket joint, elliptical femoral condyles on a flat tibia plateau and a revolute joint, respectively. The origin of the pelvis reference frame was fixed at the midpoint of line connecting the left anterior superior iliac spine (LASIS) to right anterior superior iliac spine (RASIS). The origin of femoral, tibia and foot reference frames were fixed at knee joint center, ankle joint center and toe, respectively. The 3-orthogonal axes at the pelvic, femur and tibia had the following direction:

X-axis was the anterior-posterior axis. It was positive when x pointed to the anterior direction.

Y-axis was the mediolateral axis. It was positive when y pointed to the lateral direction.

Z-axis was the vertical axis. It was positive when z pointed to the superior direction.

The 3-orthogonal axes at the foot:

X-axis was the vertical axis. It was positive when x pointed to the superior direction.

Y-axis was the mediolateral axis. It was positive when y pointed to the lateral direction.

Z-axis was the anterior-posterior axis. It was positive when z pointed to the posterior direction.

The origin and insertion coordinates of muscles were derived from Delp (1990). Since the model of Delp was developed from a 180-cm tall male, coordinates were scaled to suit an individual runner using the scaling factors presented in table B1.

Table B1 Landmark for bone scaling.

Axis	**Scaling factor**
Pelvic Z[1]	ASIS-hip center Z coordinate difference
Femoral Z[1]	Femoral length
Tibial Z[1]	Tibial length
Foot Z[2]	Heel - toe Z coordinate difference

1 = derived from Brand et al. (1982)
2 = revised from Kepple et al. (1994). His scaling factor for the length of foot (Foot Z) was the heel-the fifth metatarsal Z coordinate difference.

Delp (1990) reported the coordinates of muscle origin and insertion in the reference frame of each segment. To derive those coordinates in the global reference

frame for the calculation of moment arm lengths all coordinates in the segmental reference frames were transformed to the global reference frame. An example of two link segments attached by a muscle is shown in Figure B1. An equation (7) was used for transforming the coordinates from the segmental to the global reference frames (Amirouche, 1992; Kepple et al., 1994):

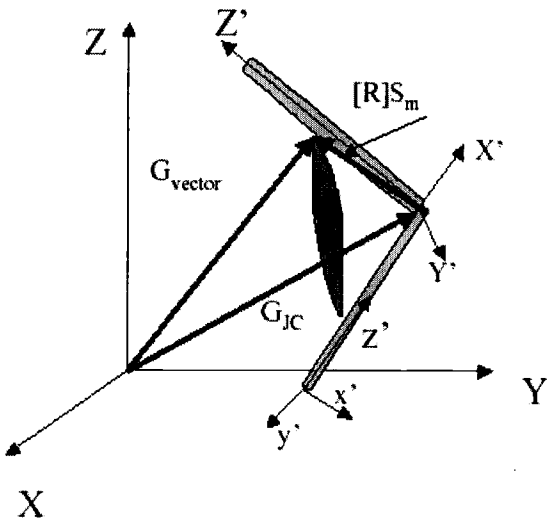

Figure B1. An illustration of two connected segments attached by a muscle. x', y', z' and X',Y', Z' are segmental axes of the first and the second segments, respectively. X, Y, Z are global axes of the global reference frame. G_{vector} is a vector coordinate in the global reference frame from the global origin to a point on the segment. R is a 3 by 3 rotational matrix transformed from the segmental reference axes to the global axes. S_m is the muscle coordinate in the segmental reference frame reported by Delp. G_{JC} is a vector coordinate in the global reference frame from the global origin to the segmental origin.

$$G_{vector} = [R]S_m + G_{JC} \qquad (7)$$

G_{vector} is a vector coordinate in the global reference frame from the global origin to a point on the segment. R is a 3 by 3 rotational matrix transformed from the segmental reference axes to the global axes. S_m is the muscle coordinate in the segmental reference frame reported by Delp. G_{JC} is a vector coordinate in the global reference frame from the global origin to the segmental origin.

The origin and insertion coordinates of muscles in the global reference frame were used for determining muscle moment arm lengths using the method of Hawkins (1992). Refer to figure B2.

$$L1 = ((Oy - Jcy)^2 + (Oz - Jcz)^2)\ ½ \quad (8)$$

$$L2 = ((Iy - Jcy)^2 + (Iz - Jcz)^2)\ ½ \quad (9)$$

$$L3 = ((Oy - Iy)^2 + (Oz - Iz)^2)\ ½ \quad (10)$$

$$ß = \cos^{-1}[(L2^2 + L3^2 - L1^2)/(2*L2*L3)] \quad (11)$$

$$MA = L2 \sin(ß) \quad (12)$$

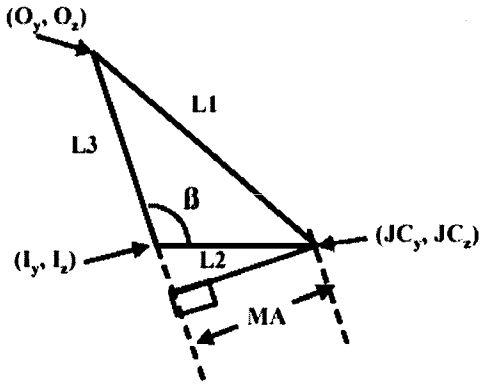

Figure B2. The geometry of the joint center and the origin and insertion of muscle used for the calculation of muscle moment arm lengths. O is muscle origin. I is muscle insertion. J is joint center. y is y-axis of global reference frame. z is z-axis of global reference frame. MA is muscle moment arm length. ß is an angle between L2 and L3.

Review of the optimization

Optimization is a method widely used for predicting muscle forces. It requires the assumption that the body selects muscles for a given mechanical function according to minimized physiological criterion. One of these criteria is selected to be the objective function of optimization. The physiological criteria for objective functions have been proposed as both linear and non-linear functions. The linear objective functions are the minimization of muscle force, muscle stress and muscle power while the non-linear objective functions are the minimization of fatigue and

metabolic energy expenditure. These criteria are written as the following (Crowninshield, 1983; Dul et al., 1984; Collin, 1995; Prilutsky and Zatsiorsky, 2002):

1) Force criterion: This criterion minimizes the sum of an individual muscle force.

$$\text{Minimize} \quad \sum_{i=1}^{N} f_i \qquad (13)$$

i is the number of muscle force and f_i is the tensile force developed in the i^{th} muscle.

2) Stress criterion: This criterion leads to the minimization of maximum stress.

$$\text{Minimize} \quad \max \{f_i / PCSA_i\} \qquad (14)$$

$PCSA_i$ is the physiological cross-sectional area of the i^{th} muscle.

3) Power Criterion: This criterion minimizes instantaneous muscle power.

$$\text{Minimize} \quad \sum_{i=1}^{N} W_i \qquad (15)$$

W_i is work done by the i^{th} muscle during the time between data frames (n-1) and n.

4) Fatigue Criterion: This criterion is based on the relationship between muscle force and maximum time of contraction. The muscle force-endurance relationship was proposed as

$\log T = -n \log f + c$

T is the maximum time of contraction. f is contraction force. n and c are the experimental constants. The estimated value of n from the statics and dynamics contractions was in the range of 1.4 to 5.1. The mean of n was equal to 3.0.

In 1983, Crowninshield proposed a muscle stress-endurance relationship as shown in figure B3. Muscle stress is a ratio of muscle force and its cross-sectional area. It inversely relates to the maximum endurance time. To maximize endurance

time muscle stress has to be at a minimum (Crowninshield and Brand, 1981; Crowninshield, 1983).

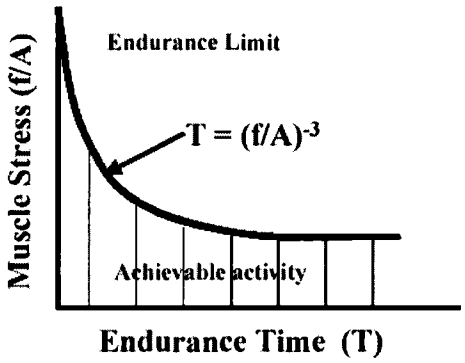

Figure B3. A muscle stress-endurance relationship.

Crowninshield and team proposed the objective function of fatigue as being the minimizing stress of each muscle. This stress equation is a power function and can be written as:

$$\text{Minimize} \quad \sum_{i=1}^{j} (f_i/PCSA_i)^n \qquad \text{while} \quad n>1 \qquad (16)$$

n is the exponent in the muscle endurance-force relationship. Its range is equal to 1.4-5.1 and its average value is equal to 3.0.

Based on the cat model in the Petrofsky and Lind experiment (1979), muscle with relatively more slow-twitch fibers has a greater endurance time. In 1984, Dul and his colleagues proposed the objective function of fatigue criterion as

$$\text{Minimize} \quad \max \{1/T_i\} \qquad i= 1,2,3,\ldots,n \qquad (17)$$

T_i is endurance time of the i^{th} muscle and can be estimated from:

$$T_i = a_i(f_i/ f_{imax}100)^{p}_i$$

f_i is the i^{th} muscle force. f_{imax} is maximum isometric force of the i^{th} muscle. a_i and p_i are the muscle parameters depending on the percentage of slow twitch fiber (S_i) of that muscle.

$$a_i = \exp(3.48 + 0.169\ S_i)$$

$$p_i = -0.25-0.036\ S_i$$

4) Metabolic energy expenditure criterion: The objective function of this criterion is shown as the following (Prilutsky and Zatsiorsky, 2002):

$$\text{Minimize} \quad f = \sum_{i=1}^{j} a_i^p * F_{imax} * v_{imax} * \Phi[v_i / v_{imax}] \qquad p = 1,2 \qquad (18)$$

f is the metabolic rate of the i^{th} muscle. Function Φ determines the metabolic cost. F_{imax} and v_{imax} are maximum muscle force and maximum velocity of the i^{th} muscle, respectively. v_i is instantaneous velocity of the i^{th} muscle. a_i is an unknown normalized activation of the i^{th} muscle. It range is between 0 and 1 and sought by minimizing f.

The selected objective function is subject to the equality constraints composed of the muscle moment equations of all joints in the model. For the four-link segmental model of the lower extremity, these equality constraints can be written as the following:

$$M_a = \sum_{i=1}^{j} d_{ai} * F_i \qquad (19)$$

$$M_k = \sum_{i=1}^{j} d_{ki} * F_i \qquad (20)$$

$$M_h = \sum_{i=1}^{j} d_{hi} * F_i \qquad (21)$$

where M_a, M_k, and M_h are the resultant moments at ankle, knee and hip joints, respectively. d is moment arm length of the i^{th} muscle. F_i is the force of the i^{th} muscle that results in the moment at that joint.

Since muscle develops only a tensile force and the amount of force should not exceed the maximum isometric force, then the optimization is also subject to these inequality constraints:

$$F_1, F_2, F_3, F_4, \ldots, F_n \geq 0 \qquad (22)$$

$$F_1, F_2, F_3, F_4, \ldots, F_n \leq \text{maximum isometric force} \qquad (23)$$

The maximum muscle force of the i^{th} muscle is estimated from $\sigma * PCSA_i$. σ is the muscle stress.

Without constraints, the objective function produces unrealistic muscle force estimations (Challis, 1997). The individual muscle force prediction will be restricted within physiologically realistic boundaries by subjecting the objective function to these constraints.

The validity of each objective function. Among the linear criteria, the minimized muscle force criterion selects the muscle that has the longest moment arm first. If force of the selected muscle exceeds its maximum force, the muscle with the next largest moment arm is selected. The minimized muscle stress criterion selects the muscle that has the largest product of moment arm and physiological cross-sectional area first. The second largest product will be selected when the stress of the first selected muscle reaches its maximum stress (Dul et al., 1984). These two criteria result in the orderly recruitment of muscles and cannot predict synergistic actions of muscles. Collin (1995) compared the solutions of these two criteria and those of the minimum power criterion with the pattern provided by Electromyography (EMG) during walking. The predicted patterns of muscular activities differed from the EMG patterns at certain instants of gait. Moreover, both the minimized muscle force and minimized muscle stress criteria failed to predict an antagonistic action of muscles.

In contrast, the minimized sum of the cubed muscle stress in fatigue criterion and minimized energy expenditure could predict 1) reciprocal co-activation of one-joint antagonist muscles, 2) co-activation of one-joint synergists with their two-joint antagonists, 3) the synergist of muscles crossing the same joint, 4) a strong relationship between force and the activation of two-joint muscles and moments at the two joints. Another fatigue criterion, which minimizes the maximum of the set $\{1/T_i\}$, could predict cat muscle forces with a smaller error compared to the minimized sum of the cubed muscle stress. However, the latter showed a slightly higher correlation between predicted and measured muscle activation patterns. Prilutsky and his colleague (2002) suggested that these criteria were reasonable for tasks with sub-maximal effort, such as walking, running, cycling, load-lifting, and contact force tasks.

One and multi-degree of freedom optimizations. Binding and his colleagues (2000) compared force-sharing among the synergistic muscles between one (ankle joint) and two-degree-of-freedom (ankle and knee joints) models. The force-sharing among three muscles around the ankle joint of a cat was used for validity testing. Two fatigue criteria, minimized sum of cubed muscle stresses (equation 16) and minimized max $\{1/T_i\}$(equation 17), were tested. They reported that the one-degree-of-freedom optimization could not provide adequate solutions and should not be used for the prediction of individual muscle force. In contrast, two and multi-degree-of-freedom approaches could predict force-sharing patterns observed in the experiment. The force-sharing pattern found in the two-degree-of-freedom approach was due to the loop relationship formed by the ankle and knee moments.

Static and dynamic optimization. There are two types of optimization: static and dynamic. Static optimization, an inverse dynamics approach, assumes that the value of the objective function does not depend on time. Muscle forces are calculated for each time instant of the movement. In contrast, dynamic optimization, a forward dynamics approach, solves the objective function that depends on time. Muscle forces and the performance criterion are treated as time-dependent state variables. The limitations of these two methods are 1) accurate inverse dynamics data are needed for static optimization and 2) a number of physiological parameters are needed for dynamic optimization (Prilutsky and Zatsiorsky, 2002; Anderson et al., 2001). Unfortunately, some of these parameters are still unknown.

In 2001, Anderson and Pandy compared muscle forces and joint contact forces predicted from static and dynamic optimizations. The objective function used for the static optimization was the minimized sum of squared muscle stresses. The objective function was both subjected to and not subjected to physiological constraints. The physiological constraints were the force-length-velocity properties of the muscle. The criterion for the dynamic optimization was the ratio between a computation of the total metabolic energy consumed and the change in position of the center of mass in the direction of progression. They selected this objective function for the study because it

showed that people select walking speeds to minimize the metabolic energy expended per unit distance traveled. Comparing the solutions of the static and dynamic optimizations, the results were very similar. The predicted force patterns from both techniques were also similar to those of EMG. Therefore, they concluded that static optimization was adequate for predictions of muscle and joint contact force. Moreover, the activation dynamics and the force-length-velocity properties of the muscle could be neglected because the solutions of physiological and non-physiological constraints were the same.

REFERENCES

Amirouche, F.M.L. (1992). *Computational methods in multibody dynamics.* (pp.16-22). Prentice-Hall, Englewood Cliffs, New Jersey.

Anderson, F.C., & Pandy, M.G. (2001). Static and dynamic optimization solutions for gait are practically equivalent. *Journal of Biomechanics*, **34**, 153-161.

Binding, P., Jinha, A., & Herzog, W. (2000). Analytic analysis of the force sharing among synergistic muscles in one-and two-degree of freedom models. *Journal of Biomechanics*, **33**, 1423-1432.

Brand, R.A., Crowninshield, R.D., Wittstock, C.E., Pedersen, D.R., Clark, C.R., & Krieken, F.M.V. (1982). A model of lower extremity muscular anatomy. *Journal of Biomechanical Engineering*, **104**, 304-310.

Challis, J.H. (1997). Producing physiologically realistic individual muscle force estimations by imposing constrains when using optimization techniques. *Medical Engineering and Physics*, **19**, 253-61.

Collins, J.J. (1995). The redundant nature of locomotor optimization laws. *Journal of Biomechanics*, **28**, 251-267.

Crowninshield, R.D., & Brand, R.A. (1981). A physiologically based criterion of muscle force prediction in locomotion. *Journal of Biomechanics*, **14**, 793-801.

Crowninshield, R.D. (1983). A physiologically based criterion for muscle force predictions on locomotion. *BULLETIN of the Hospital for Joint Diseases Orthopaedic Institute*, **XLIII**, 164-170.

Delp, S.L. (1990). Surgery simulation: a computer graphics system to analyze and design musculoskeletal reconstructions of the lower limb. Dissertation, Stanford University, California.

Dul, J., Johnson, G.E., Shiavi, R., & Townsend, M.A. (1984). Muscular synergism II: A minimum fatigue criterion for load sharing between synergistic muscles. *Journal of Biomechanics*, **17**, 675-684.

Hawkins, D. (1992). Software for determining lower extremity muscle-tendon kinematics and moment arm lengths during flexion/extension movements. *Computer Biological Medicine,* **22**, 59-71.

Hibbeler, R.C. (1997). Engineering mechanics statics and dynamics (8^{th} Ed.). Prentice-Hall, Upper Saddle River, New Jersey.

Kepple, T.M., Arnold, A.S., Stanhope, S.J., & Siegel, K.L. (1994). Assessment of a method to estimate muscle attachments from surface landmarks: a 3-D computer graphics approach. *Journal of Biomechanics*, **27**, 365-371.

Petrofsky, J.C., & Lind, A.R. (1979). Isometric endurance in fast and slow muscles in cat. *American Journal of Physiology*, **236**, C185-C191.

Prilutsky, B.I., & Zatsiorsky, V.M. (2002). Optimization-based models of muscle coordination. *Exercise and Sport Science Reviews*, **30**, 32-38.

Appendix C

APPENDIX C

THE MUSCLE ORIENTATIONS OF A TYPICAL RUNNER

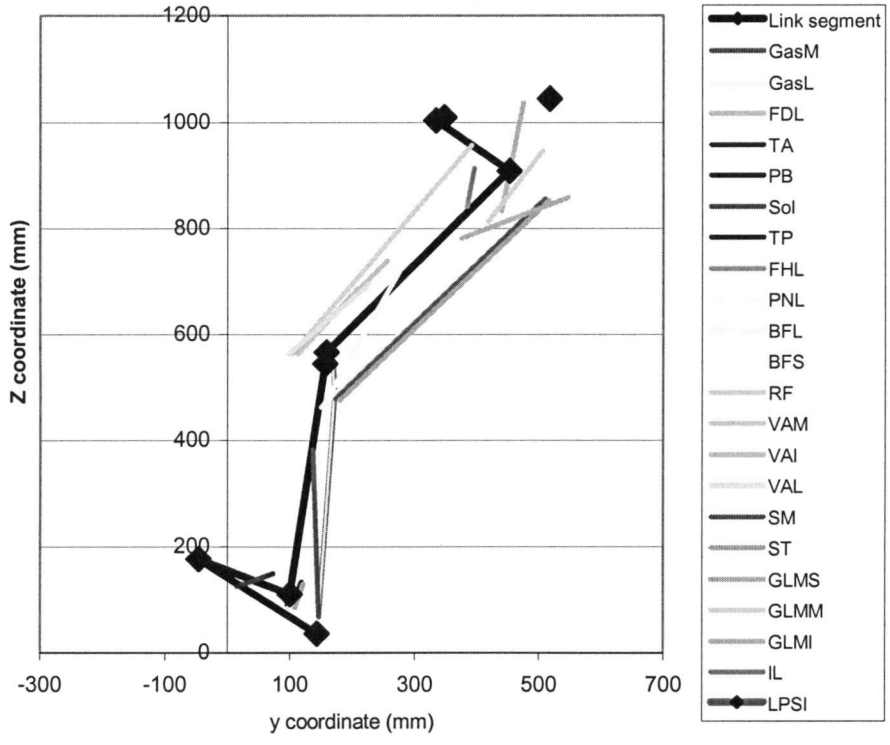

Figure C1. The sagittal view of a lower limb segment attached with 21 muscles at the initial contact. Negative Y-coordinates represent a forward direction. GasM is the medial gastrocnemius. GasL is the lateral gastrocnemius. FDL is the flexor digitorum longus. TA is the tibialis anterior. PB is the peroneus brevis. Sol is the soleus. TP is the tibialis posterior. FHL is the flexor hallucis longus. PNL is the peroneus longus. BFL is the biceps femoris long head. BFS is the biceps femoris short head. RF is the rectus femoris. VAM is the vastus mediallis. VAI is the vastus intermedius. VAL is the vastus laterallis. SM is the semimembranosus. ST is the semitendinosus. GLMS is the superior gluteus maximus. GLMM is the middle gluteus maximus. GLMI is the inferior gluteus maximus. IL is the iliacus. LPSI is the left posterior superior iliac spine.

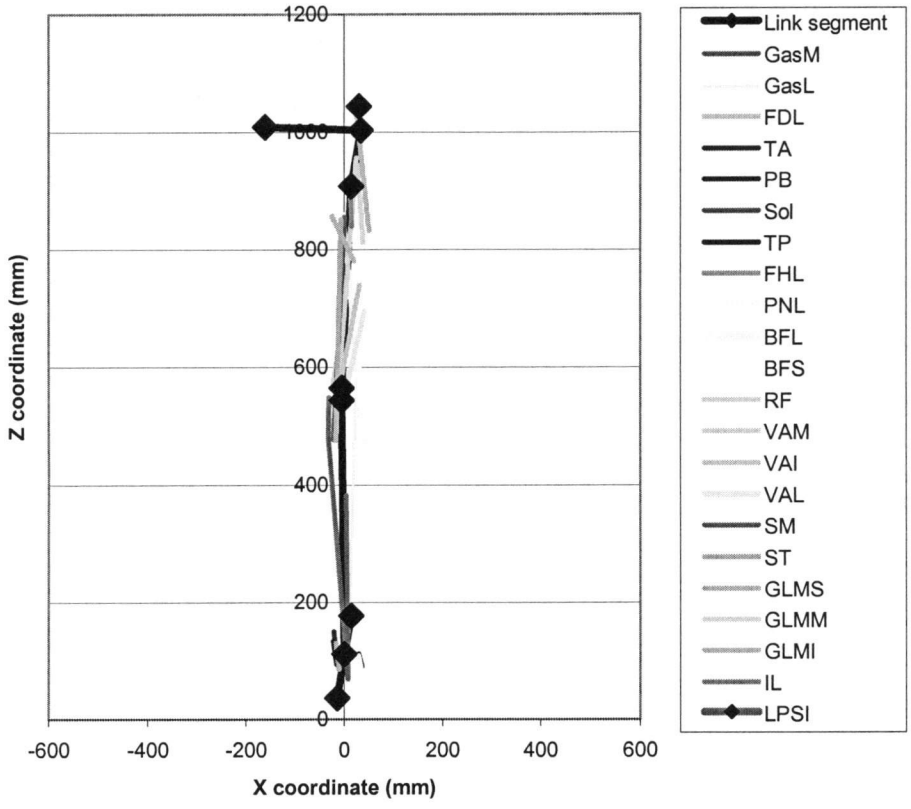

Figure C2.The frontal view of a lower limb segment attached with 21 muscles at the initial contact. Negative X-coordinates represent a medial side. GasM is the medial gastrocnemius. GasL is the lateral gastrocnemius. FDL is the flexor digitorum longus. TA is the tibialis anterior. PB is the peroneus brevis. Sol is the soleus. TP is the tibialis posterior. FHL is the flexor hallucis longus. PNL is the peroneus longus. BFL is the biceps femoris long head. BFS is the biceps femoris short head. RF is the rectus femoris. VAM is the vastus mediallis. VAI is the vastus intermedius. VAL is the vastus laterallis. SM is the semimembranosus. ST is the semitendinosus. GLMS is the superior gluteus maximus. GLMM is the middle gluteus maximus. GLMI is the inferior gluteus maximus. IL is the iliacus. LPSI is the left posterior superior iliac spine.

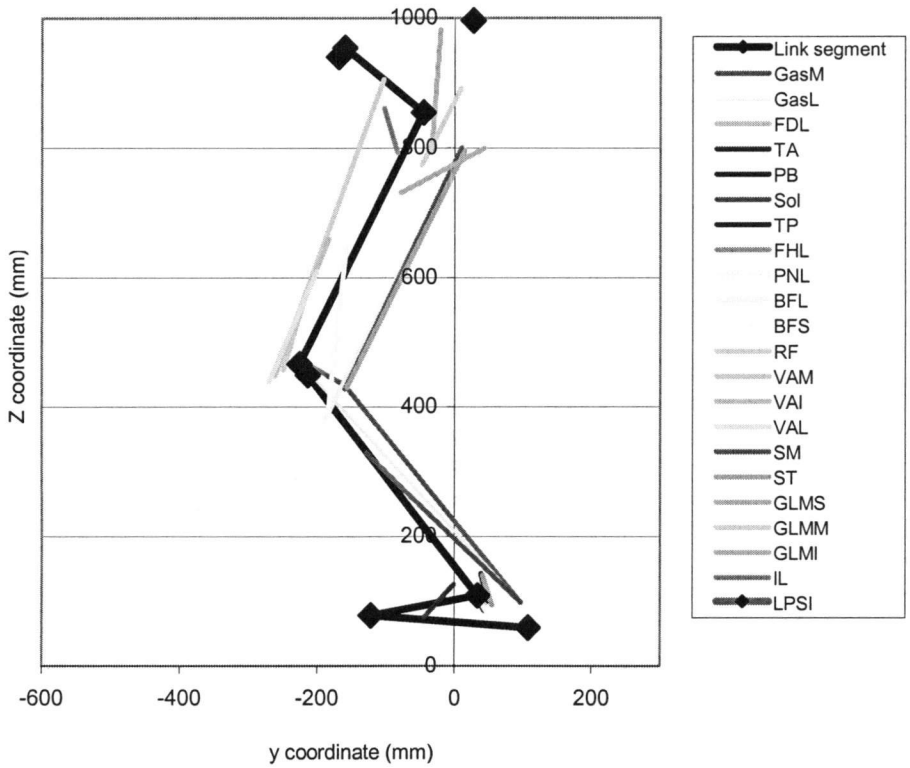

Figure C3. The sagittal view of a lower limb segment attached with 21 muscles at mid stance. Negative Y-coordinates represent a forward direction. GasM is the medial gastrocnemius. GasL is the lateral gastrocnemius. FDL is the flexor digitorum longus. TA is the tibialis anterior. PB is the peroneus brevis. Sol is the soleus. TP is the tibialis posterior. FHL is the flexor hallucis longus. PNL is the peroneus longus. BFL is the biceps femoris long head. BFS is the biceps femoris short head. RF is the rectus femoris. VAM is the vastus mediallis. VAI is the vastus intermedius. VAL is the vastus laterallis. SM is the semimembranosus. ST is the semitendinosus. GLMS is the superior gluteus maximus. GLMM is the middle gluteus maximus. GLMI is the inferior gluteus maximus. IL is the iliacus. LPSI is the left posterior superior iliac spine.

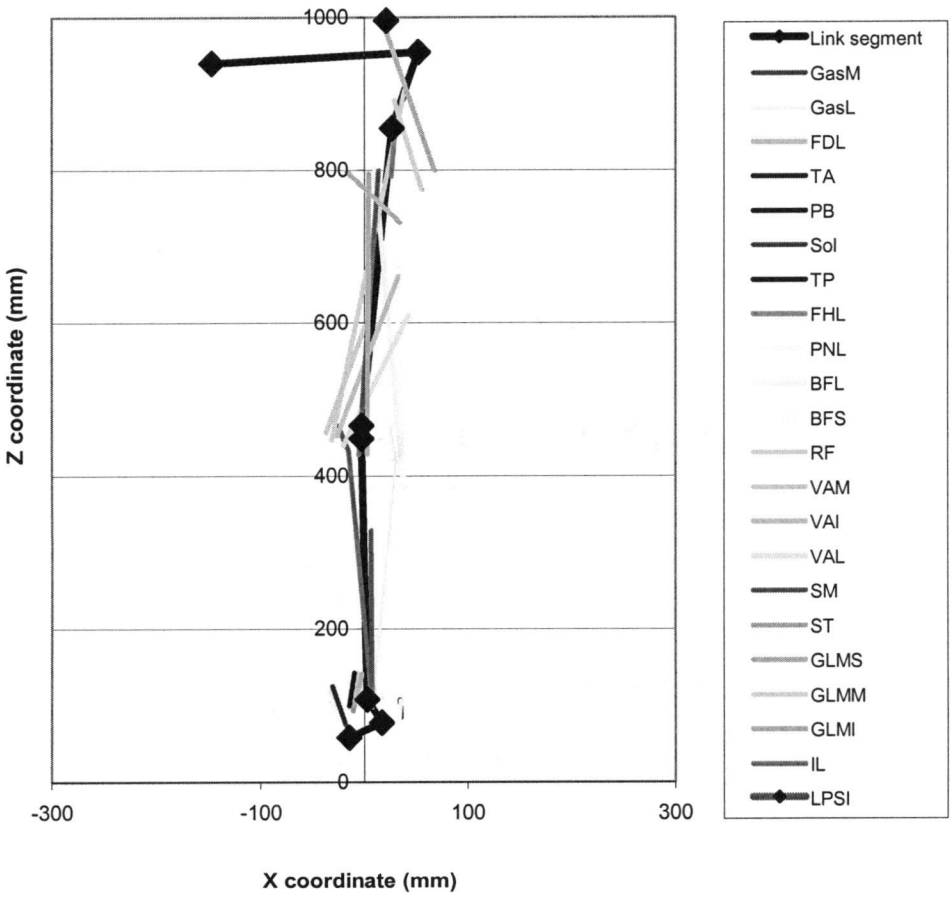

Figure C4. The frontal view of a lower limb segment attached with 21 muscles at mid stance. Negative X-coordinates represent a medial side. GasM is the medial gastrocnemius. GasL is the lateral gastrocnemius. FDL is the flexor digitorum longus. TA is the tibialis anterior. PB is the peroneus brevis. Sol is the soleus. TP is the tibialis posterior. FHL is the flexor hallucis longus. PNL is the peroneus longus. BFL is the biceps femoris long head. BFS is the biceps femoris short head. RF is the rectus femoris. VAM is the vastus mediallis. VAI is the vastus intermedius. VAL is the vastus laterallis. SM is the semimembranosus. ST is the semitendinosus. GLMS is the superior gluteus maximus. GLMM is the middle gluteus maximus. GLMI is the inferior gluteus maximus. IL is the iliacus. LPSI is the left posterior superior iliac spine.

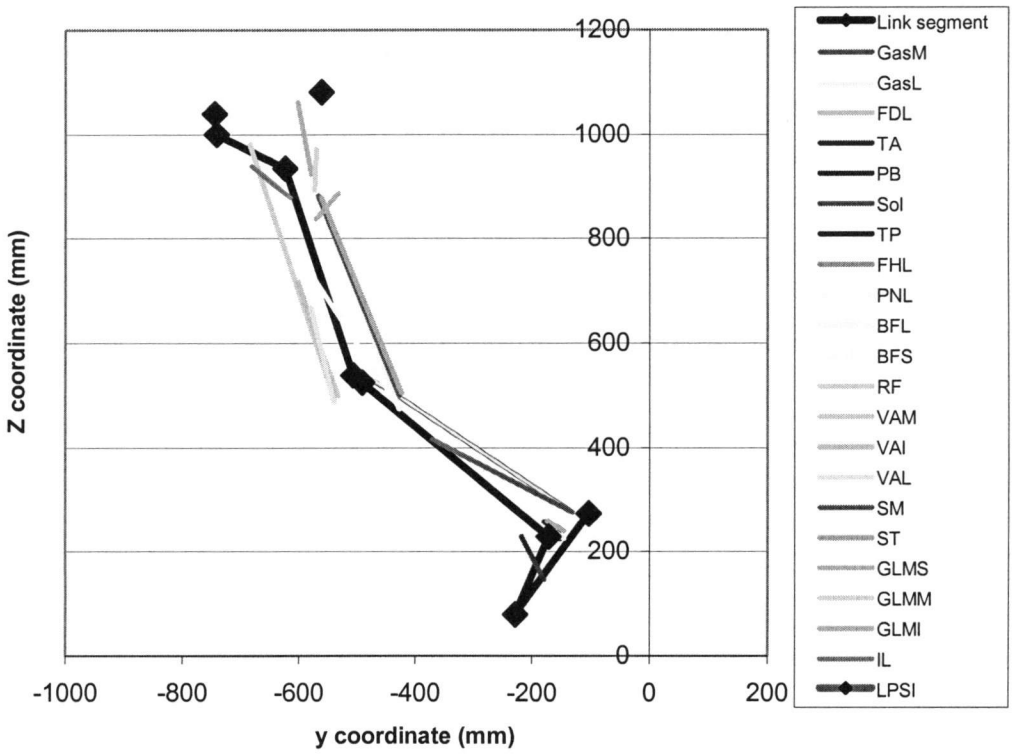

Figure C5. The sagittal view of a lower limb segment attached with 21 muscles at the toe off. Negative Y-coordinates represent a forward direction. GasM is the medial gastrocnemius. GasL is the lateral gastrocnemius. FDL is the flexor digitorum longus. TA is the tibialis anterior. PB is the peroneus brevis. Sol is the soleus. TP is the tibialis posterior. FHL is the flexor hallucis longus. PNL is the peroneus longus. BFL is the biceps femoris long head. BFS is the biceps femoris short head. RF is the rectus femoris. VAM is the vastus mediallis. VAI is the vastus intermedius. VAL is the vastus laterallis. SM is the semimembranosus. ST is the semitendinosus. GLMS is the superior gluteus maximus. GLMM is the middle gluteus maximus. GLMI is the inferior gluteus maximus. IL is the iliacus. LPSI is the left posterior superior iliac spine.

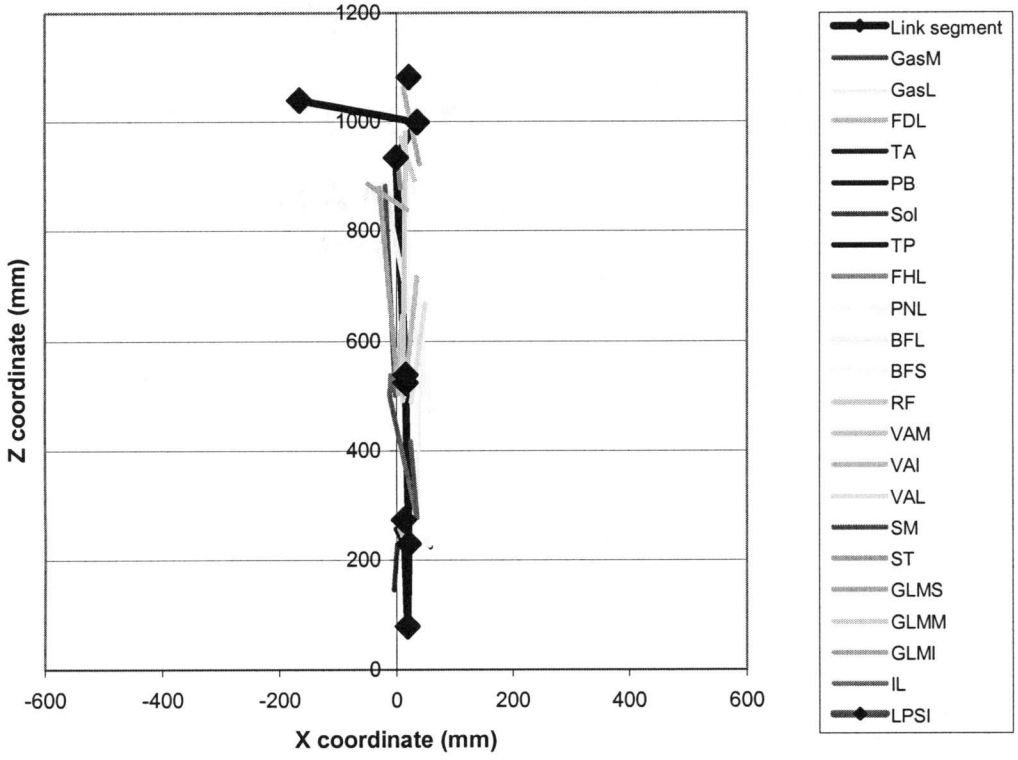

Figure C6. The frontal view of a lower limb segment attached with 21 muscles at the toe off. Negative X-coordinates represent a medial side. GasM is the medial gastrocnemius. GasL is the lateral gastrocnemius. FDL is the flexor digitorum longus. TA is the tibialis anterior. PB is the peroneus brevis. Sol is the soleus. TP is the tibialis posterior. FHL is the flexor hallucis longus. PNL is the peroneus longus. BFL is the biceps femoris long head. BFS is the biceps femoris short head. RF is the rectus femoris. VAM is the vastus mediallis. VAI is the vastus intermedius. VAL is the vastus laterallis. SM is the semimembranosus. ST is the semitendinosus. GLMS is the superior gluteus maximus. GLMM is the middle gluteus maximus. GLMI is the inferior gluteus maximus. IL is the iliacus. LPSI is the left posterior superior iliac spine.

Appendix D

APPENDIX D
INFORMED CONSENT DOCUMENT

Project Title: Do running and fatigued running relate to stress fractures of the tibia?

Principal Investigator: Brian K. Bay, Department of Exercise and Sport Science and Mechanical Engineering.

Research Staff: Siriporn Sasimontonkul, Department of Exercise and Sport Science

purposes

Stress fractures of the tibia (or shin bone) are weaknesses in the bone and are more likely to occur in distance runners. They result from small loads applying to bone repetitively. It is also possible that muscle fatigue may contribute to stress fractures, but currently there is no evidence to support this hypothesis.

This is a research study. The purposes of this research are 1) to determine whether the loads applied to bone while running could result in bone injury, especially stress fractures of the tibia and 2) to determine whether muscle fatigue from prolonged running changes the loads applied to bone and increases the risk of bone injury.

We are inviting you to participate in this research study because you are a male runner, aged between 20 to 35 years. You also meet the following criteria: (a) You currently run either about 20 – 60 miles per week or about 6-10 miles per day at least 3 day a week, (b) While running you hit the ground with your heels first, (c) You are currently injury free, especially of stress fractures, and have no abnormal running pattern such as running with limp, and (d) You have no history of or current cardiovascular disease/chest pain. For this study, 10 male runners will be asked to participate.

The purpose of this consent form is to give you the information you will need to help you decide whether to be in the study or not. Please read the form carefully. You may ask any questions about the research, what you will be asked to do, the possible risks and benefits, your rights as a volunteer, and anything else about the

research or this form that is not clear. When all of your questions have been answered, you can decide if you want to be in this study or not. This process is called "informed consent". You will be given a copy of this form for your records.

procedures

If you agree to participate, you will have a single testing session that will last for approximately 3-3.5 hours. You will be asked to wear running shoes and shorts. The study will be conducted in rooms 8 and 15 in the basement of Women's Building at Oregon State University. The following procedures are involved in this study.

1) The questionnaire. You will be asked to complete a questionnaire that asks about your current health, injury status and history, as well as your training status.

2) The measuring of anthropometrics. Your body weight will be measured using a scale. While standing, your height and leg length (the length from hip to ankle) will be measured using a measuring tape. The widest diameter of knee and ankle will be measured using a caliper. This procedure will last about 10 minutes.

3) The determination of the baseline strengths of the thigh and leg muscles. After a short warm up, you will be asked to sit on a dynamometer (a machine which measures the strength of muscle through resistance) in order to measure the baseline strengths of thigh and leg muscles. You will extend and flex your left leg and left foot against the dynamometer attachment five times each, respectively. Each time, you will extend or flex as hard as you can for 3-5 seconds and the dynamometer will adjust the resistance force according to your strength. These processes will last about 30 minutes.

4) The recording of the lower leg's motion and the forces exerted on the foot before running exercise. Reflective markers will be attached to your skin and clothing using double-sided marking tape at the front and the back of the hip, left thigh, left knee, left ankle, left heel and left second toe. You will then be asked to run 6 trials (less than 10 meters each) at the speed of 3.5 - 4 m/s (7.8 - 9 mi/hr). It is a medium,

comfortable, pace (6:40 – 7:40 min/mi) and equivalent to the speed that most recreational runners use for running. All parts of your left foot will need to hit a force-measuring plate, mounted within the floor, in order to accurately record the forces exerted on your foot. Cameras will record the motion of the markers but your image won't be visible in the recordings. These processes will last about 20 minutes.

5) Running exercise. The ratings of perceived exertion (RPE) will be used to rate your perception of exertion while running, that is, how strenuous the running feels to you. This perception of exertion depends mainly on the fatigue in your leg muscles. You will be asked to use a scale from 6 to 20, where 6 means "no exertion at all" and 20 means "maximal exertion". A chart of this scale will be shown to you and the researcher will explain how to use it before running. A big chart of this scale will be shown to you again when it is time for rating. Thereafter, a heart rate monitor will be strapped around your chest and wrist in order to monitor your heart rates every 15 minutes.

You will be asked to run on a treadmill at your preferred running speed. After 5 –10 minutes of running, you will evaluate how strenuous this running feels to you. The running speed will be increased if you feel that it is "extremely light" (scale of 7) or "very light" (scale of 9). A speed that you rate as "lightly heavy" (scale of 11) will be used in this study so that leg muscle fatigue can occur after about 1-1:15 hours. You will rate your perception of exertion every 15 minutes of running. After you feel that it is "very heavy" (scale of 17), you will stop running. If you request a chance to rest or to stop exercising at any time, the request will be honored immediately. The strengths of leg muscles will be evaluated immediately using the dynamometer. If the strengths of the leg muscles are about 25-30% less than their initial values, the running exercise will be complete. If this condition is not met, without taking a rest, you will continue running on the treadmill using the previous pace and the leg muscle strengths will be evaluated every 15 minutes. The running will be completed when either the leg muscle strengths are about 25-30% less than their initial values or you become exhausted, whichever occurs first. This procedure should last about 1- 1:15 hours, but

may last longer depending on your fitness level. If muscle fatigue does not occur within 1-1:15 hours, you will be asked if you are willing to continue running.

6) The recording of the lower leg's motion and the forces exerted on the foot after running exercise. You will be asked to perform another 6 trials of running across a force-measuring plate while we record the motion of the markers attached to your body. This procedure will be as described in section 4, and will last about 20 minutes.

7) The determination of the strengths of the thigh and leg muscles after completing all tests. You will be asked to sit on the dynamometer and to extend and flex your left leg and left foot against the dynamometer attachment. The procedure is the same as that described in section 3. The muscle strengths will be recorded. This process will last about 20 minutes.

risks

The risks that can happen in the study are the same as those that can occur during running. There is a possibility that you could fall during running, which could result in skin abrasions or bruises. To minimize this risk, we will recommend that you grab the front or the side rails of the treadmill if you are losing your balance. Muscle soreness may be associated with the prolonged running and exhaustion. To minimize the potential for muscle soreness, you will be instructed to stretch your muscles, especially the leg muscles, both before and after the running exercise. Fainting may result from excessive sweating. To minimize this risk, you will drink plain water intermittently while running.

With maximum-effort exercise, there is also the possibility of fainting, an irregular, fast, or slow heartbeat, and in rare instances, chest pain, stroke, or death. This study, however, involves only medium-effort exercise, and these events are extremely rare in healthy people under 35 years of age with relatively good training status and fitness level. However, the following efforts will be made to minimize these risks. Your heart rate will be monitored while running and the researcher will observe any abnormal signs while you run. You will be asked to report any unusual symptoms

that you experience before, during, or after the running exercise. For your safety, you should report these symptoms and you should not run if you are not feeling well. While running, you will periodically be asked to rate how you are feeling and your fatigue level. **The running will be stopped at any time that you request it.** The running will also be stopped immediately if your heartbeat feels irregular or if you have chest discomfort, shortness of breath, or signs of fainting, such as cold hands and dizziness.

An individual trained and currently certified in CPR techniques will be present during the testing phases of this project. If you experience a cardiac event, the researcher will call 911 for an emergency ambulance immediately and you will be instructed to lie down. The researcher will take your pulse every 1 to 5 minutes and stay with you until an emergency ambulance arrives.

benefits

There are no foreseeable direct benefits to you as a result of participating in this project. However, if you desire, your individual test results will be sent to you after completing the process of the analysis.

Your participation may advance the understanding of the mechanism of stress fractures of the tibia that are likely to occur in distance runners. The researcher anticipates that the runners in general should also benefit from this study by knowing how much load is put on bone while running and whether or not this load can result in the weakness of bone.

Costs and compensation

There will not be any cost to you for participating in this study. Compensation will be made available to participants for completing various phases of the study, $30 for completing all phases of the study. If you stop partway through the study, you will receive the pro-rated compensation for having participated. For example, withdrawal

after 1 hour will result in $10 of compensation to you; withdrawal after 2 hours will result in $20 of compensation.

confidentiality

Records of participation in this research project will be kept confidential to the extent permitted by law. A code number will be used to identify any test results or other information you provide. Also, no identifiable images of you will be recorded or saved, since the cameras that will record your movements see only the reflective markers that will be taped to you. In the event of any report or publication from this study, your identity will not be disclosed. Results will be reported in a summarized manner in such a way that you cannot be identified.

research related injury

In the event of research related injury, compensation and medical treatment is not provided by Oregon State University.

Voluntary participation

Taking part in this research study is voluntary. You may choose not to take part at all. If you agree to participate in this study, you may stop participating at any time. If you decide not to take part, or if you stop participating at any time, your decision will not result in any penalty or loss of benefits to which you may otherwise be entitled. Any data collected from you may be included in the study results, even if you choose to stop partway through the study. If you stop partway through the study, you will receive the pro-rated compensation as described in "Costs and Compensation" section.

questions

Questions are encouraged. If you have any questions about this research project, please contact: Siriporn Sasimontonkul, at (541) 752-9699 or by e-mail at sasimons@onid.orst.edu or contact: Brian Bay, at (541) 737-7024 or by e-mail at Brian.Bay@oregonstate.edu. If you have questions about your rights as a participant, please contact the Oregon State University Institutional Review Board (IRB) Coordinator, at (541) 737-3437 or by e-mail at IRB@oregonstate.edu or by mail at 312 Kerr Administration Building, Corvallis, OR 97331-2140.

Your signature indicates that this research study has been explained to you, that your questions have been answered, and that you agree to take part in this study. You will receive a copy of this form.

Participant's Name (printed):

_____

_____ _____

(Signature of Participant) (Date)

Researcher statement

I have discussed the above points with the participant or, where appropriate, with the participant's legally authorized representative, using a translator when necessary. It is my opinion that the participant understands the risks, benefits, and procedures involved with participation in this research study.

_____ _____

(Signature of Researcher) (Date)